POLYMERIC TUBES PREPARED FROM POLY(VINYL ALCOHOL) FIBER TEMPLATES

by

Jesmi Çavuşoğlu

B.S., Chemistry, Marmara University, 2005

M.S., Chemistry, Boğaziçi University, 2009

Submitted to the Institute for Graduate Studies in
Science and Engineering in partial fulfillment of
the requirements for the degree of
Doctor of Philosophy

Graduate Program in Chemistry

Boğaziçi University

2016

POLYMERIC TUBES PREPARED FROM POLY(VINYL ALCOHOL) FIBER TEMPLATES

APPROVED BY:

Assoc. Prof. A. Ersin Acar (Thesis Supervisor)	…….
Prof. Selim Küsefoğlu (Thesis Co-Advisor)	…….
Prof. Duygu Avcı Semiz	…….
Prof. İlknur Doğan	…….
Prof. Atilla Güngör	…….
Ediz Taylan, Ph.D.	…….

DATE OF APPROVAL: 17.05.2016

ACKNOWLEDGEMENTS

I am indebted to many people in writing this thesis. First and foremost, I would like to express my sincere and profound gratitude to my thesis supervisor Prof. Selim Küsefoğlu for the continuous guidance during my Ph.D. study, for his motivation and encouragement. It was an invaluable experience for me to work with him.

Besides my advisor, I would like to thank the rest of my thesis committee: Assoc. Prof. A. Ersin Acar, Prof. Duygu Avcı Semiz, Prof. İlknur Doğan, Prof. Atilla Güngör, and Dr. Ediz Taylan for their careful and constructive review of the final manuscript and for their insightful comments.

I would especially like to thank Dr. Bilge Gedik Uluocak for her help in Scanning Electron Microscopy imaging.

I thank my friends in Chemistry Department Dr. Şule Erol, Sevgi Sarıgül, Dr. Selda Erkoç for all the fun times we had in these years. In particular I am grateful to Assist. Prof. Gökhan Çaylı and Dr. Cem Öztürk for very helpful discussions.

Last but not the least; my deepest thanks go to my family for their endless love, continuous moral support and encouragement throughout these years.

ABSTRACT

POLYMERIC TUBES PREPARED FROM POLY(VINYL ALCOHOL) FIBER TEMPLATES

In this study, the fabrication of covalently crosslinked polymeric tubes by using poly(vinyl alcohol) (PVA) fiber templates has been demonstrated. The crosslinking on the surface of PVA fiber templates was achieved by two different methods. In the first method PVA surface hydroxyl groups were reacted with difunctional crosslinkers. Crosslinking took place with several dialdehydes and diisocyanates, respectively. The conditions were adjusted to allow the reaction to occur only on the surface and unreacted PVA inner core was removed from crosslinked fibers. Tubular structures which have adjustable shell thicknesses were succesfully fabricated by glutaraldehyde (GA) and 1,6-hexamethylene diisocyanate (HMDI) crosslinked PVA microfibers. Ultraviolet-visible spectroscopy was used to investigate load/release properties of these tubular hydrogels with changing shell thicknesses. Fluorescein dye molecules were used for imaging and the succesful absorption of dye molecules inside the shells was observed by optical microscopy. Furthermore, hydrophilicity differences were predicted between the outer and the inner shells. The feasibility of this method in fabrication of nanotubes was also investigated. In the second method PVA fibers were first reacted with acryloyl chloride and 3-trimethoxysilyl propylmethacrylate, respectively, to get double bond functionalized PVA fibers. These pendant double bonds were used to photopolymerize the surface of PVA with other mono and/or difunctional acrylate monomers. It was observed that during dissolution of the inner core, the shells were ruptured which may be due to a rigid network formation by photopolymerization. Therefore, it was found that the first crosslinking method is more suitable to prepare such hollow structures whose shells can be adjusted in terms of crosslinking and thickness. It was concluded that such materials may have potential applications in entrapment and release of several molecules.

ÖZET

POLYVİNİL ALKOL ELYAF ŞABLONLARI KULLANILARAK POLİMERİK TÜBÜLER YAPILARIN ELDESİ

Bu çalışmada poly(vinil alkol) (PVA) elyafların şablon olarak kullanılmasıyla kovalent çapraz bağlı polimerik tübüler yapıların eldesi gösterilmiştir. PVA elyafların çapraz bağlanması iki farklı yöntemle gerçekleştirilmiştir. Uygulanan birinci yöntemde PVA elyaf yüzeyindeki hidroksil grupları PVA ile reaksiyona girebilen bifonksiyonel monomerler kullanılarak çapraz bağlanmıştır. Bu amaçla çeşitli dialdehit ve diizosiyant monomerleri kullanılmıştır. Reaksiyon şartları çapraz bağlanmanın sadece yüzeyde gerçekleşebilmesi için ayarlanmıştır ve reaksiyona girmemiş PVA elyafların iç kısımlarından ayrılmıştır. PVA mikron boyutlu elyafların glutaraldehit (GA) ve 1,6- heksametilen diisosiyanat (HMDI) ile çapraz bağlanması sonucu değişik çeper kalınlıklarına sahip tübüler yapılar elde edilmiştir. Tübüler ve hidrojel benzeri özellik gösteren bu yapıların değişen çeper kalınlıkları ile yükleme ve salınım özellikleri Ultraviyole-görünür bölge spektroskopisi ile incelenmiştir. Görüntüleme için floresein boya molekülleri kullanılmış ve tübüler çeperlerde boya moleküllerinin başarılı absorpsiyonu optik mikroskop ile görüntülenmiştir. Bununla birlikte iç ve dış çeperler arasında hidrofilik bir farkın olduğu da tespit edilmiştir. Bu çapraz bağlanma yönteminin nano boyutlu tübüler yapıların eldesine uygunluğu da tartışılmıştır. Uygulanan ikinci yöntemde ise PVA elyafları akriloil klorür ve 3-trimetoksisilil propilmetakrilat ile reaksiyona sokularak yüzeylerine çift bağ grupları aşılanmıştır. Bu çift bağ grupları diğer mono ve/veya bifonksiyonel akrilat grupları ile PVA elyaf yüzeylerini fotopolimerize etmek için kullanılmışlardır. Bu şekilde elde edilen çeperler oldukça kırılgan bir yapıya sahip oldukları için reaksiyona girmemiş PVA elyaf şablonlarının ayrılması sırasında parçalanmışlardır. Bu nedenle bahsedilen ilk yöntemin çeper kalınlıkları ve çapraz bağlanma oranı ayarlanabilir içi boş tübüler yapıların eldesi için daha uygun olduğu bulunmuştur. Sonuç olarak bu tür malzemelerin çeşitli moleküllerin yükleme ve salınımı gibi potansiyel uygulamalarının olabileceği görülmüştür.

TABLE OF CONTENTS

ACKNOWLEDGEMENTS iii

ABSTRACT iv

ÖZET v

TABLE OF CONTENTS vi

LIST OF FIGURES xi

LIST OF TABLES xix

LIST OF ABBREVIATIONS xxi

1. INTRODUCTION 1

1.1. Fabrication Methods of Tubular Structures. 1

1.1.1. Emulsion Polymerization. 1

1.1.2. Self-assembly of Macromolecules 2

1.1.3. Template-Directed Synthesis 3

1.1.4. Electrospinning 5

1.1.4.1. Co-axial Electrospinning. 6

1.1.5. Tubes by Fiber Templates (TUFT Process) 7

1.1.5.1. Template Fibers 9

1.1.5.2. Wall Materials. 10

1.1.6. Covalently Crosslinked Polymeric Tubes by Fiber Templates 10

1.2. Poly(vinyl Alcohol) 11

1.3. Modifications of PVA. 13

1.4. Physical Crosslinking of PVA 14

1.4.1. Freeze-thawing 14

1.4.2. Heat-treatment or Annealing. 15

1.4.3. Irradiation 15

1.4.4. Composite Formation 15
1.5. Chemical Crosslinking of PVA 16
1.5.1. Radical Formation 16
1.5.2. Reaction with Aldehydes 16
1.5.3. Reaction with Dialdehydes 17
1.5.4. Reaction with Diisocyanates 18
1.5.5. Reaction with Sodium Tetraborate 19
1.5.6. Reaction with Epichlorohydrin (EPC) 19
1.5.7. Reaction with Polycarboxylic Acids 20
1.5.8. Reaction with Acid Chlorides 21
1.5.9. Reaction with Alkoxysilanes 22
2. RESEARCH OBJECTIVES 24
3. EXPERIMENTAL 28
3.1. Materials and Apparatus 28
3.1.1. Materials 28
3.1.2. Apparatus 28
3.2. Preparation of PVA Fibers 29
3.3. Preparation of PVA Films 30
3.4. Preparation of Glutaraldehyde Crosslinked PVA Fibers and Films 30
3.4.1. Swelling Behaviour of GA Crosslinked Fibers 32
3.4.2. Dye Loading into GA Crosslinked PVA Tubular Structures 32
3.4.3. Dye Loading Efficiency of GA Crosslinked PVA Tubular Structures . . 32
3.4.4. Dye Release and Diffusion Studies of GA Crosslinked PVA Tubular Structures 33
3.5. Preparation of Glyoxal Crosslinked PVA Fibers 33
3.5.1. Swelling Behaviour of GLY Crosslinked Fibers 34
3.6. Preparation of Hexamethylene Diisocyanate Crosslinked PVA Fibers 34

3.6.1. Swelling Behaviour of HMDI Crosslinked Fibers 35
3.6.2. Dye Loading into HMDI Crosslinked PVA Tubular Structures 36
3.6.3. Dye Loading Efficiency of HMDI Crosslinked PVA Tubular Structures 37
3.6.4. Dye Release and Diffusion Studies of HMDI Crosslinked PVA Tubular Structures 37
3.7. Preparation of Isophorone Diisocyanate Crosslinked PVA Fibers 37
3.8. Preparation of 2,4-Toluene Diisocyanate Crosslinked PVA Fibers 38
3.9. Grafting of Acryloyl Chloride on PVA Fibers 38
3.10. Grafting and/or Crosslinking of 3-trimethoxysilyl propylmethacrylate on PVA Fibers 38
3.11. Surface Photopolymerization of Double Bond Functionalized PVA Fibers. . . 38
3.12. Dissolution of PVA Templates from Crosslinked Fibers and Films 39
4. RESULTS AND DISCUSSION 40
4.1. Poly(vinyl alcohol) Fibers 40
4.2. Fabrication and Characterization of Dialdehyde Crosslinked PVA Tubular Structures 41
4.2.1. Crosslinking Reaction of PVA with Glutaraldehyde 41
4.2.2. FTIR Characterization of GA Crosslinked PVA Fibers 42
4.2.3. Determination of Crosslinking Density for GA Crosslinked PVA Fibers by Swelling 48
4.2.4. Removal of the Core from GA Crosslinked PVA Fibers 51
4.2.4.1. The effect of PVA fiber length. 55
4.2.4.2. The effect of crosslinked wall thickness. 56
4.2.5. Parameters That Affect Tube Wall Thickness of GA Crosslinked PVA Tubes 57
4.2.6. Dye Loading Properties of GA Crosslinked PVA Tubes 60

4.2.7. Dye Diffusion and Release Properties of the GA Crosslinked PVA Tubes 63
4.2.8. Contact Angle Measurements of GA Crosslinked PVA Films 65
4.2.9. Crosslinking of PVA Nanofibers with Glutaraldehyde 66
4.2.10. Crosslinking of PVA with Glyoxal. 67
4.2.11. FTIR Characterization of GLY Crosslinked PVA Fibers 68
4.2.12. Determination of Crosslinking Density for GLY Crosslinked PVA Fibers by Swelling 71
4.2.13. Removal of the Core from GLY Crosslinked PVA Fibers. 72
4.3. Fabrication and Characterization of Diisocyanate Crosslinked PVA Tubular Structures 73
4.3.1. Crosslinking Reaction of Poly(vinyl alcohol) with Hexamethylene Diisocyanate. 74
4.3.2. FTIR Characterization of PVA Fibers Reacted with HMDI in Different Solvents 74
4.3.3. Determination of Crosslinking Density for HMDI Crosslinked PVA Fibers by Swelling 84
4.3.4. Removal of the Core from HMDI Crosslinked PVA Fibers. 85
4.3.5. Parameters That Affect Tube Thickness in HMDI Crosslinked Fibers . 89
4.3.6. Dye Loading Properties of HMDI Crosslinked PVA Tubes 91
4.3.7. Dye Diffusion and Release Properties of the HMDI Crosslinked PVA Tubes 93
4.3.8. Contact Angle Measurements of HMDI Crosslinked Films 95
4.3.9. Crosslinking of Poly(vinyl alcohol) Nanofibers with HMDI 96
4.3.10. Crosslinking of PVA with Other Diisocyanates 97
4.3.11. Removal of the Core from IPDI and 2,4-TDI Crosslinked PVA Fibers. 101

4.4. Modification of Poly(vinyl alcohol) with Acryloyl Chloride or Alkoxysilane and Crosslinking of Modified Fibers with Mono- or Difunctional Hardeners. 102

4.4.1. Grafting of Acryloyl Chloride on PVA Fibers and FTIR Characterization of the Product 103

4.4.2. Grafting of 3-trimethoxysilyl propylmethacrylateon PVA Fibers and FTIR and SEM Characterization of the Product 104

4.4.3. Surface Photopolymerization of Modified PVA Fibers and Characterization of Fibers after Complete Dissolution of Templates . 108

5. CONCLUSIONS 111

REFERENCES 112

LIST OF FIGURES

Figure 1.1. Polyaniline nanomaterials prepared by emulsion polymerization. 2

Figure 1.2. The general structures of rod-coil block copolymers in solution. 3

Figure 1.3. Template-directed synthesis of tubular structures. 4

Figure 1.4. Polystyrene (PS) nanotubes prepared by wetting of ordered porous alumina membrane templates. 5

Figure 1.5. The common setup and working principle of electrospinning. 6

Figure 1.6. Schematic illustration of coaxial-electrospinning setup and fabrication process of core-shell fibers. 7

Figure 1.7. The TUFT process, general concept for the preparation of polymer tubes (a), polymer/metal hybrid tubes (b), and core-shell tubes (c). 8

Figure 1.8. Template polymer candidates: poly (L-lactide) (PLA) (a), poly(methylmethacrylate) (PMMA) (b), poly(ethyleneoxide) (PEO) (c), poly(tetramethylene adipamide) (PA) (d).Poly(vinylalcohol) (PVA) (e). . 9

Figure 1.9. SEM images of PPX tubes obtained by coating electrospun PLA fibers by CVD and subsequent degradation of PLA template fibers. 10

Figure 1.10. The general strategy used in fabrication of covalently crosslinked tubular structures.. 11

Figure 1.11. Conventional method for the synthesis of PVA. 12

Figure 1.12. Thermal degradation of poly(vinyl alcohol) in nitrogen atmosphere. . . . 13

Figure 1.13. Schematic representation of a hydrogel structure. 14

Figure 1.14. General mechanism for the reaction between aldehydes and alcohols. . . 16

Figure 1.15. Crosslinking reaction between PVA with glyoxal 17

Figure 1.16. Crosslinking reaction of PVA with glutaraldehyde 17

Figure 1.17. General reaction of PVA with isocyanate. 18

Figure 1.18. Crosslinking reaction of PVA with a diisocyanate. 18

Figure 1.19. Crosslinking reaction of PVA with sodium tetraborate.. 19

Figure 1.20. Crosslinking reaction of PVA with epichlorohydrin. 19

Figure 1.21. Esterification reaction between PVA and lactic acid. 20

Figure 1.22. Intermolecular (a) and intramolecular (b) esterification reactions between PVA and maleic acid. 20

Figure 1.23. Acryloyl chloride grafted PVA. 21

Figure 1.24. Examples of polymerizable monomers used for crosslinking of AC grafted PVA; 1,6-hexanedioldiacrylate (HDODA) (a), n-butylacrylate (nBA) (b), ethylene glycol dimethacrylate (EGDMA) (c), polyethylene glycol diacrylate (PEGDA) (d) and 2-hydroxyethyl methacrylate (HEMA) (e).. 21

Figure 1.25. General structure of an organoalkoxysilane. 22

Figure 1.26. Hydrolysis of an organoalkoxysilane. 22

Figure 1.27. Hybrid formation with PVA organic backbone and silane functionalized groups. 23

Figure 1.28. 3-trimethoxysilyl propylmethacrylate (MPS). 23

Figure 2.1. Schematic representation of the first strategy applied in the fabrication of covalently crosslinked polymeric tubes. 26

Figure 2.2. Schematic representation of the second strategy applied in the fabrication of covalently crosslinked polymeric tubes. 27

Figure 4.1. Morphologies of PVA nanofibers (a), and PVA microfibers (b). 40

Figure 4.2. FTIR spectra of neat PVA (a) and PVA crosslinked in 0.002M (b), 0.01M (c), 0.02M (d), 0.2M (e), 0.5M (f), and 1M (g) glutaraldehyde solutions.. 44

Figure 4.3. Expected crosslinked products by the reaction between PVA and GA. . . 45

Figure 4.4. Absorbance ratio of hydroxyl (3300 cm^{-1}) to a reference peak (2900 cm^{-1}) on crosslinked PVA with different GA content in reaction solution. 46

Figure 4.5. Absorbance ratio of aldehyde (1720 cm^{-1}) to a reference peak (2900 cm^{-1}) on crosslinked PVA with different GA content in reaction solution. 47

Figure 4.6. Absorbance ratio of the bands 1141 cm^{-1} to 1096 cm^{-1} on crosslinked PVA with different GA content in reaction solution. 48

Figure 4.7. Effect of different GA content in reaction solutions on the swelling of crosslinked PVA in water.. 50

Figure 4.8. TG curves of neat PVA fibers (a), PVA fibers crosslinked in 0.02M GA (b), 0.2M GA (c) solutions. 51

Figure 4.9. DTG curves of neat PVA fibers (a), PVA fibers crosslinked in 0.02M GA (b), 0.2M GA (c) solutions. 52

Figure 4.10. GA crosslinked PVA fibers after 1 min dissolution in water at 70°C (Scale: 100 μm, PVA fiber used was crosslinked by 0.2M GA solution). 53

Figure 4.11. GA crosslinked PVA tubes before (a) and after dialysis (b). 54

Figure 4.12. GA crosslinked PVA tubular structures after 2 min (a), 5 min (b), 10 min (c), 30 min (d) dissolution in water at 70°C 54

Figure 4.13. SEM images of the uncut (a) and cut GA crosslinked fibers (b) after dissolution. 56

Figure 4.14. GA crosslinked PVA tubes (a) and rolled tubular polymeric films (b) after too long dissolution in water at 70°C. 57

Figure 4.15. Cross sections of lightly crosslinked (a) and highly crosslinked PVA fibers (b) (Scale: 50μm).. 58

Figure 4.16. SEM images of crosslinked PVA polymeric tubes prepared in 0.02 M (a and b) and 0.2 M (c and d) glutaraldehyde solutions. 59

Figure 4.17. SEM images of the surface of PVA polymeric tubes crosslinked in 0.2M glutaraldehyde solutions. 60

Figure 4.18. Optical microscopy images of fluorescein loaded PVA polymeric tubes crosslinked in 0.02M and 0.2M glutaraldehyde solutions. 61

Figure 4.19. Initial dye concentrations of PVA polymeric tubes crosslinked in 0.02M and 0.2M glutaraldehyde solutions. 62

Figure 4.20. Plot of the released amount of fluorescein dye versus time for PVA polymeric tubes crosslinked in 0.02M and 0.2M glutaraldehyde solutions. 64

Figure 4.21. Effect of dye loading on the release from PVA tubular hydrogels crosslinked with 0.2M GA concentration. 64

Figure 4.22. SEM images of crosslinked PVA nanofibers in 0.02M (a) and 0.2M (b) glutaraldehyde solutions and their dissolved products, respectively (c and d). 67

Figure 4.23. FTIR spectra of neat PVA (a) and PVA crosslinked in 0.002M (b) and 0.01M (c) glyoxal solutions. 69

Figure 4.24. Expected crosslinked products by the reaction between PVA and GLY.....70

Figure 4.25. SEM images of crosslinked PVA fibers in 0.002M (a) and 0.1M (b) GLY solutions. 72

Figure 4.26. FTIR spectra of PVAcrosslinked with 0.1M HMDI solutions prepared in DMF (a), acetone (b), and toluene (c). 76

Figure 4.27. Expected products by the reaction between PVA and HMDI. 78

Figure 4.28. The reaction of isocyanates with moisture (water) and monomers with amine functionalities. 79

Figure 4.29. FTIR spectra of neat PVA (a) and PVA crosslinked in 0.01M (b), 0.04M (c), 0.1M (d), 0.2M (e), and 0.3M (f) HMDI solutions in dimethyl formamide. 81

Figure 4.30. Absorbance ratio of the peak at 3300 cm^{-1} to a reference peak (2900 cm^{-1}) on crosslinked PVA with different HMDI content in reaction solution.. 82

Figure 4.31. Absorbance ratio of the peak at 1693 cm^{-1} to a reference peak (2900 cm^{-1}) on crosslinked PVA with different HMDI content in reaction solution.. 82

Figure 4.32. Absorbance ratio of the peak at 1141 cm^{-1} to a reference peak (1090 cm^{-1}) on crosslinked PVA with different HMDI content in reaction solution. 83

Figure 4.33. Effect of different HMDI content in reaction solutions on the swelling of crosslinked PVA in water.. 85

Figure 4.34. TG curves of neat PVA fibers (a), PVA fibers crosslinked in 0.1M (b), 0.2M (c), and 0.3M (d) HMDI solutions.. 86

Figure 4.35. DTG curvesof neat PVA fibers (a), PVA fibers crosslinked in 0.1M HMDI (b), 0.2M HMDI (c), and 0.3M (d) solutions. 87

Figure 4.36. HMDI crosslinked PVA fibers after 1 min (a) and 5 min (b) 30 min (c) dissolution in water at 70°C (PVA fiber used was crosslinked by 0.2M HMDI concentration).. 88

Figure 4.37. SEM images of crosslinked PVA polymeric tubes in 0.01M (a), 0.04M (b), 0.1M (d), 0.2M (e), 0.3M HMDI solutions and bulk crosslinked fibers in 1M HMDI solution.. 90

Figure 4.38. SEM imageof the surface of PVA polymeric tubes crosslinked in 0.2MHMDI solutions (a) and optical microscopy image (b) of these tubes after loaded with fluorescein dye. 91

Figure 4.39. Initial dye concentrations of PVA polymeric tubes crosslinked in 0.1M, 0.2M and 0.3M HMDI solutions. 92

Figure 4.40. Plot of per cent release of fluorescein dye versus time for PVA polymeric tubes crosslinked in 0.1M, 0.2M and 0.3M HMDI solutions.. 94

Figure 4.41. Effect of dye loading on the fluorescein released from PVA tubular hydrogels crosslinked in 0.2M HMDI concentration.. 95

Figure 4.42. SEM images of crosslinked PVA nanofibers in 0.1M HMDI solution (a) and its product after water dissolution (b). 96

Figure 4.43. FTIR spectra of PVA (a) and PVA crosslinked in 0.2M IPDI (b) and 0.2M 2,4-TDI solutions in DMF.. 99

Figure 4.44. Expected products by the reaction between PVA and IPDI. 98

Figure 4.45. Expected products by the reaction between PVA and 2,4-TDI. 100

Figure 4.46. SEM images showing the surface of crosslinked PVA fibers in 0.2M IPDI solution before dissolution (a and b), after 2 min dissolution (c), after c omplete dissolution (d), and the surface of crosslinked PVA fibers (e) and film (f) in 0.2M 2,4-TDI solution before dissolution. . . 102

Figure 4.47. FTIR spectra of PVA (a) and acryloyl chloride grafted PVA (PVA-g-AC) (b) 105

Figure 4.48. Expected product after the grafting of 3-trimethoxysilyl propylmethacrylate on PVA. 104

Figure 4.49. FTIR spectra of PVA (a) and 3-trimethoxysilyl propylmethacrylate modified PVA (PVA-g-MPS) (b). 106

Figure 4.50. SEM images showing PVA fibers and their surface morphologies before (a and b) and after (c and d) 3-trimethoxysilyl propylmethacrylate modification 107

Figure 4.51. SEM images of dissolved PVA-*g*-AC fibers after dip coating with PEGDA (a), HDODA (b) and HEMA (c) (100 wt% each in 0.5M solution).. 109

Figure 4.52. SEM images of dissolved PVA-*g*-AC (a and b) and PVA-*g*-MPS (c and d) fibers after dip coating with HEMA/PEGDA(80/20) prepared in 1M solution.. 110

LIST OF TABLES

Table 3.1. Reaction conditions used in fabrication of GA crosslinked microfibers. 31

Table 3.2. Reaction conditions used in fabrication of GLY crosslinked microfibers. 34

Table 3.3. Reaction conditions used in fabrication of HMDI crosslinked microfibers. 36

Table 3.4. The ratios of photopolymerizable crosslinkers used as shell materials. . . 39

Table 4.1. Vibration band frequencies of PVA and GA crosslinked PVA. 43

Table 4.2. Effect of pH on swelling of PVA fibers crosslinked in 0.2M GA solution. 49

Table 4.3. Loading amount of PVA polymeric tubes crosslinked in 0.02M and 0.2M glutaraldehyde solutions. 61

Table 4.4. Effect of pH on release properties. 63

Table 4.5. Contact angles (θ) of PVA and GA crosslinked PVA films. 66

Table 4.6. Absorbance ratios of several FTIR bands belong to PVA, crosslinked PVA in 0.002 and 1M GLY solutions.. 71

Table 4.7. Vibration band frequencies of PVA and HMDI crosslinked PVA 80

Table 4.8. Effect of pH on swelling of PVA fibers crosslinked in 0.2M HMDI solution. 84

Table 4.9. The degradation temperatures and loss percentages of neat PVA fiber (a), PVA fibers crosslinked in 0.02M GA (b), 0.2M GA (c), 0.1M HMDI (d), 0.2M HMDI (e), and 0.3M HDI solutions. 87

Table 4.10. Loading amount of PVA polymeric tubes crosslinked in 0.1M, 0.2M and 0.3M HMDI solutions. 93

Table 4.11. Effect of pH on release percentage of dye from HMDI crosslinked PVA tubes 94

Table 4.12. Contact angle (θ)values of PVA and HMDI crosslinked PVA films. . . . 96

Table 4.13. Absorbance ratios of several FTIR bands belong to PVA and PVA-*g*-AC. 103

LIST OF ACRONYMS/ABBREVIATIONS

2,4-TDI	2,4-Toluene diisocyante
AC	Acryloyl chloride
ATR	Attenuated Total Reflectance
DMF	Dimethyl formamide
DTG	Differential Thermogravimetry
EtOH	Ethanol
FTIR	Fourier Transform Infrared
GA	Glutaraldehyde
GLY	Glyoxal
HCl	Hydrochloric Acid
HEMA	2-hydroxyethyl methacrylate
HDODA	1,6-hexanedioldiacrylate
HMDI	1,6-hexamethylene diisocyanate
IPDI	Isophorone diisocyanate
MPS	3-trimethoxysilyl propylmethacrylate
PEGDA	Poly(ethylene glycol) diacrylate
PVA	Poly(vinyl alcohol)
PVAc	Poly(vinyl acetate)
SEM	Scanning Electron Microscopy
TGA	Thermogravimetric Analysis
THF	Tetrahydrofuran
UV-Vis	Ultraviyolet-visible

1. INTRODUCTION

The design and fabrication of confinement structures such as spheres and tubes on micrometer and submicrometer scale have received great attention due to their potential applications in a broad range of areas such as electronics, sensors, seperation, catalysis, medicine, encapsulation and controlled release technology. Both inorganic (glass, ceramics, metals) and organic (polymers, biomolecules) materials have been processed with these dimensions. In particular, tubular objects in micro- and nanoscale have attracted special attention due to high anisotropy and their huge surface to volume ratio. Hollow polymeric tubes with such dimensions may be used to store or transport gasses or fluids, for applications in the area of catalysis, ion exchange microelectronics, drug release or even encapsulation [1-12].

1.1. Fabrication Methods of Tubular Structures

The generation of hollow polymeric structures, hollow tubes in particular, can be achieved through suspension or emulsion polymerization methods, self-assembly of macromolecules, template directed synthesis, electrospinning and combination of electrospinning and vapor deposition polymerization methods, among others.

1.1.1. Emulsion Polymerization

Emulsion polymerization is simple, economic, and environmentally friendly method used in fabrication of polymeric tubes. For instance, conducting nano and micron size tubes of polyaniline (PANi) and polypyrolle (PPy) can be prepared by this method [13, 14]. By adjusting the thermodynamic and kinetic parameters, micelles, with morphologies of spheres, hollow spheres and tubular structures can be obtained by emulsion polymerization (Figure 1.1) [15, 16].

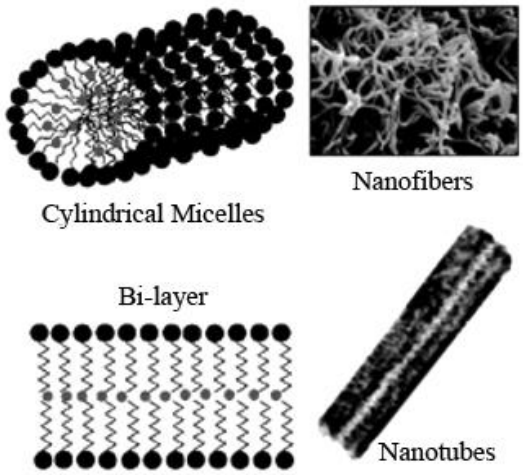


Figure 1.1. Polyaniline nanomaterials prepared by emulsion polymerization [17].

1.1.2. Self-assembly of Macromolecules

Polymeric tubes can be prepared *via* self-assembly of macromolecules such as amphiphilic and rod-coil block copolymers. Hydrophobic and hydrophilic parts can self-assemble into tubes by H-bonding and π-π interactions at a molecular level [18]. The morphology of self-assembled amphiphilic block copolymers is dictated by the lowest Gibbs free energy [19]. The free energy of self-assembly of amphiphilic diblock copolymers is contributed by the stretching energies of the surface (shell) and core chains, and the interfacial energy between the core and solvent [20, 21]. If core/solvent interfacial tension increases, stretching of the core and surface (shell) as well as micelle number and size will increase. Above a critical interfacial tension, spherical-to-cylindrical micelle transition occures [22].

Rod-coil block copolymers in coil-selective solvents micelles are formed with the rods packed in the core. Due to different packing geometries of the rods, the shape of micelles may be spherical, wormlike, or elliptical. As the rod length increases, tubular vesicles are preferred due to lower interfacial curvature. In rod-selective solvents rods are packed on the outside of the self-assembled structures. Tubular vesicles are formed in coil-rich systems due to increased interfacial area per coil block. When the coil block is small relative to the rod block, strong separation of the coil from the rod occurs and solvent results in segregation

of the coil into cores which forms spherical or wormlike micelles (Figure 1.2).

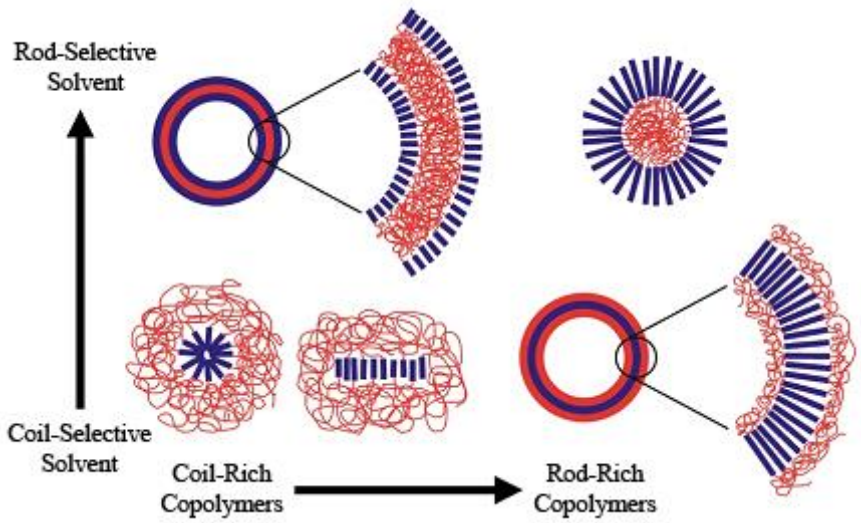


Figure 1.2. The general structures of rod-coil block copolymers in solution [23].

However, the formation of tubular structures by emulsion polymerization and self-assembly is influenced by too many factors and the dimension of these tubes is very hard to control and the preparation of long tubular structures is difficult.

1.1.3. Template-Directed Synthesis

Template-directed synthesis method has attracted tremendous attention in fabrication of tubular polymeric, inorganic and metal structures in various dimensions due to its generality and versatility [24-29].

The synthesis is carried out within the pores of a micro- or nanoporous template membrane. The membrane contains cylindrical pores with uniform diameters that extend through the entire thickness of the membrane. The most commonly used porous templates are alumina membranes. In addition, mesoporous silica membranes [30], mesoporous zeolites [31, 32] and “track-etch” polymeric membranes containing randomly distributed channels with uniform diameters have also been used as templates.

In this method when porous templates are brought into contact with polymer solutions or melts, a thin surface film will cover the pore walls in the initial stages of wetting since the cohesive driving forces for complete filling are much weaker than the adhesive forces [28]. Wall wetting and complete filling of the pores thus take place on different time scales. Complete filling of the pores can be prevented by thermal quenching in case of melts or solvent evaporation in case of solutions, resulting in the formation of tubular structures. If complete filling occurs, instead of tubular structures polymeric fibrils are obtained (Figure 1.3). Melt-processable polymers (e.g. polytetetrafluoroethylene, polystyrene, and polymethyl methacrylate etc.), blends or multi-component polymer solutions can be formed into tubes (Figure 1.4) [28, 33-35]. Due to its versatility, the template-directed synthesis method is also proved to be a promising approach for providing functionalized polymeric tubes.

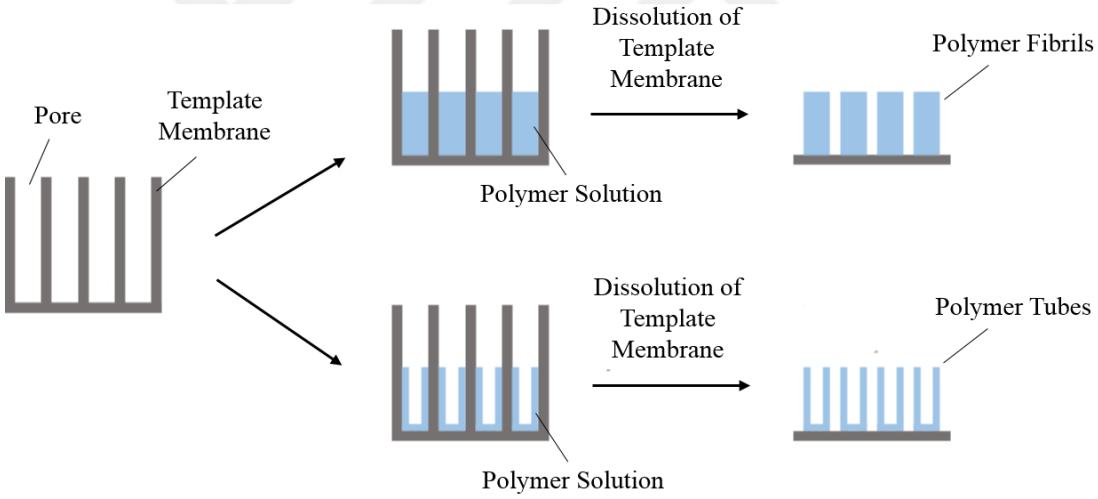


Figure 1.3. Template-directed synthesis of tubular structures.

Despite its versatile features, the template-directed synthesis method has some limitations, such as too low yield for practical applications, no free standing tubules due to the need of removal sacrificial templates which may lead to collapse of tubes synthesized, and limited tubule length by the membrane thickness.

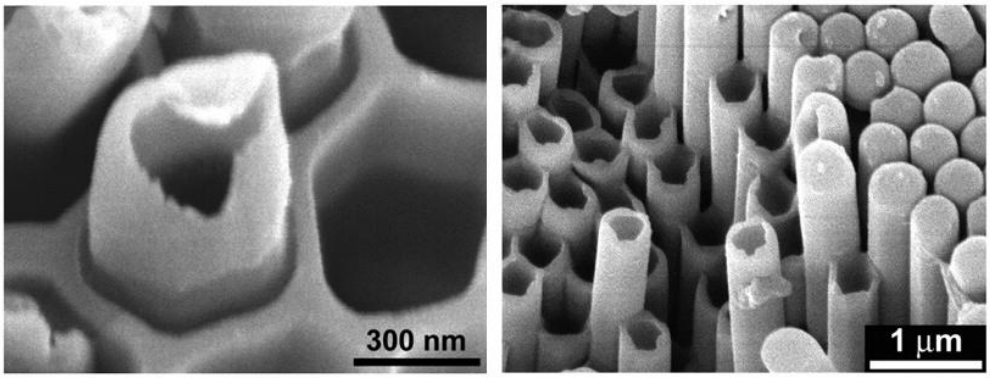


Figure 1.4. Polystyrene (PS) nanotubes prepared by wetting of ordered porous alumina membrane templates [28].

1.1.4. Electrospinning

Electrospinning (also called electrostatic spinning) provides a simple and versatile method for the large scale continuous fabrication of micro- and nanofibers with core-sheath, hollow or porous structures from a wide range of materials [36, 37]. It uses electrical charge to draw fine (on the micro or nano scale) fibers from a polymer solution or melt [38]. Electrospinning occurs when the applied electrical voltage exceeds a critical electrical potential at which the electrostatic force overcomes the surface tension of the polymer solution. The common setup and working principle is shown in Figure 1.5. A high voltage power supply creates a charge aggregation into the polymer solution or melt at the spinneret of syringe. Under pulling of electrostatic force, polymer liquid is drawn and got a "Taylor cone" at the end part of spinneret, then drawn out from spinneret as the "Liquid jet". Due to electrostatic repulsion of the charges in the polymer liquid, it is drawn thinner and thinner, as the fiber spin part. In this process, ultrathin fibers solidify or dry rapidly, and then fibers are collected on the "Collector".

The diameter and morphology of the fibers can be influenced by process variables [39] and solution properties [40] such as applied voltage, solution concentration, molecular weight of polymer, surface tension of solution, dielectric constant of the solvent, and solvent conductivity.

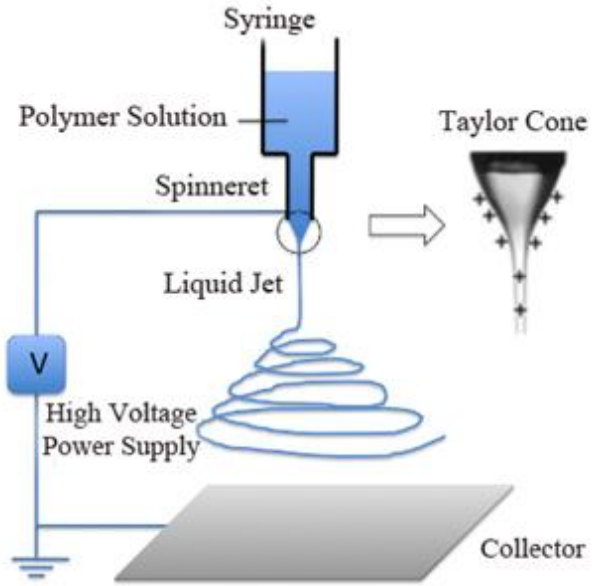


Figure 1.5. The common setup and working principle of electrospinning [41].

1.1.4.1. Co-axial Electrospinning. Core-sheath tubular structures can be prepared by coaxial spinning using concentric capillary spinnerets (Figure 1.6) [42]. The outer needle is attached to the container including the sheath solution and the inner needle is connected to the container holding the core solution. Under high voltage, the electrospinning liquid is drawn out from spinneret and forms a "Compound Taylor cone" with a core-sheath structure. The formation and fabrication of core-sheath fibers depend on the formation of core-sheath Taylor cone. In order to get a nice "Compound Taylor cone" it should be kept in dynamic stabilization which is achieved by adjusting injection speed of inner and outer fluids.

Polymeric microtubes by coaxial electrospinning of polycaprolactone core and poly(ethylene oxide) shell solutions was reported [43]. Evaporation of the core solution through the shell allows the formation of tubular structures.

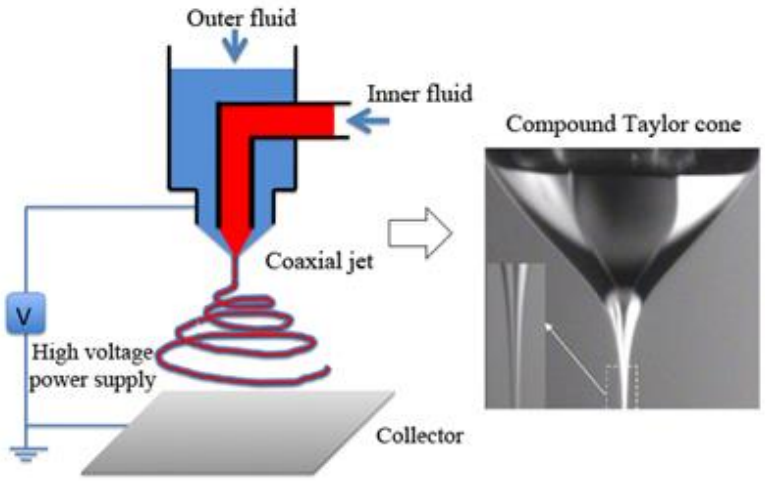


Figure 1.6. Schematic illustration of coaxial-electrospinning setup and fabrication process of core-shell fibers [41].

1.1.5. Tubes by Fiber Templates (TUFT Process)

Tubular structures have also been prepared by a combination of electrospinning and several deposition polymerization techniques. A fiber-based template technique which can be used in fabrication of polymer, metal and hybrid meso- and nanotubes in a large scale was reported [2,44]. The method is termed as TUFT process (Tubes by Fiber Templates). The general concept is to coat thin degradable polymer fibers with the desired wall materials using various deposition techniques. Tubes are formed after selective removal of the core material by thermal decomposition, solvent extraction or irradiation (Figure 1.7).

TUFT process mainly consists of three crucial steps:

- Preparation of degradable or dissolvable polymer template fibers by electrospinning
- Surface modification of template fibers with desired wall materials by different deposition techniques. This happens frequently by vapor phase deposition of polymers, metals, or glass [2]
- Removal of polymer template fibers by heat treatment, dissolving in selective solvents or irradiation

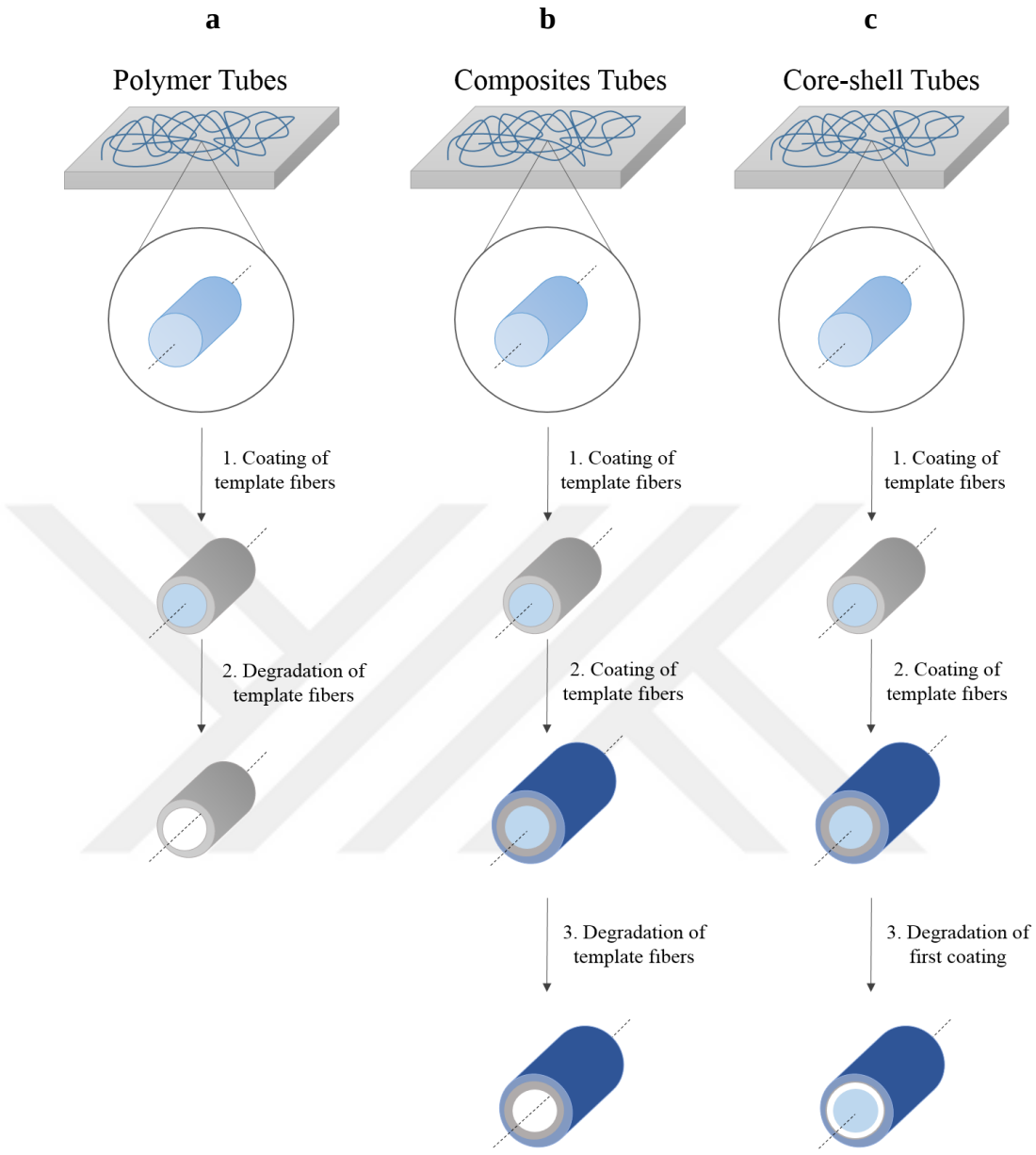


Figure 1.7. The TUFT process, general concept for the preparation of polymer tubes (a), polymer/metal hybrid tubes (b), and core-shell tubes (c).

The TUFT process has many advantages over the other techniques. It can produce tubular structures in a large scale; it enables to fabricate free-standing polymeric tubes or tubular webs; the inner diameter of the tubes can be manipulated in a broad range from a few nanometer to several microns; the tube length and the wall thickness can be controlled at will depending on the amount of the coating material.

1.1.5.1. Template Fibers. The approach of using electrospun polymer fibers as templates provides great versatility for the design of tubular structures with controlled dimensions [45]. The inner diameter of the polymer tubes prepared by this method depends on the diameter of the template fibers. In order to be used in TUFT process the template polymeric fibers should be prepared from fiber processable polymers, stable in coating conditions, solvent-extractable or thermal degredable at a lower temperature than the decomposition temperature of the wall materials. Some fiber template candidates are shown in Figure 1.8.

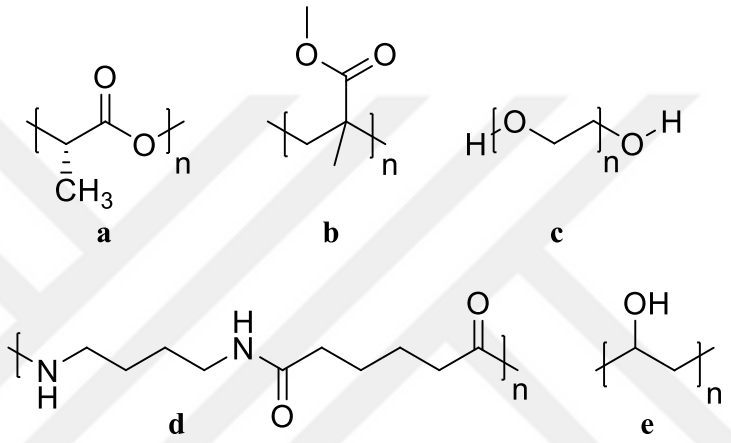


Figure 1.8. Template polymer candidates: poly (L-lactide) (PLA) (a), poly(methyl methacrylate) (PMMA) (b), poly(ethyleneoxide) (PEO) (c), poly(tetramethylene adipamide) (PA) (d).Poly(vinylalcohol) (PVA) (e).

The selection of template core polymer is critical to the process. There are many available core polymer template candidates which can be electrospun into fibers and extracted with suitable solvents or thermally degraded under heat. A key requirement is that core fibers should be stable during coating but should degrade or dissolve under the conditions that leave the wall material intact. For instance, poly(ethyleneoxide) (PEO) and poly (L-lactide) (PLA) are selected as suitable template fibers since they can be extracted in chloroform or they can be removed from the core by means of thermal degradation since they have a relatively low decomposition temperature of 235-255°C [46, 54]. Poly(tetramethylene adipamide) (PA) and poly(methyl methacrylate) (PMMA) are the other core material candidates that can be romoved by formic acid extraction [47, 52] and poly(vinyl alcohol) (PVA) which can be removed either by thermal decomposition or by dissolving in water.

1.1.5.2. Wall Materials. Different types of materials such as metal, ceramic, glass, semiconductor and polymers can be used as wall materials in TUFT process. Since polymer tubes are not as brittle as metal or glass tubes and can be easily functionalized, they are desirable for a broad range of applications. Wall materials should remain intact during removal process of template fibers. For instance, gold and aluminum coated fibers can be prepared by physical vapor deposition of the metal [38]. Further pyrolysis of aluminum coated fibers resulted in Al_2O_3/Al hybrid tubes. Glass or TiO_2 coated fibers are obtained via sol-gel technique [48]. Poly(p-xylene) (PPX) can be an ideal wall material which is applied on fibers by chemical vapor deposition technique (CVD) [44]. PPX tubes obtained by coating electrospun PLA fibers by CVD is shown in Figure 1.9. PPX has good thermal stability (melting point at about 420^{o}C) and excellent chemical inertness against all kinds of reagents and solvents which make easy to remove template fibers without any problem. Another important advantage of PPX coating is that it can form pin-hole coating layers on polymer template fibers with uniform thickness. Because PPX formation by CVD is quantitative, it is possible to adjust the thickness of PPX coating by controlling the amount of starting materials.

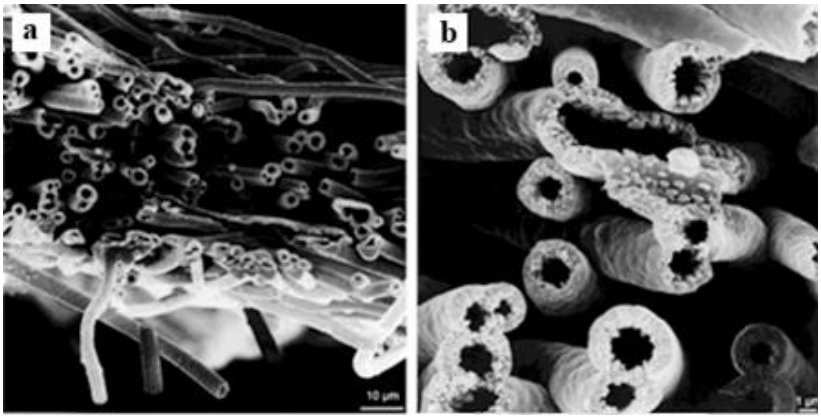


Figure 1.9. SEM images of PPX tubes obtained by coating electrospun PLA fibers by CVD and subsequent degradation of PLA template fibers [45].

1.1.6. Covalently Crosslinked Polymeric Tubes by Fiber Templates

In all of the literature examples using TUFT process in fabrication of tubular structures there is no covalent interaction between template fibers and wall materials. Fiber templates

have been used as solid supports for materials that form the outer layer (shell). In this study the fabrication of covalently crosslinked polymeric tubes by using functional fiber templates has been shown. As a general concept, the outer surface polymer chains of thin functional fibers are crosslinked and the unreacted core is selectively removed. Tubular structures essentially the same diameter as the fiber are formed. This study is the first example that uses functional groups of template fiber itself to get a crosslinked shell. The general strategy is depicted in Figure 1.10.

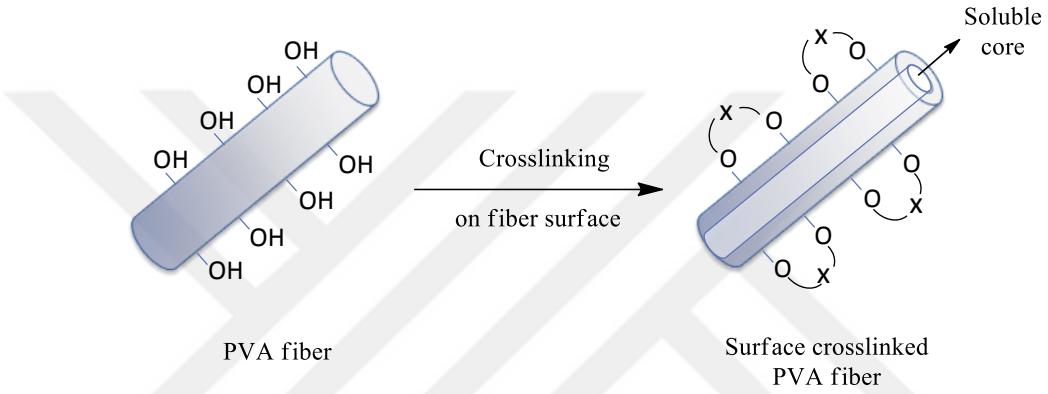


Figure 1.10. The general strategy used in fabrication of covalently crosslinked tubular structures.

The main advantage of this method is that it enables the fabrication of crosslinked polymeric tubes having various amount of crosslinking densities showing hydrogel properties. The shells of these tubes will show a hydrophilicity difference which may lead to interesting applications. The inner side of the tubes will include more unreacted –OH functional groups which makes inner core more hydrophilic then the tube shell.

1.2. Poly(vinyl Alcohol)

Among a variety of polymers poly(vinyl alcohol) (PVA) is a suitable candidate due to its solubility in water, thermal degradability at sufficiently low tempatures, its excellent electospinning or melt spinning processable properties, chemical resistance, -OH functional groups and good mechanical properties.

PVA is a hydrophilic, nontoxic, biocompatible, and semicrystalline polymer derived from hydrolysis (or alcoholysis) of poly (vinyl acetate) (PVAc) (Figure 1.11) [49-51]. In practise acetate hydrolysis is not complete and both hydroxyl and acetate groups exist on the backbone. Poly(vinyl alcohol-co-vinyl acetate) is represented by a proportion in mol per cent "m" and "n-m", respectively [52].

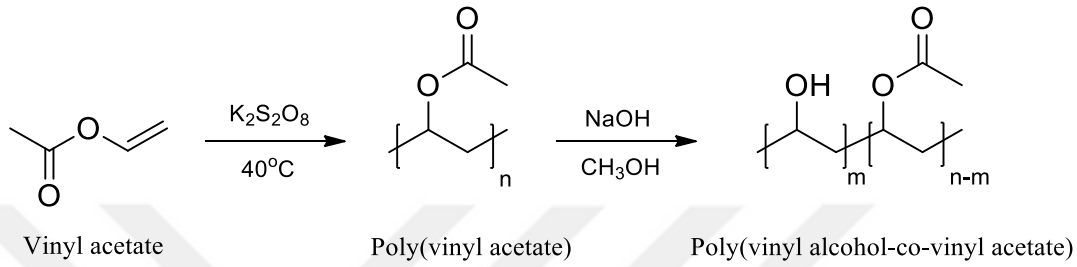


Figure 1.11. Conventional method for the synthesis of PVA.

Commercial PVA is available in highly hydrolyzed (degree of hydrolysis about 91 to 99 per cent) and partially hydrolyzed grades (degree of hydrolysis from 87 to 89 per cent). The degree of hydrolysis (DH) or the content of acetate groups in PVA affects its chemical properties, crystallizability, and solubility [53, 54]. The partially hydrolized grade contains residual acetate groups which reduces the degree of crystallinity, lowers the melting point, gives a greater aqueous solubility, increases its ability to adhere to hydrophobic surfaces. Conversely, highly hydrolyzed grades have a high degree of crystallinity, a low aqueous solubility (require 90°C for 30 min for a complete dissolution), improved stability in organic solvents and adhesion onto hydrophilic surfaces [55]. PVA with DH between 87-89 per cent has lower mechanical and water resistance than a PVA with DH between 98 and 99.9 per cent. Consequently, the potential to interact with other polar monomers or polymers would be expected to vary as a function of DH.

PVA can be easily processed into fibers and films with desirable hydrophilicity and biocompatibility.

The dissolution of PVA depends on the nature of the solvent, the temperature and the extent of hydrolysis in the polymer and molecular weight. PVA fibers and films used in this study have DH between 88 and 98 per cent and molecular weight around 88000-98000

g/mol. Therefore, they are completely soluble in water and partially soluble in DMSO and DMF at 90°C. On the other hand, they are not soluble in solvents like ethanol, toluene, tetrahydrofuran, and dichloromethane. Water solubility of PVA makes it an ideal candidate for use in the tube formation scheme shown in Figure 1.10.

Thermal decomposition of PVA fibers under nitrogen atmosphere is shown in Figure 1.12. PVA starts to decompose at 240°C and the decompostion rate reaches a maximum value at 430°C. Due to low decompositon temperature thermal degradation as well as solvent extraction may be a way to remove template fibers.

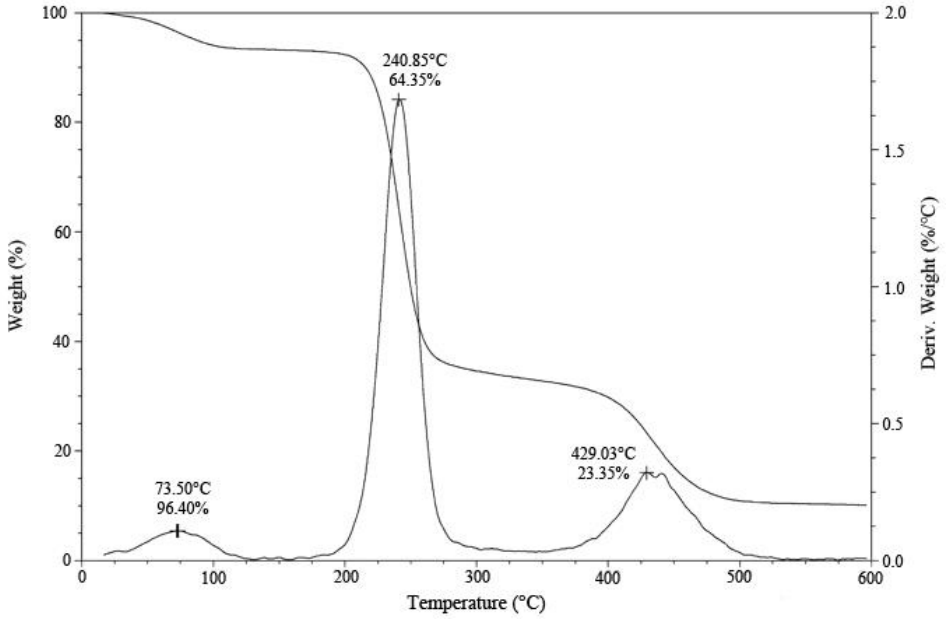


Figure 1.12. Thermal degradation of poly(vinyl alcohol) in nitrogen atmosphere.

1.3. Modifications of PVA

PVA is an excellent candidate to be used as template fibers because its abundant hydroxyl groups on its backbone can be crosslinked by physical or chemical methods with multifunctional crosslinking agents. The same hydroxyl groups can be readily modified to attach growth factors, adhesion proteins, or other biologically active molecules [56-58]. Crosslinking as well as modification of PVA through its hydroxyl groups can further bring new application areas for this material. One such outcome is the formation of PVA

hydrogels, which have been widely investigated for biomedical and biotechnological applications [59-64].

There are many studies showing the objective of evaluating the uses of PVA hydrogels in the area of controlled release drug delivery [52, 65-67]. Hydrogels are crosslinked polymers which are glassy in dehydrated state but swell to become an elastic gel upon water penetration. Physical properties of hydrogels are similar with human tissues due to high water capacity and low interfacial tension with water and biological fluids [68, 69]. If a drug is entrapped within the swelling matrix, it will dissolve and diffuse out through the swollen network into surrounding aqueous environment. Such schemes are used in controlled delivery of drugs. General representation of a hydrogel structure is shown in Figure 1.13.

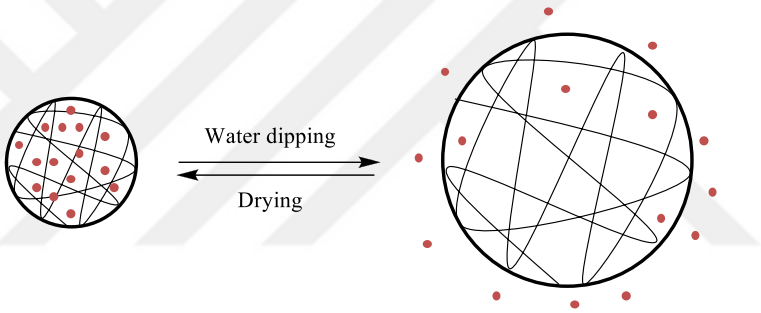


Figure 1.13. Schematic representation of a hydrogel structure.

1.4. Physical Crosslinking of PVA

The physical modification results in a molecular rearrangement on PVA chains forming high tacticity crystalline regions. This crosslinking technique is used where toxic residual crosslinking agents are avoided [70, 71]. The main physical modifications reported in the literature are freeze-thawing, heat-treatment or annealing, irradiation, and composite formation.

1.4.1. Freeze-thawing

PVA molecules can form intra- and inter-chain hydrogen bonds when dissolved in water. In this technique PVA aquous solution is submitted to freezing and thawing

cycles. By repeated freezing-thawing process, insoluble PVA can be obtained, probably due to the formation of inter-chain hydrogen bonding and the presence of new crystalline regions that act as crosslinks [72, 73].

1.4.2. Heat-treatment or Annealing

This process involves heating of an aquous solution of polymer followed by slow cooling until a complete evaporation of solvent is achieved. Heat-treatment or annealing of PVA at elevated temperatures can form crystallities, which serve as physical crosslinks [74].

1.4.3. Irradiation

The use of electron beam or gamma irradiation of aqueous solutions of PVA to obtain crosslinked, water-insoluble hydrogels is a well-known and documented technique [74-76]. Irradiation has been shown to be also useful for crosslinking water-swollen PVA films [77]. $H\cdot$ and $OH\cdot$ radicals from water molecules abstract the H atom(s) from $-CH_2$ and/or -CH(OH) groups of PVA to form the polymer radicals. The crosslinked network results from the coupling reaction of produced polymer radicals. Since oxygen is believed to cause the degradation of PVA during irradiation, the crosslinking reaction should be performed in the absence of dissolved oxygen [78].

1.4.4. Composite Formation

Composites of PVA with other polymers like polyethylene oxide, starch, gelatin, poly(lactic acid) and acrylonitrile butadiene styrene/polyethylene wax form homogenous blends where interaction forces are generated at a particle level. Intermolecular complexation among molecules with secondary binding forces, such as Coulomb forces, hydrogen bonding, Van der Waals forces, charge-transfer interactions restrict the mobility of polymer chains resulting in formation of composites of PVA which improves physicochemical properties [79, 80].

1.5. Chemical Crosslinking of PVA

PVA functionalization or crosslinking by chemical modifications has become very attractive since all multifunctional compounds capable of reacting with hydroxyl groups can be used to obtain tridimensional networks in PVA [81, 82]. The great accessibility and reactivity of PVA is attributed to its geometric conformation and its interaction with the solvent used. With this method toxic residues from reagents used could remain in the final crosslinked products.

1.5.1. Radical Formation

In this process polymerization reaction is initiated with a free radical generator. The free radicals are bonded to PVA, leading to an internal polymerization which increases molecular weight and hydrophobicity. Due to the presence of radicals which may have toxic effects in the final product, this reaction is not prefered [75, 83].

1.5.2. Reaction with Aldehydes

It is well known that hydroxyl groups of PVA react with aldehydes in acidic medium *via* formation of acetal bonds [84, 85]. By addition of an alcohol to the carbonyl group of an aldehyde a hemiacetal, an intermediate specie, is formed which then becomes an acetal after the addition of a second alcohol molecule. The general reaction is shown in Figure 1.14.

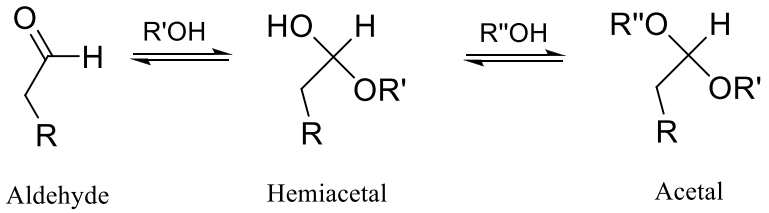


Figure 1.14. General mechanism for the reaction between aldehydes and alcohols.

1.5.3. Reaction with Dialdehydes

The reaction between a dialdehyde and hydroxyl groups of PVA is carried out in acidic medium under mild conditions. This reaction occurs *via* acetal bond formation and this happens twice for each aldehyde end present to give stable 6-membered cyclic acetals [86, 87]. Common dialdehydes used as crosslinking agents for PVA are glyoxal (Figure 1.15) and glutaraldehyde (GA) (Figure 1.16).

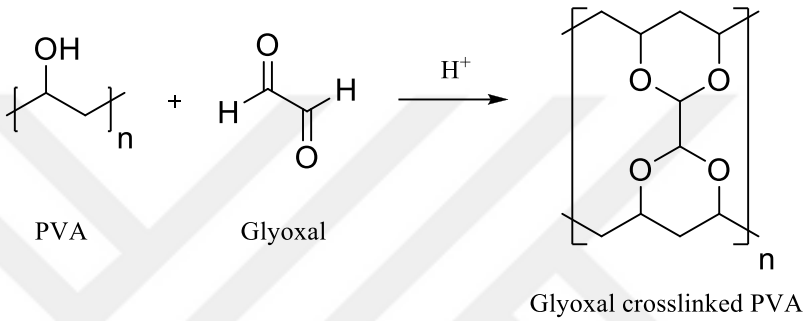


Figure 1.15. Crosslinking reaction between PVA with glyoxal.

There are two possibilities in the reaction between GA and PVA. Both aldehyde groups of GA may react with PVA to form intermolecular (a) and/or intramolecular (b) crosslinks, either makes PVA insoluble. Only one aldehyde end may react with PVA and the other may remain unreacted (c) (Figure 1.16).

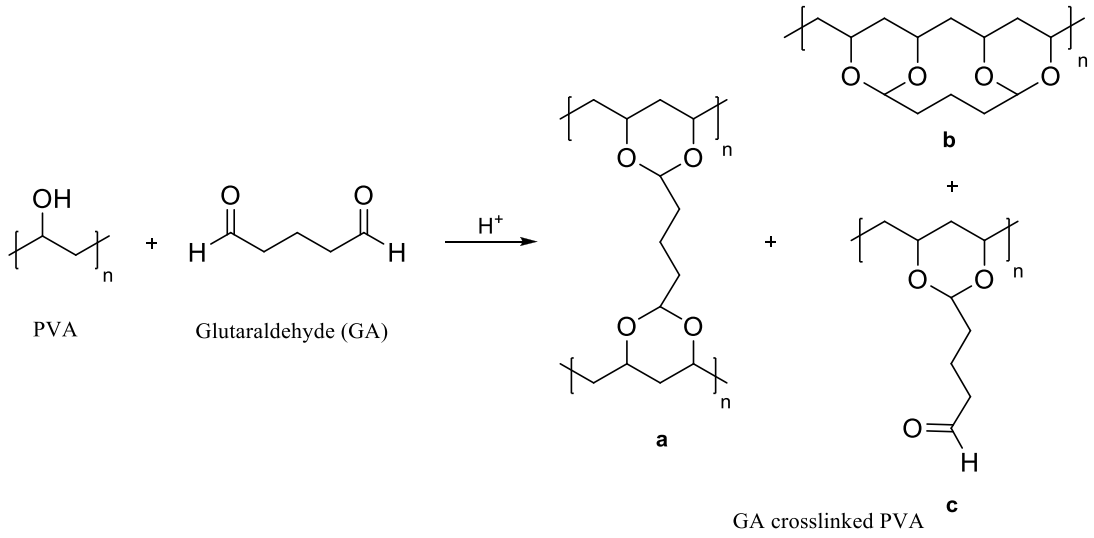


Figure 1.16. Crosslinking reaction of PVA with glutaraldehyde.

1.5.4. Reaction with Diisocyanates

Alcohols react with isocyanates to form carbamates is a well known reaction (Figure 1.17). Therefore, crosslinking of PVA may be achieved by reacting hydroxyl groups along the polymer chain with diisocyanates. The crosslinking happens when two isocyanate ends react with PVA via formation of urethane bridges. The reaction results in the formation of intermolecular (a) and/or intramolecular crosslinks (b), shown in Figure 1.18. The resulting membranes were insoluble in common polar or nonpolar solvents, indicating their crosslinked nature [88]. Unlike dialdehydes, if only one end of isocyanate react with PVA there will be no crosslinking reaction.

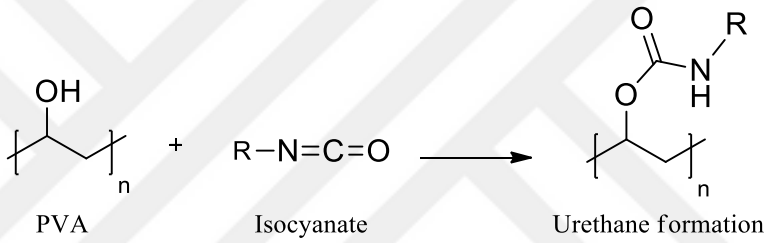


Figure 1.17. General reaction of PVA with isocyanate.

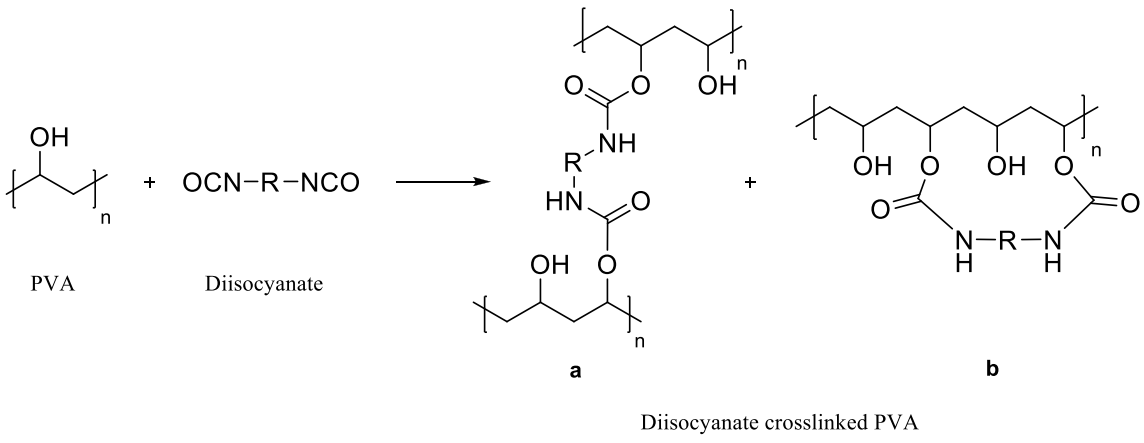


Figure 1.18. Crosslinking reaction of PVA with a diisocyanate.

1.5.5. Reaction with Sodium Tetraborate

PVA reacts with sodium tetraborate and forms a cyclic compound (Figure 1.19). The reaction is very sensitive to pH of the aquous medium and the concentration of sodium tetraborate [89].

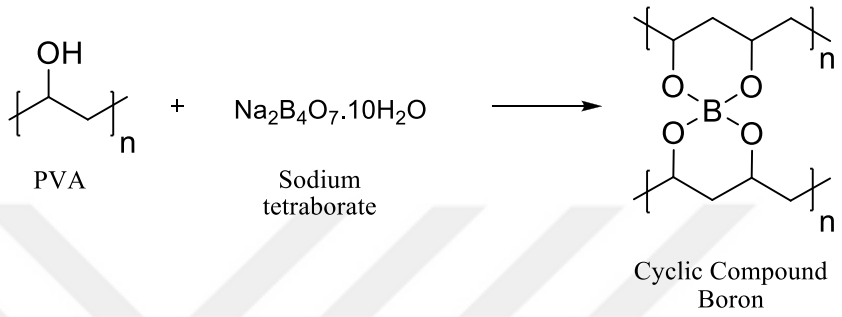


Figure 1.19. Crosslinking reaction of PVA with sodium tetraborate.

1.5.6. Reaction with Epichlorohydrin (EPC)

Epichlorohydrin (EPC) acts as a bifunctional molecule toward hydroxyl groups under basic conditions (Figure 1.20) [90].

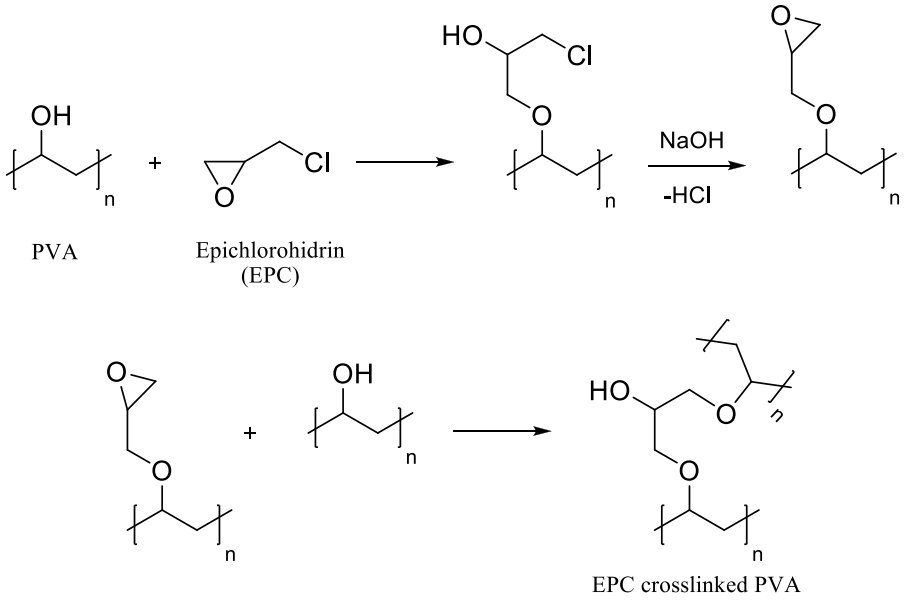


Figure 1.20. Crosslinking reaction of PVA with epichlorohydrin.

1.5.7. Reaction with Polycarboxylic Acids

The reaction between a carboxylic acid and an alcohol is known as esterification and leading to the formation of an ester. Lactic acid (Figure 1.21), maleic acid (Figure 1.22) [91], sulfosuccinic acid [92], acrylic acid and methacrylic acid [93] are the most common used acids to fabricate crosslinked hydrogels with PVA.

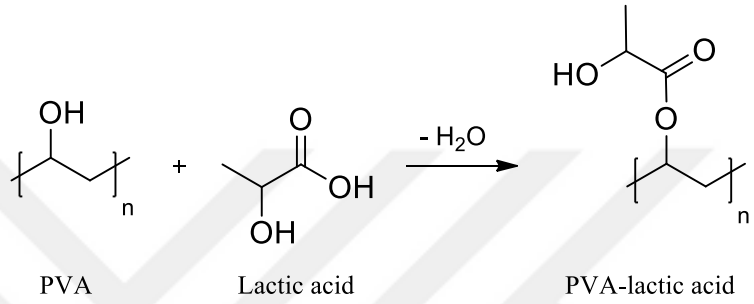


Figure 1.21. Esterification reaction between PVA and lactic acid.

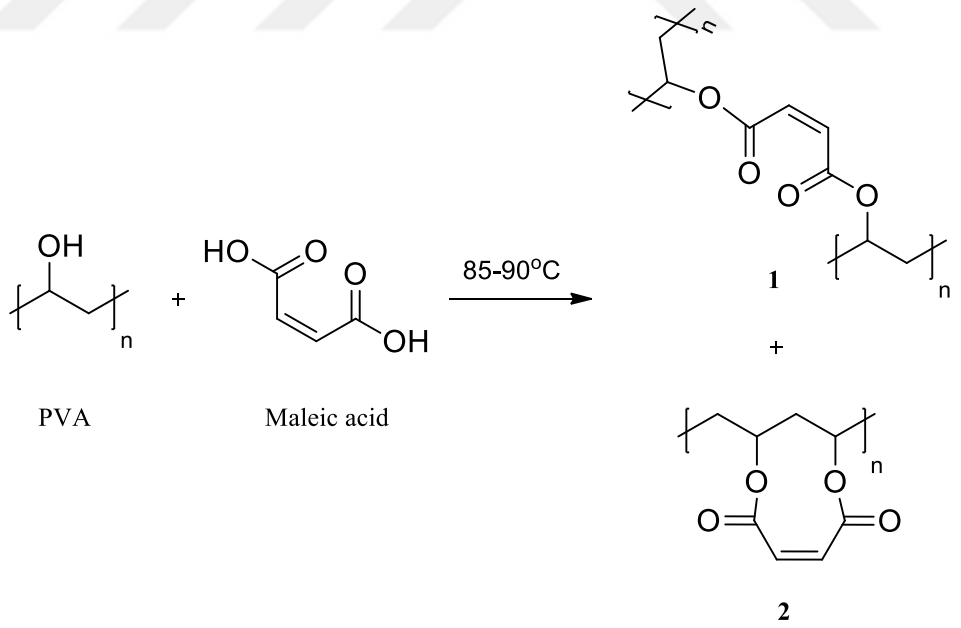


Figure 1.22. Intermolecular (a) and intramolecular (b) esterification reactions between PVA and maleic acid.

1.5.8. Reaction with Acid Chlorides

The esterification reaction of acryloyl chloride with PVA is shown in Figure 1.23. Photoreactive PVA can be prepared by grafting photo-crosslinkable groups on the pendant hydroxyl groups [94].

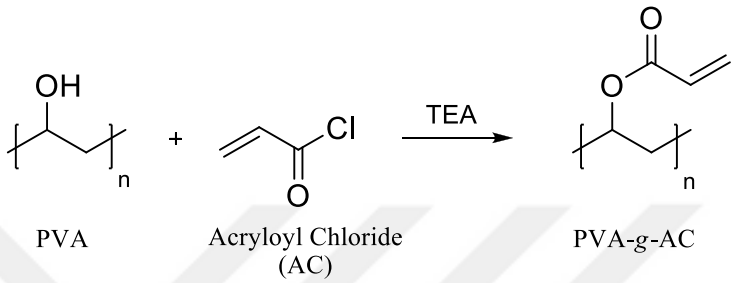


Figure 1.23. Acryloyl chloride grafted PVA.

Photoreactive PVA derivatives form crosslinked hydrogels with other double bond functionalized monomers within minutes in the presence of a non-toxic photoinitiator upon exposure to long wavelength ultraviolet light (UV). Some examples of photo-polymerizable monomers are shown in Figure 1.24. Furthermore, unreacted pendant hydroxyl groups provide sites for further crosslinking or the attachment of bioactive molecules, such as peptides, to signal cell attachment, proliferation, differentiation, or migration [95, 96].

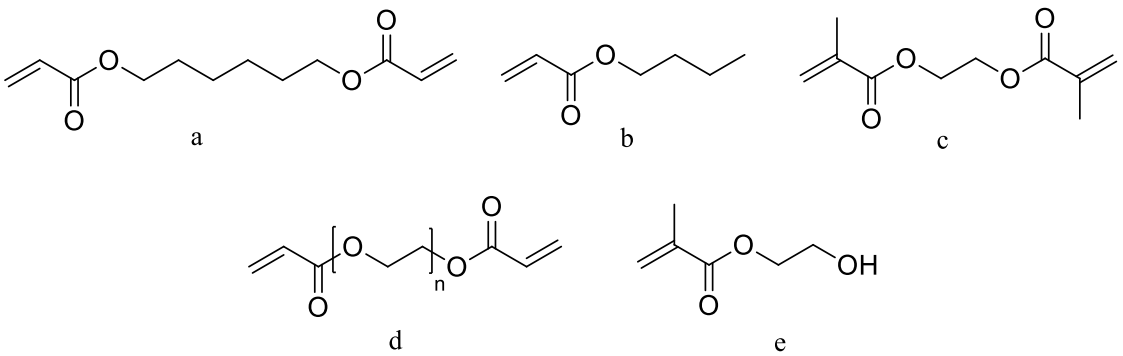


Figure 1.24. Examples of polymerizable monomers used for crosslinking of AC grafted PVA; 1,6-hexanedioldiacrylate (HDODA) (a), n-butylacrylate (nBA) (b), ethylene glycol dimethacrylate (EGDMA) (c), polyethylene glycol diacrylate (PEGDA) (d) and 2-hydroxyethyl methacrylate (HEMA) (e).

1.5.9. Reaction with Alkoxysilanes

Hybrid formation of PVA with organoalkoxysilanes such as tetraethoxysilane (TEOS), 3-mercaptopropyltrimethoxysilane (MPTMS) and 3-glycidoxypropyltrimethoxysilane (GPTMS) in acidic medium was reported in the literature [97]. The interaction between organic and inorganic phases occurs at nano or molecular scale resulting in nanocomposites with large interfaces [98]. These composites have the properties of both organic polymers and silica, so called hybrid organic-inorganic materials. They are also termed as 'ceramers' and 'ormosils' (organically modified silicates) or 'ormocers' (organically modified ceramics). Figure 1.25 shows the general structure of an organoalkoxysilane.

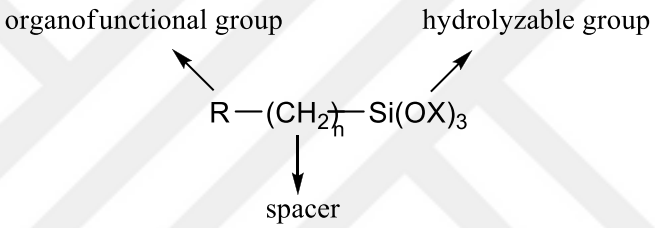


Figure 1.25. General structure of an organoalkoxysilane.

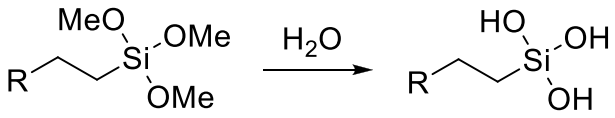


Figure 1.26. Hydrolysis of an organoalkoxysilane.

Silanol ends of hydrolized organoalkoxysilanes (Figure 1.26) readily available to condense with PVA chains and with themselves as shown in Figure 1.27. By modifying PVA surface with an organoalkoxysilane having double bond functionality such as 3-trimethoxysilyl propylmethacrylate (Figure 1.28) photoreactive PVA derivatives can be prepared.

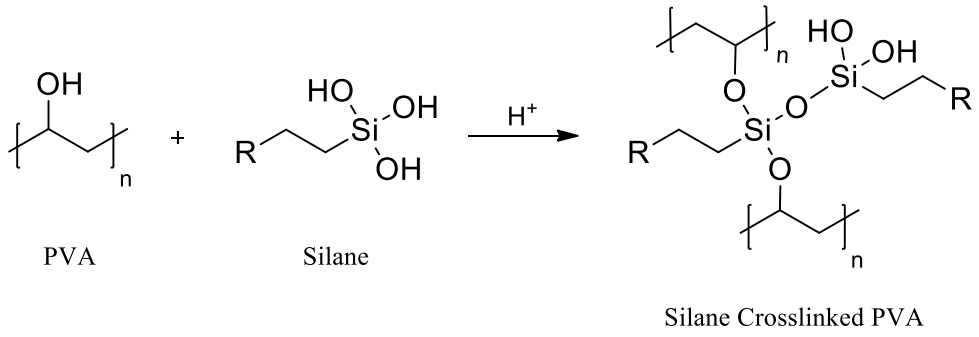


Figure 1.27. Hybrid formation with PVA organic backbone and silane functionalized groups.

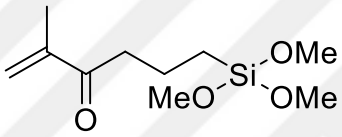


Figure 1.28. 3-trimethoxysilyl propylmethacrylate (MPS).

2. RESEARCH OBJECTIVES

The aim of this study is to demonstrate the fabrication of covalently crosslinked polymeric microtubes by using poly(vinyl alcohol) (PVA) fiber templates. Compared to the other fiber template methods reported in the literature, in this study PVA fibers are not only used as solid supports but also their reactive sites are used to design the shells of tubular structures.

The general concept for the formation of tubular structures is to take hydroxyl functional PVA template fibers and selectively crosslink only their surface polymer chains and finally remove unreacted core. This is the first example that uses reactivity of fiber templates to get a crosslinked shell having a hydrophilicity difference which may lead to interesting applications. The outer shell of the tubes obtained by this method is expected to have a relatively hydrophobic property while the inner side of the shells are more hydrophilic due to high concentration of unreacted hydroxyl groups located on the inside walls. Two strategies will be applied for the crosslinking of PVA fiber templates which are depicted in Figure 2.1 and Figure 2.2.

In the first strategy difunctional crosslinkers such as dialdehydes or diisocyanates are absorbed onto the surface of PVA fibers, and reacted to get a crosslinked outer shell and an unreacted inner core which can be removed after surface reaction is completed (Figure 2.1).

The second strategy is to functionalize PVA fiber surface with polymerizable monomers and react the grafted PVA fiber with other mono and/or difunctional reactive monomers to get water insoluble crosslinked network on the fiber surface and after the removal of unreacted PVA core to fabricate polymeric hollow structures (Figure 2.2, X represents a PVA reactive group). For functionalization of PVA fibers the monomers should have two ends; a PVA reactive end which is used to graft PVA chains and a photopolymerizable end, usually an acrylate, which will be used for further crosslinking.

In both of these two strategies it is crucial to keep the reaction only on the surface. PVA fibers should be stable during grafting and crosslinking reactions. Solvent used in these

reactions should not dissolve fiber templates. However, unreacted inner core should be removed under conditions that leave the crosslinked shell intact. Since crosslinked shell is covalently bonded to PVA fiber, for easy dissolution the shell should swell and be flexible to allow water penetration inside which is necessary for complete removal of the core. The system has been designed by taking into account all of these parameters.

The shells of tubular structures formed will be characterized in terms of crosslinking and thickness. Due to their surface properties, the shells are expected to behave like hydrogel materials. Therefore, the possibility of these hollow structures to be used in entrapment and release of molecules will be investigated, using flourescein dye as a model imaging molecule.

In general microfibers have been used in this study. However, the technique and crosslinking reactions which are applicable on microfibers will be investigated in order to check the applicability of this method for nanofibers.

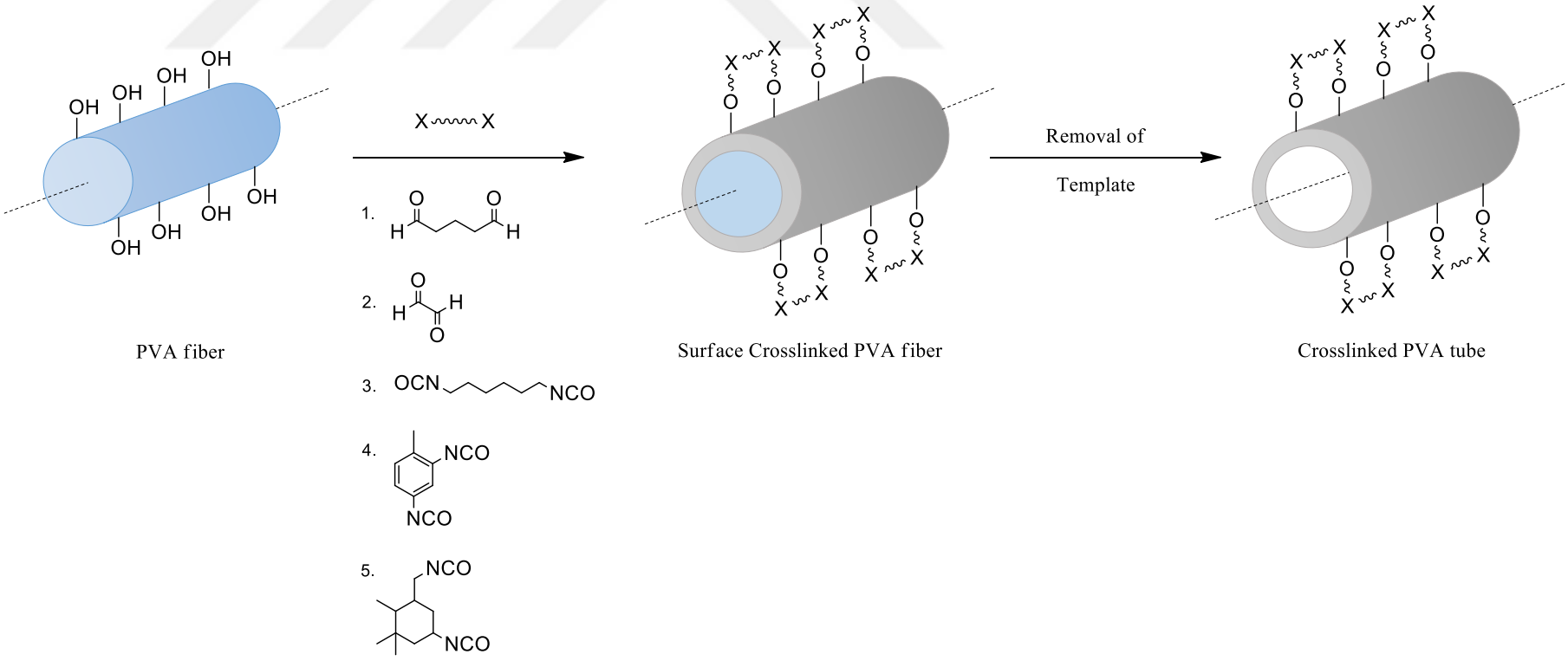


Figure 2.1. Schematic representation of the first strategy applied in the fabrication of covalently crosslinked polymeric tubes.

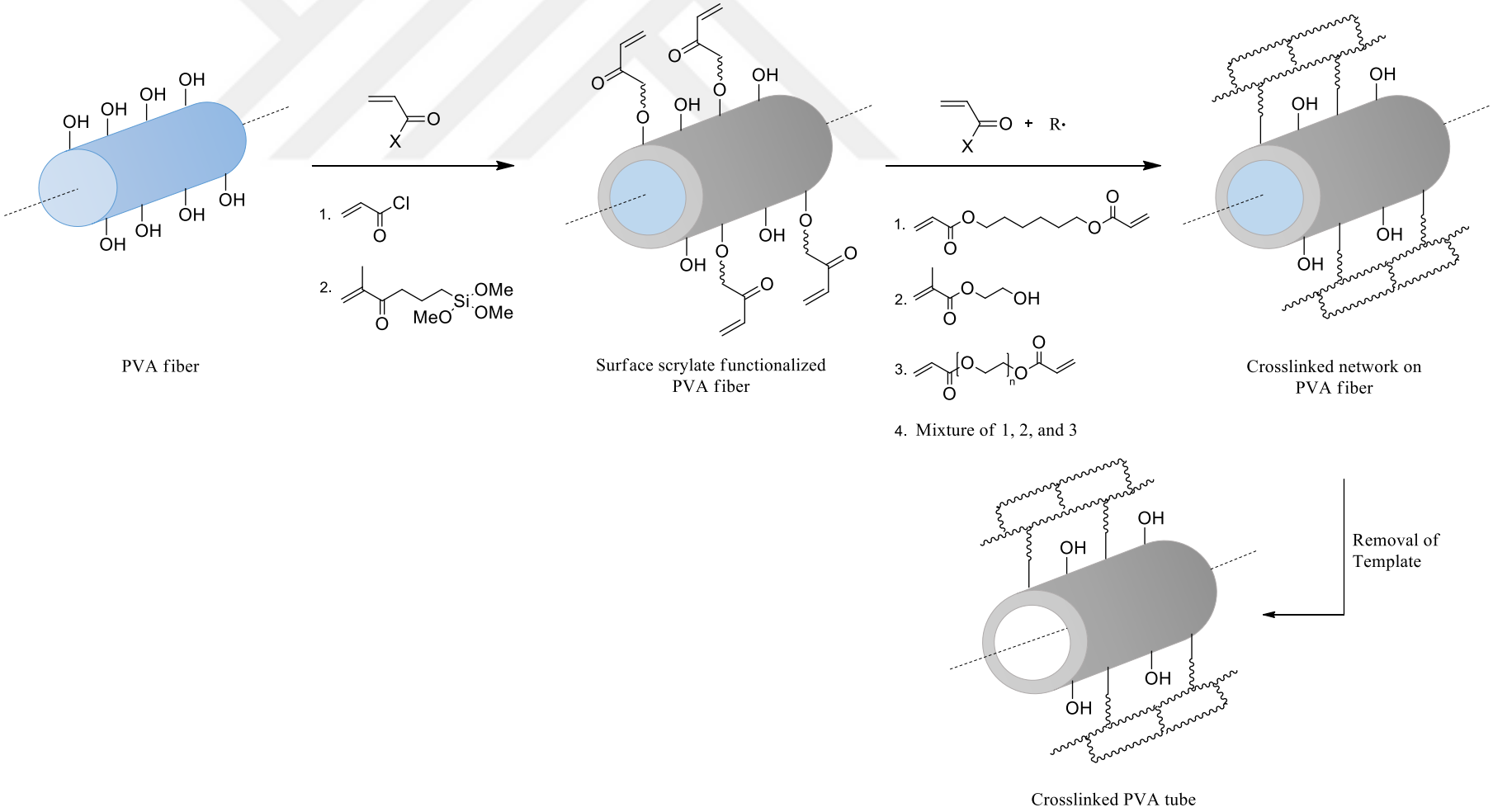


Figure 2.2. Schematic representation of the second strategy applied in the fabrication of covalently crosslinked polymeric tubes.

3. EXPERIMENTAL

3.1. Materials and Apparatus

3.1.1. Materials

Poly(vinyl alcohol) (PVA) microfibers and nanofibers were obtained from Beijing Guanghui Textile Co., LTD (China) and Prof. Uslu research group (Turkey), respectively. 98 per cent hydrolyzed PVA powder was purchased from Aldrich (U.S.). The solvents ethanol, dichloromethane, tetrahydrofuran, dimethylformamide, acetone were supplied by Merck (Germany) and used as received. Glutaraldehyde (25 per cent in water) and glyoxal solution (40 per cent in water), Irgacure 651, 2-hydroxyethyl methacrylate, poly(ethylene glycol) diacrylate (Mn=575), 1,6-hexanedioldiacrylate, and Fluorescein were purchased from Sigma Aldrich (U.S.). 1,6-hexamethylene diisocyanate, 2,4-toluene diisocyanate, isophorone diisocyanate, acryloyl chloride, and triethylamine were obtained from Fluka (U.S.). 3-trimethoxysilyl propylmethacrylate was obtained from Cam Elyaf A.Ş (Turkey).

3.1.2. Apparatus

Fourier Transform Infrared Spectroscopy (FTIR) analyses of all crosslinked samples were done usingThermo Nicolet 380 FT-IR spectrometer with Smart Diamond ATR. FTIR was used to characterize specific chemical groups in the materials. All samples were analyzed by using Attenuated Total Reflectance (ATR) mode. FTIR spectra were obtained within the range of 4000 to 400 cm^{-1} during 32 scans at 2 cm^{-1} resolution with the substraction of background and they were normalized and major vibration bands were associated with chemical groups.

To examine the morphological characteristics of fibers and films, samples were viewed using scanning electron microscope (SEM) ESEM-FEG/EDAX Philiphs XL-30 instrument operating at 10 and 20 kV. All samples were supported on carbon tapes and sputtered with gold before examination.

Dye loaded crosslinked tubular structures were examined using a Zeiss Axio Observer inverted microscope with a Zeiss Filter set 38 (excitation BP 470/40, emission BP 525/50). Images were processed using Zeiss AxioVision software. Measurements on several samples as well as various locations on the same sample were conducted to ensure minimal experimental errors in obtaining representative values.

UNICAM UV/VIS Spectrometer UV2 was used to investigate load and release properties of fluorescein dye molecules from tubular structures obtained.

Contact angle measurements were performed using KSV CAM 101 contact angle instrument. Contact angles were measured by the sessile drop method using water at room temperature. Each contact angle reported was the mean value of ten measurements taken at different positions on the film. The contact angles were measured on both sides of the films and averaged.

Thermogravimetric Analysis (TGA) was used to determine thermal properties of crosslinked tubular structures. Experiments were performed on a TA Q50 apparatus from ambient to 600°C with a heating rate of 10°C/min. The samples were placed in an open platinium pan under nitrogen.

A Radium Ralutec 9W/78 UVA lamp (k=350-400nm), placed at a distance of 6 cm from the samples, was used as UV light source for photopolymerizations.

3.2. Preparation of PVA Fibers

Micron size PVA fibers prepared by melt spinning were chopped into apx. 10 cm pieces and suspended in dichloromethane for 5 h and rinsed with dichloromethane twice to remove sizing agents and dried under vacuum before crosslinking reaction.

Nano size PVA fibers prepared by electrospinning were used as received. PVA nanofibers were dryed overnight for characterization and further reactions.

3.3. Preparation of PVA Films

A 7 per cent PVA solution was prepared by dissolving 3.5 g polymer in 50 mLof Milli-Q water at 90°C with continuous stirring for 3 h. This solution was cast onto microscope slides by rolling a glass rod over the surface. Extreme care was taken in drying process to ensure complete drying. After two days of open air drying, films were kept at 60°C in vacuum for two days. FTIR showed that the water peak at 1650 cm^{-1} was completely eliminated.

3.4. Preparation of Glutaraldehyde Crosslinked PVA Fibers and Films

For surface crosslinking, PVA fibers and films were treated with glutaraldehyde (GA) in a non-solvent. Several concentrations of GA in ethanol (EtOH) were prepared and pH was adjusted to 2 with 1M hydrochloric acid (HCl) solution. In a typical procedure the films and fibers were placed in the solution of GA (water/HCl/EtOH mixture, at pH=2) and GA was absorbed onto these surfaces for several minutes. It is important to state that PVA films used were cast on microscope slides so that only one side of the films was accessible to crosslinker solutions. After removal of these films and fibers from these solutions, excess GA solution was washed off with EtOH. The GA-absorbed fibers and films were crosslinked at several temperatures and reaction times.The concentration of solutions used were 0.002, 0.01, 0.02, 0.2, 0.5, and 1M. Crosslinked fibers and films were extracted in EtOH to remove residual unreacted crosslinkers from surface and dried. Reaction conditions are summarized in Table 3.1. In general the reactions with PVA films and microfibers were carried out at 50°C for 2.5 h after allowing the monomer solutions to diffuse in the surface of PVA for 5 minutes. Star (*) labelled conditions became succesful in tubular formation from micron size fibers.

According to our experience from microfibers the crosslinker concentrations used were 0.02M and 0.2M for PVA nanofiber mats. They were kept in these solutions for 10 seconds and washed immediately with EtOH to remove excess crosslinkers from the surface. The crosslinking reaction for nanofibers was carried out at 50°C for 2.5 h.

The dissolution process of unreacted PVA templates from crosslinked fibers and films will be discussed in the section 3.12.

Table 3.1. Reaction conditions used in fabrication of GA crosslinked microfibers.

Conc. (M)	Diff. Time (min)	React. Temp. (°C)	React. Time (h)	Conc. (M)	Diff. Time (min)	React. Temp. (°C)	React. Time (h)	Conc. (M)	Diff. Time (min)	React. Temp. (°C)	React. Time (h)
0.002	1	50	1,5	0.01	1	50	1,5	0.02	1	50	1,5
			2,5				2,5				2,5
			4				4				4
		70	1,5			70	1,5			70	1,5
			2,5				2,5				2,5
			4				4				4
	5	50	1,5		5	50	1,5		5	50	1,5
			2,5				2,5				2,5*
			4				4				4
		70	1,5			70	1,5			70	1,5*
			2,5				2,5				2,5
			4				4				4
	10	50	1,5		10	50	1,5		10	50	1,5
			2,5				2,5				2,5
			4				4				4
		70	1,5			70	1,5			70	1,5
			2,5				2,5				2,5
			4				4				4
0.2	1	50	1,5	0.5	1	50	1,5	1	1	50	1,5
			2,5				2,5				2,5
			4				4				4
		70	1,5			70	1,5			70	1,5
			2,5				2,5				2,5
			4				4				4
	5	50	1,5		5	50	1,5		5	50	1,5
			2,5*				2,5				2,5
			4				4				4
		70	1,5*			70	1,5			70	1,5
			2,5				2,5				2,5
			4				4				4
	10	50	1,5		10	50	1,5		10	50	1,5
			2,5				2,5				2,5
			4				4				4
		70	1,5			70	1,5			70	1,5
			2,5				2,5				2,5
			4				4				4

3.4.1. Swelling Behaviour of GA Crosslinked Fibers

The dried and pre-weighed GA crosslinked samples were immersed in water at room temperature for 84 h during which period the polymer attained equilibrium swelling. The polymers were taken out and reweighed after wiping the surface gently at specific time intervals.

All swelling measurements in water were done with PVA fibers crosslinked in 0.002, 0.01, 0.02, 0.2, 0.5, and 1M GA solutions. For swelling measurements the crosslinked fibers were used after dissolution of their unreacted PVA cores. All fibers were succesfully crosslinked by these monomer solutions but some of them became lightly crosslinked and lost their tubular shape after dissolution. The results obtained were used to show the change in degree of swelling with the concentration of GA monomer solution.

In order to investigate the pH effect on the swelling properties of the tubes, swelling measurements were done in aquous solutions at pH=5 and pH=9 with PVA fibers which were crosslinked in 0.2M GA solutions.

3.4.2. Dye Loading into GA Crosslinked PVA Tubular Structures

A 10 mg/mL solution of fluorescein dye was used to load the GA crosslinked PVA tubular structures. Three different concentrations 0.020, 0.011, and 0.005 per cent (w/v per cent) were prepared from this fluorescein solution and used for loading dye molecules into the PVA tubes that were crosslinked in 0.02M and 0.2M GA reaction solutions. Fluorescein dye of each solution was adsorbed onto GA crosslinked PVA tubes by immersing these tubes in dye solutions for 24 h with continuous stirring. Tubes were then air dried for 24 h and vacuum dried at 50^{o}C for 4 h. Fluorescein dye over the surface of the tubes was washed with water at room temperature for 3 times and the tubes were vacuum-dried again.

3.4.3. Dye Loading Efficiency of GA Crosslinked PVA Tubular Structures

To determine the fluorescein loaded in each tube, the loaded tubes were soaked in fresh water. After 24 h the absorbance of the soaking medium was measured

spectrophotometrically at 454 nm. In order to establish the relationship between the UV absorbance of fluorescein, at 454 nm, and the concentration of the fluorescein solutions, a calibration curve was drawn for standard solutions ranging from 0.023 to 0.094 mmol fluorescein/L.

3.4.4. Dye Release and Diffusion Studies of GA Crosslinked PVA Tubular Structures

All experiments were carried out at pH=5, water, and pH=9 at 37±0.5°C. Since there was no difference observed between the diffusion of fluorescein molecules at different pH values after 1h release, all the release studies were done in water. The amount of release at different time intervals was determined spectrophotometrically at 454 nm. After each observation, tubes were put in 3 mL fresh solutions. The amount of dye released was calculated by comparing the absorbance with the standard curve prepared with pure dye.

3.5. Preparation of Glyoxal Crosslinked PVA Fibers

Several concentrations of glyoxal (GLY) in ethanol were prepared and pH was adjusted to 2 with 1M HCl solution. In a typical procedure PVA microfibers were placed in the solution of GLY (water/HCl/EtOH mixture, at pH=2) and GLY was allowed to be absorbed onto the fiber surfaces for several minutes. After removal of these fibers from these solutions, excess GLY solution was washed off with ethanol. The GLY-absorbed fibers were crosslinked at several temperatures and reaction times. The concentration of solutions used were 0.002 and 0.1M. Crosslinked fibers were extracted in ethanol to remove residual unreacted monomers from surface and dried. Reaction conditions are summarized in Table 3.2.

The dissolution process of unreacted PVA templates from crosslinked fibers will be discussed in the section 3.12.

3.5.1. Swelling Behaviour of GLY Crosslinked Fibers

The dried and pre-weighed GLY crosslinked samples were immersed in water at room temperature for 84 h. The polymers were taken out and reweighed after wiping the surface gently at specific time intervals.

All swelling measurements were done with PVA fibers crosslinked in 0.002 and 0.1M GLY solutions. During crosslinking reaction the monomer diffusion time was kept constant as 2 minutes as well as reaction time and temperature which is 2.5 h at 50^{o}C. Distilled water was used as a swelling medium since the crosslinked fibers do not show any pH dependance property like GA crosslinked fibers. For swelling measurements the crosslinked structures were used after dissolution of unreacted PVA core. However it was observed that all of the fibers became bulk crosslinked.

Table 3.2. Reaction conditions used in fabrication of GLY crosslinked microfibers.

Conc. (M)	**Diff. Time (min)**	**React. Temp. (°C)**	**React. Time (h)**	**Conc. (M)**	**Diff. Time (min)**	**React. Temp. (°C)**	**React. Time (h)**
0.002	1	50	1,5	0.1	1	50	1,5
			2,5				2,5
			4				4
		70	1,5			70	1,5
			2,5				2,5
			4				4
	2	50	1,5		2	50	1,5
			2,5				2,5
			4				4
		70	1,5			70	1,5
			2,5				2,5

3.6. Preparation of Hexamethylene Diisocyanate Crosslinked PVA Fibers

For the surface crosslinking polymer films and fibers were treated with 1,6-hexamethylene diisocyanate (HMDI) in dimethyl formamide (DMF) which is a good solvent for PVA. Several concentrations of HMDI in DMF were prepared without any catalyst. In a

typical procedure the films and fibers were placed in the solution of HMDI and it was absorbed onto these surfaces for several minutes. It is important to state that PVA films used were cast on microscope slides so that only one side of the films was accessible to crosslinker solutions. After removal of these films and fibers from these solutions, excess crosslinker solution was washed off with DMF. The HMDI-absorbed fibers and films were crosslinked at several temperatures and reaction times. The concentration of solutions used were 0.01, 0.04, 0.1, 0.2, and 0.3M. Crosslinked fibers and films were extracted in tetrahydrofuran (THF) to remove residual unreacted crosslinkers from the surface and dried. In general the reactions with PVA films and microfibers were carried out at 70^{o}C for 8 h under N_2 atmosphere after allowing the monomer solutions to diffuse in the surface of PVA for 4 minutes. Star (*) labelled conditions became succesful in tubular structure formation from micron size fibers.

Surface reactions were also conducted with crosslinker solutions prepared in acetone and toluene to compare the extent of surface reaction in solvents having different polarities. 0.1M of HMDI solutions in toluene, acetone and DMF were used as crosslinking media. PVA microfibers were kept in these solutions for 4 minutes and crosslinked at 70^{o}C for 8 h under N_2 atmosphere.

According to our experience from microfibers the crosslinker concentration used was 0.1M for PVA nanofiber mats. The fibers were kept in these solutions around 2 seconds and washed immediately with DMF to remove excess crosslinkers from the surface. The crosslinking reaction for nanofibers was carried out at 70^{o}C for 8 h.

The dissolution process of unreacted PVA templates from crosslinked fibers and films will be discussed in the section 3.12.

3.6.1. Swelling Behaviour of HMDI Crosslinked Fibers

The dried and pre-weighed HMDI crosslinked samples were immersed into water at room temperature for 84 h. The polymers were taken out and reweighed after wiping the surface gently at specific time intervals.

Table 3.3. Reaction conditions used in fabrication of HMDI crosslinked microfibers.

Conc. (M)	Diff. Time (min)	React. Temp. (°C)	React. Time (h)	Conc. (M)	Diff. Time (min)	React. Temp. (°C)	React. Time (h)	Conc. (M)	Diff. Time (min)	React. Temp. (°C)	React. Time (h)
0.01	1	70	5	0.04	1	70	5	0.1	1	70	5
			8				8				8
	4	70	5		4	70	5		4	70	5
			8				8				8*
	8	70	5		8	70	5		8	70	5
			8				8				8
0.2	1	70	5	0.3	1	70	5				
			8				8				
	4	70	5		4	70	5				
			8*				8*				
	8	70	5		8	70	5				
			8				8				

All swelling measurements were done with PVA fibers crosslinked in 0.01, 0.04, 0.1, 0.2, and 0.3M HMDI solutions. For swelling measurements the crosslinked fibers were used after dissolution of their unreacted PVA cores. All fibers were succesfully crosslinked by these monomer solutions but some of them became lightly crosslinked and lost their tubular shape after dissolution. The results obtained are used to show the change in degree of swelling with the concentration of crosslinker solution.

In order to investigate the pH effect on the swelling properties of the tubes, swelling measurements were done in aquous solutions at pH=5 and pH=9 for PVA fibers which were crosslinked in 0.2M HMDI solutions.

3.6.2. Dye Loading into HMDI Crosslinked PVA Tubular Structures

A 10 mg/mL solution of fluorescein dye was used to load the HMDI crosslinked PVA tubular structures.Three different percentages of fluorescein solutions 0.020, 0.011, and 0.005 per cent (w/v per cent) were prepared from this solution and used for loading dye molecules into the PVA tubes that were crosslinked in 0.1, 0.2 and 0.3M HMDI solutions. Fluorescein dye of each solution was adsorbed onto HMDI crosslinked PVA tubes by immersing these tubes in dye solutions for 24 h with continuous stirring. Tubes were then

air dried for 24 h and vacuum dried at 50^{o}C for 4 h. Fluorescein dye over the surface of the tubes was washed with water for 3 times and the tubes were vacuum-dried.

3.6.3. Dye Loading Efficiency of HMDI Crosslinked PVA Tubular Structures

To determine the fluorescein loaded in each tube crosslinked in 0.1, 0.2 and 0.3M HMDI solutions, the loaded tubes were soaked in water. After 24 h the absorbance of the soaking medium was measured spectrophotometrically at 454 nm. In order to establish the relationship between the UV absorbance of fluorescein, at 454 nm, and the concentration of the fluorescein solutions, a calibration curve was drawn for standard solutions ranging from 0.023 to 0.094 mmol fluorescein/L.

3.6.4. Dye Release and Diffusion Studies of HMDI Crosslinked PVA Tubular Structures

All experiments were carried out in pH=5, water, and pH=9 at 37±0.5°C. Since there was no difference observed between the diffusion of fluorescein molecules at different pH values after 1 h release, all the release studies were done in water. The amount of release at different time intervals was determined spectrophotometrically at 454 nm. After each observation, tubes were put in 3 mL fresh solutions. The amount of dye release was calculated by comparing the absorbance with the standard curve prepared with pure dye.

3.7. Preparation of Isophorone Diisocyanate Crosslinked PVA Fibers

PVA fibers were treated with isophorone diisocyanate (IPDI) in DMF. In a typical procedure the PVA fibers were placed in 0.2M solution of IPDI which was absorbed onto these surfaces for 4 minutes. Immediately after removal of these fibers from the solution, excess crosslinker was washed off with DMF. The IPDI-absorbed fibers were crosslinked at 70°C for 8 h. The crosslinking conditions were choosen according to our previous experience with HMDI.

The dissolution process of unreacted PVA templates from crosslinked fibers will be discussed in the section 3.12.

3.8. Preparation of 2,4-Toluene Diisocyanate Crosslinked PVA Fibers

PVA fibers were treated with 2,4-toluene diisocyanate (2,4-TDI) in DMF. In a typical procedure the PVA fibers were placed in 0.2M solution of 2,4-TDI which was absorbed onto these surfaces for 4 minutes. Immediately after removal of these fibers from the solution, excess crosslinker was washed off with DMF. The 2,4-TDI -absorbed fibers were crosslinked at 70°C for 8 h. The crosslinking conditions were choosen according to our previous experience with HMDI.

The dissolution process of unreacted PVA templates from crosslinked fibers will be discussed in the section 3.12.

3.9. Grafting of Acryloyl Chloride on PVA Fibers

PVA microfibers were reacted with 3 fold excess acryloyl chloride (AC) in the presence of triethylamine (TEA) in toluene at room temperature for 48 h. Grafted fibers were rinsed with toluene and dried.

3.10. Grafting and/or Crosslinking of 3-trimethoxysilyl propylmethacrylate on PVA Fibers

The reaction of PVA with 3-trimethoxysilyl propylmethacrylate (MPS) occurs in acidic medium. The fibers were introduced to an acidic solution (water/HCl/THF mixture, at pH=2) of MPS (concentration=1.77 M) and kept in 5 minutes with gentle stirring and they were removed from the solution and rinsed thoroughly in water and THF. Excess solvent was evaporated from the surface. The fibers were reacted at 50°C for 1 h.

3.11. Surface Photopolymerization of Double Bond Functionalized PVA Fibers

Polymerizable crosslinkers applied as shell materials were 1,6-hexanedioldiacrylate (HDODA), 2-hydroxyethylmethacrylate (HEMA), and poly(ethyleneglycol) diacrylate (PEGDA). The ratios used are summarized in Table 3.4. 0.5, and 1M concentrations of each crosslinker and/or mixed crosslinker solutions were prepared in dichloromethane. Irgacure

651 was used as photoinitiator as 1 per cent per weight of all crosslinker amount. Double bond functionalized PVA fibers were immersed into these solutions and pulled out of the solution immediately and exposed to UV light in 4 minutes. A Radium Ralutec 9W/78 UVA lamp (k=350-400nm), placed at a distance of 6 cm from the samples, was used as UV light source. After curing these fibers were rinsed with dichloromethane and dried.

The dissolution process of unreacted PVA templates from crosslinked fibers will be discussed in the section 3.12.

Table 3.4. The ratios of photopolymerizable crosslinkers used as shell materials.

Crosslinker	**Weight (%)**	**Crosslinker**	**Weight (%)**
HDODA	100	HEMA+PEGDA	90+10
HEMA	100	HEMA+PEGDA	80+20
PEGDA	100	HEMA+PEGDA	70+30

3.12. Dissolution of PVA Templates from Crosslinked Fibers and Films

In a general procedure the inner core of crosslinked PVA fibers was dissolved in water at 70^{o}C. The dissolution time for each crosslinked shell was optimized according to their crosslinking density, shell thickness and fiber length. The inner core of PVA microfibers needed more time than nanofibers to be dissolved completely. Precipitation of PVA inside and outside of the tubes obtained was removed from the shells of nascent tubes by dialysis against water at room temperature. Unreacted sides of PVA films were also dissolved in the similar conditions. PVA fibers and films were freeze-dryed before SEM examination.

4. RESULTS AND DISCUSSION

4.1. Poly(vinyl alcohol) Fibers

Poly(vinyl alcohol) (PVA) nanofibers prepared by electrospinning and PVA microfibers which were prepared by melt spinning have 300 nm and 60 μm average diameters, respectively. Scanning electron microscopy (SEM) images of the neat PVA fibers are shown in Figure 4.1.

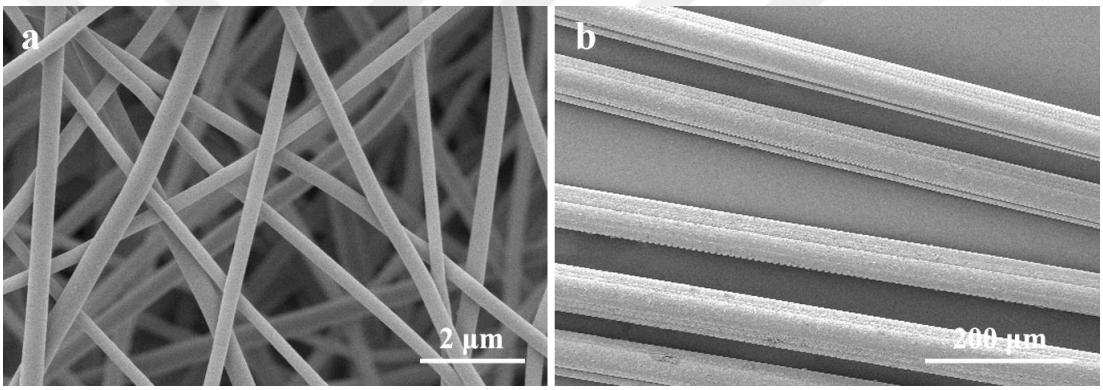


Figure 4.1. Morphologies of PVA nanofibers (a), and PVA microfibers (b).

FTIR spectrum clearly reveals the major peaks associated with PVA (Figure 4.2a) and Table 4.1 summarizes the most characteristic bands and their respective assignment. Absorptions of asymmetrical and symmetrical stretchings of C–H from alkyl groups in the backbone are υ= 2941 and 2908 cm^{-1}, respectively. Strong bands for free –OH groups (non-bonded –OH stretching band at υ= 3650-3600 cm^{-1}), and hydrogen bonded–OH groups (υ= 3550-3200 cm^{-1}) can be observed [99]. Due to the presence of hydrophilic forces coming from the interaction between –OH groups, intramolecular and intermolecular hydrogen bondings are expected to occur among PVA chains. The two peaks at 1420 and 1372 cm^{-1} are from the secondary –OH in-plane bending and C–H wagging vibrations, respectively. The band at υ= 1141 cm^{-1} represents C–C symmetrical stretchings which is sensitive to crystallinity. Therefore, it can be used as an assesment tool of PVA since PVA is a semi-

crystalline polymer able to form several crystalline domains [99-100]. The band at 1090 cm^{-1} corresponds to the C–O stretching vibrations of PVA.

The carbonyl bands at 1666 and 1714 cm^{-1} are present in the spectrum of neat PVA which belong to residual acetate groups from the manufacture of PVA. The intensity of these peaks is weak indicating that only a few acetate groups are present in the polymer chain. There is approximately 5 per cent of unhydrolyzed polyvinyl acetate (PVAc) in the samples used. The shoulder at 1714 cm^{-1} corresponds to carbonyl group of acetate (O=C–O) [101].

4.2. Fabrication and Characterization of Dialdehyde Crosslinked PVA Tubular Structures

Reacting of PVA with dialdehydes is one of the most commonly used crosslinking techniques in the literature. When dialdehydes are used, such as glutaraldehyde or glyoxal, crosslinking reactions of PVA can be conducted under mild conditions and this reaction results in the formation of acetal bonds. Most of the literature examples were applied in bulk, there are only a few examples showing the surface crosslinking of PVA with these reagents [102-103]. In our work careful control of glutaraldehyde diffusion was made possible so that crosslinking was confined to a thin outer shell.

4.2.1. Crosslinking Reaction of PVA with Glutaraldehyde

Glutaraldehyde (GA) has been used as a crosslinking agent in the presence of an acid catalyst. In a general procedure GA was absorbed onto PVA fibers from different concentrations of aquous ethanolic solutions at pH=2. Excess GA which does not penetrate inside the fiber matrix in a given time was washed off from the fibers with ethanol. After complete crosslinking reaction, the unreacted PVA fiber templates were removed. In order to fabricate crosslinked tubular structures the reaction should be limited only on the surface. Therefore, the selection of solvent, concentration of GA monomer solutions and diffusion time of these monomer solutions inside PVA fiber matrix have a significant effect to confine the reaction on the surface.

When a solvent like water which can dissolve PVA fibers is used as a medium, PVA will swell adequately and water miscible crosslinker GA penetrates inside the fiber matrix

and the crosslinking reaction is expected to be uniformly distributed throughout the matrix. On the contrary, when a non-solvent for PVA like ethanol which is miscible with aquous GA solution is used as a medium, PVA fibers do not swell and hence crosslinking agent cannot penetrate inside the matrix and only the surface of the fibers are impregnated with GA. Therefore, by using judiciously chosen mixtures of these two solvents, it is possible to place the crosslinking agent only at the outer surface of the fibers.

Although glutaraldehyde used contains 25 per cent of water, the quantity of water is not high enough to cause any appreciable swelling. Therefore, it is predicted that the crosslinking reaction in ethanol is predominantly a surface reaction. However, increasing the concentration of GA solutions and the diffusion time of these solutions into the fiber matrix may increase the probability of bulk reaction. The reaction conditions that were tried and resulted in succesful tubular structures are shown in Experimental Part Table 3.1.

Six different concentrations of GA reaction solutions were used for FTIR and crosslinking density characterization by swelling. The diffusion time of monomers inside the fiber matrix, reaction temperature and duration were kept constant as the concentration of GA solutions was changed. All samples were used after dissolution of unreacted PVA. However, depending on the crosslinking density only some of the fibers were succesfully resulted in tubular structures. Crosslinked tubes could only be prepared from fibers that had just the right crosslinking ratio.

4.2.2. FTIR Characterization of GA Crosslinked PVA Fibers

The FTIR spectra of GA crosslinked PVA fibers are shown in Figure 4.2(b-f) and summarized in Table 4.1. There are three major changes observed in the FTIR spectra as the concentration of GA solutions is changed. The reaction of PVA with GA results in the reduction of the intensity of -OH stretching vibration peak (υ= 3310-3350 cm^{-1}). This spectral change is due to the consumption of hydroxyl groups upon reaction with aldehydes which is an indication of the formation of acetal rings. FTIR spectra of GA crosslinked PVA samples show two important bands at 2942 and 2916 cm^{-1} of C-H stretchings related to aldehydes, a dublet absorption with peaks attributed to the alkyl chain [104]. Furthermore, there is an increase in the absorbance of the peaks between 920 and 1372 cm^{-1} indicating the

formation of an acetal ring and ether linkage as a result of the reaction between hydroxyl groups and aldehydes. These bands are overlapping with PVA and broaden PVA bands in these regions.

Strong band from carbonyl group was also verified (C=O at υ= 1720-1714 cm^{-1}) and an increase in the intensity of this peak with GA concentration was observed which is an unexpected situation. According to the spectra obtained it is suggested that an excess of GA may be present even after the rinsing of crosslinked fibers with water or ethanol. Therefore, the presence of aldehyde peaks can be an evidence for unreacted pendant aldehyde groups on PVA chains created by the reaction of GA with only one of its two aldehyde groups.

Table 4.1. Vibration band frequencies of PVA and GA crosslinked PVA.

	Chemical Group	**Wavenumber (cm^{-1})**
PVA **PVA-GA**	Non bonded O-H stretching band	υ 3650-3600
PVA **PVA-GA**	O-H from intermolecular and intramolecular hydrogen bonds	υ 3550-3200
PVA **PVA-GA**	C-H from alkyl groups C-H from aldehyde	υ 2941-2908 Two peaks in υ 2942-2916
PVA **PVA-GA**	C=O of acetate C=O of aldehyde and acetate	υ 1714-1666 υ 1720-1714
PVA	Secondary –OH in plane bend. C-H wagging of CH_2	υ 1420-1372
PVA	C-C symmetrical stretching (sensitive to crystallinity)	υ 1141
PVA **PVA-GA**	C-O-C	υ 1090

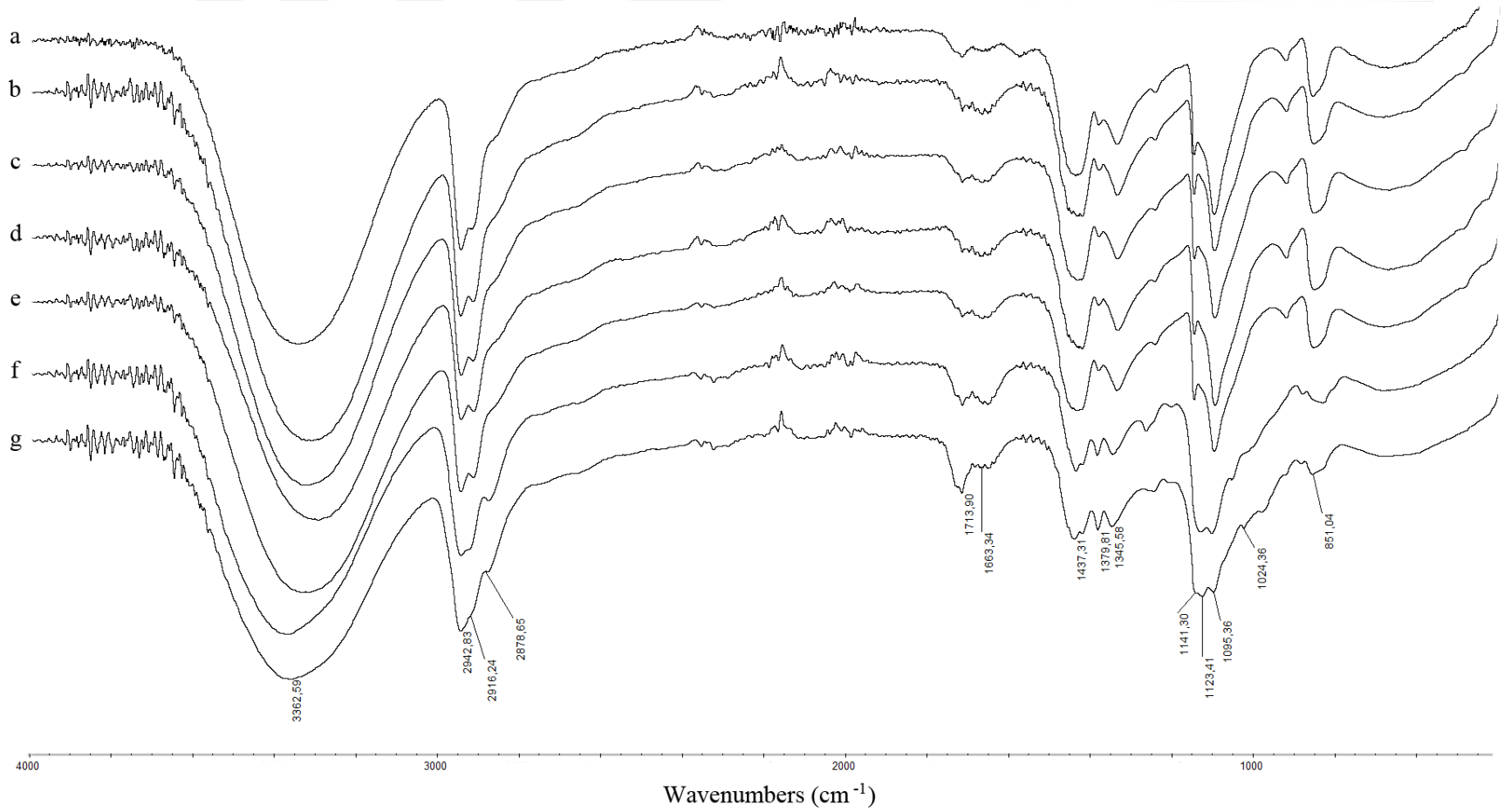
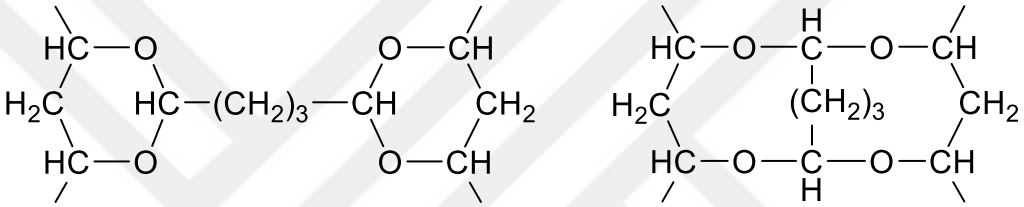
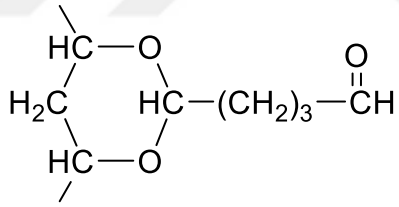


Figure 4.2. FTIR spectra of neat PVA (a) and PVA crosslinked in 0.002M (b), 0.01M (c), 0.02M (d), 0.2M (e), 0.5M (f), and 1M (g) glutaraldehyde solutions.

As a difunctional crosslinker one aldehyde group may react with hydroxyl groups of PVA chain by forming a hemiacetal structure while the other one may not react due to some conformation or kinetic limitations. Since GA is only available as an aquous solution, when GA concentration increases, the water content in the reaction medium will also increase. This causes an improved swelling of PVA. More GA molecules can be absorbed into PVA to react with more hydroxyl groups and form more crosslinks at the early stages of the reaction. The crosslinking reduces the chain mobility and reactivity of PVA leading to a reduction in reaction rate. Therefore, the probability that only one of the aldehyde groups reacts, increases with GA concentration.



a. Acetal Ring Formation



b. Aldehyde Formation by One-sided Reaction

Figure 4.3. Expected crosslinked products by the reaction between PVA and GA.

From well known reaction mechanisms in the literature and FTIR spectra analysis, typical products of the reaction between PVA and GA are shown in Figure 4.3. Four hydroxyl groups of PVA could react with one equivalent of GA if both aldehyde groups of the crosslinker had reacted. The reactions between GA and PVA can result in intermolecular (a) and/or intramolecular (b) crosslinks, both make the PVA insoluble. Figure 1.16 shows the expected crosslinking reaction products between PVA chains and GA catalyzed by hydrochloric acid. The formation of cyclic structures (Figure 4.3) are well documented [104-105]. According to the literature structure b (Figure 4.3) is formed by one-sided reaction of

GA and unreacted aldehyde pendant groups may remain on PVA chains [106] which renders the fibers insoluble in water.

In order to quantitatively analyze FTIR spectral changes, the absorbance ratios of several functional groups to several reference peaks were determined and plotted. The methylene stretching band at 2900 cm^{-1} was taken as a reference peak. The ratio of this reference peak to the peak at 3300 cm^{-1} corresponding to hydroxyl groups was plotted against GA content in the reaction solution. The graph is shown in Figure 4.4. It can be clearly observed that an increase in GA content resulted in higher degree of crosslinking and consequently the reduction of available hydroxyl groups.

The ratio of the peak at 1720 cm^{-1} corresponding to aldehyde group to the band at 2900 cm^{-1} was plotted against GA content in the reaction solution to show the presence of one-sided reaction. The graph is shown in Figure 4.5. The absorbance ratio of the aldehyde group showed a constant increase with GA concentration in reaction solution while that of hydroxyl groups decreased.

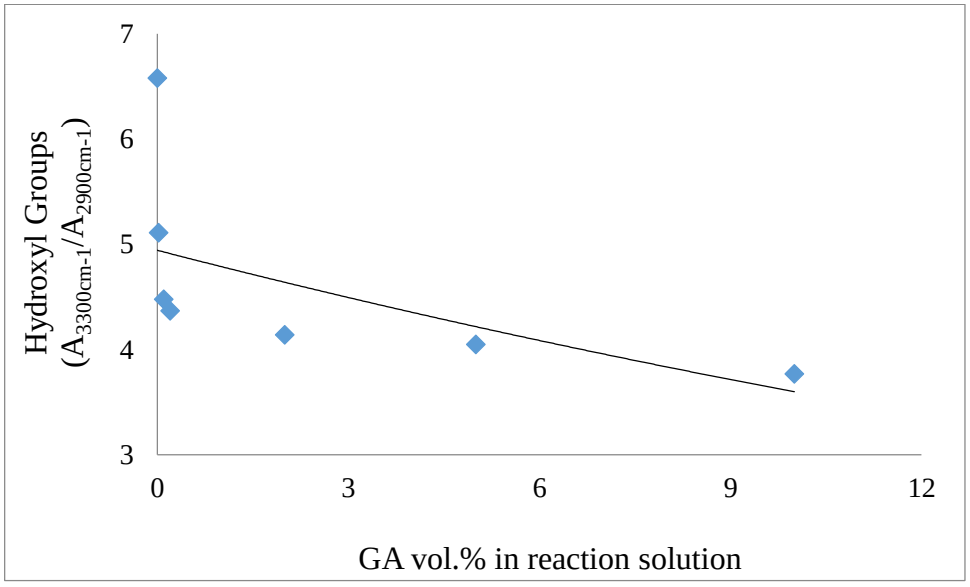


Figure 4.4. Absorbance ratio of hydroxyl (3300 cm^{-1}) to a reference peak (2900 cm^{-1}) on crosslinked PVA with different GA content in reaction solution.

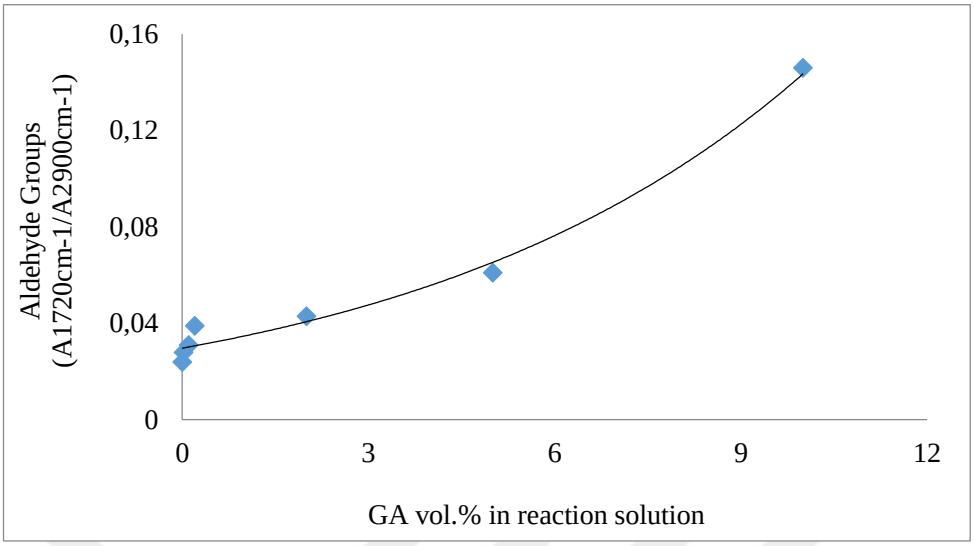


Figure 4.5. Absorbance ratio of aldehyde (1720 cm^{-1}) to a reference peak (2900 cm^{-1}) on crosslinked PVA with different GA content in reaction solution.

From absorption ratio of hydroxyl and aldehyde groups to methylene stretchings obtained from FTIR spectra, it can be said that the decrease in the number of hydroxyl groups is attributed to the acetal ring formation and the increase in absorption value of aldehyde groups is attributed to one-sided reaction. As GA content in reaction solution increases, formation of structure **b** becomes significant compared to structure **a**, as shown in Figure 4.3.

The degree of crystallinity was obtained from FTIR spectroscopy through the peak at 1141 cm^{-1} which is related to the C-C symmetric stretchings and 1096 cm^{-1} which corresponds to C-O stretchings of a portion of PVA chain where an intramolecular hydrogen bond is formed between two neighbouring –OH groups [54]. The ratio of absorbances of 1141 cm^{-1} and 1096 cm^{-1} bands was calculated for each sample obtained from reaction solutions having different GA contents. By using this ratio the correlation between crosslinking and crystallinity was established as shown in Figure 4.6. As expected, the crystalline portion depends on the number of -OH groups on PVA chain which are able to form hydrogen bonds. As GA content increases crosslinking density, the number of available –OH groups decreases which reduces crystallinity.

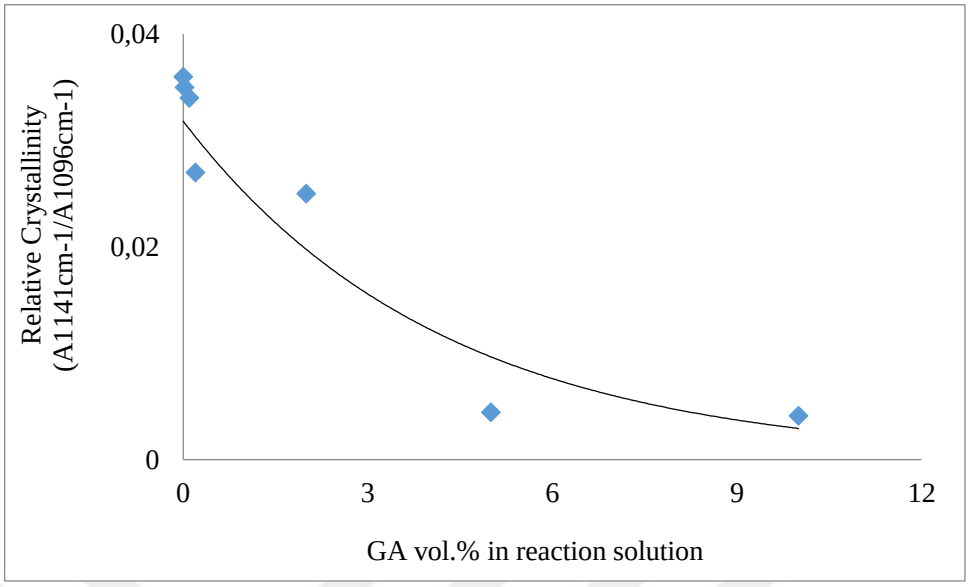


Figure 4.6. Absorbance ratio of the bands 1141 cm^{-1} to 1096 cm^{-1} on crosslinked PVA with different GA content in reaction solution.

4.2.3. Determination of Crosslinking Density for GA Crosslinked PVA Fibers by Swelling

Hydrogels are crosslinked polymers which can be used in controlled-release devices due to their swelling properties. Absorption of water leads to polymer expansion, which affects the diffusion of biological molecules or drugs and influences release kinetics. The release rate is determined by the ability of solute molecules to move through the gel networks, which change morphology during swelling due to diffusion of fluid into the polymer [63].

Swelling measurements are often used to measure the crosslink density of hydrogels. The amount of absorbed water is usually expressed as water uptake or swelling ratio as shown in the following equation:

$$\text{Degree of Swelling (\%)} = \left[\frac{Ww - Wd}{Wd}\right] \text{x}100$$

where W_d and W_w are the initial dry weight and final wet weight of the hydrogel films and fibers, respectively.

The degree of swelling is known to be dependent upon the crosslink density of polymer networks. The greater the crosslinking density, the less the degree of swelling.

It was reported in the literature that the swelling ratio depends on the hydrolysis degree of PVA films. PVA with low hydrolysis degree has acetate groups that can be hydrolyzed by addition of [OH^-] ions by raising pH. The chains then become highly ionic and these charges repel each other and increase the swelling ratio [107].

In order to investigate the effect of pH on the fibers used, swelling data were obtained for PVA fibers which were crosslinked in 0.2M GA reaction solution at 12 h time intervals at different pH values and mean value was recorded. Table 4.2 shows the variation of equilibrium swelling of GA crosslinked PVA fibers in pH 5, pH 9 and water. As this table shows there is no significant difference between swelling ratio of PVA at different pH values. In other words PVA used in this study is almost neutral regarding to pH. Since the hydroysis degree of PVA fibers used in this study is almost 95-98 per cent, the very small amount of unhydrolyzed acetate groups does not affect the swelling behaviour. Therefore, all swelling measurements were done in water.

Table 4.2. Effect of pH on swelling of PVA fibers crosslinked in 0.2M GA solution.

	Swelling (%) **Mean value ± SD (n=3)**
pH 5	168.78±0.9
water	166.47±0.6
pH 9	170.62±0.8

The effect of different GA contents in reaction solutions on the crosslinking density of PVA was studied by using swelling characteristics of the crosslinked PVA fibers. The effect of GA concentration on the swelling properties of PVA is shown in Figure 4.7.

It was observed that after crosslinking reaction with GA the resulting decrease in the hydroxyl groups of PVA has effectively reduced the affinity of the polymer for water leading to a reduction in the swelling ratio. Crosslinking of polymers also reduces the molecular mesh size of the gels for any type of diffusion and prolonged release time may be achieved by increased crosslinking [108-109].

Different GA concentrations lead to significant difference in water uptake properties of crosslinked PVA networks. By increasing the concentration of crosslinking agent chain entanglement occurs which would result in highly crosslinked rigid structure and a decreased network expansion. Lower GA concentrations on the other hand cause an increase in swelling properties. In general it may be concluded that by increase in GA concentration, the crosslinking density increases and this in turn reduces the swelling or water uptake property of the gels significantly.

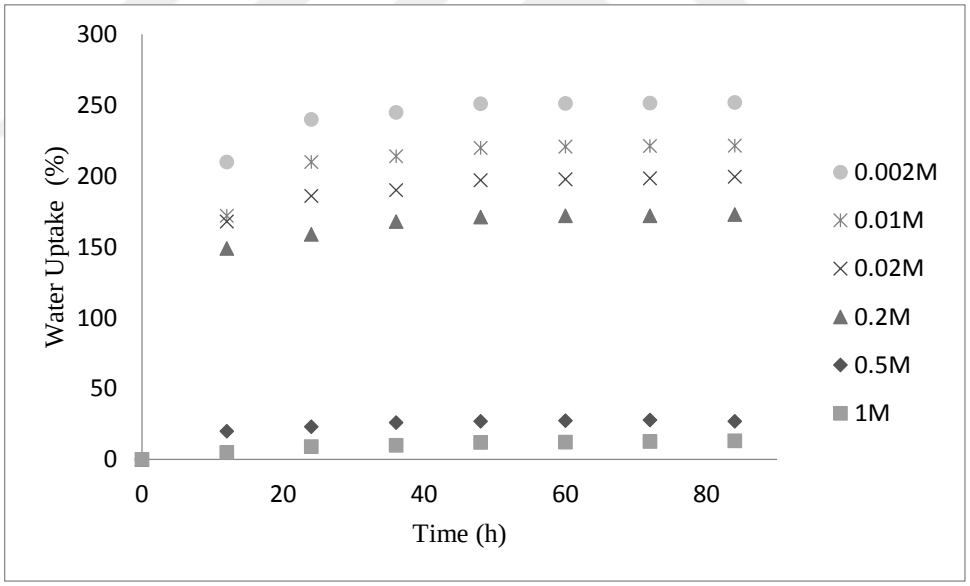


Figure 4.7. Effect of different GA content in reaction solutions on the swelling of crosslinked PVA in water.

Water uptake is 27 and 12 per cent for fibers crosslinked in 0.5M and 1M GA reaction solutions, respectively which is very low compared to the fibers crosslinked in 0.002, 0.01, 0.02, and 0.2M GA reaction solutions. This shows that in high crosslinker concentrations the

reaction may not be limited to the surface since all crosslinkers penetrate inside the fiber matrix and cause bulk crosslinking. This will be discussed in core template removal section.

4.2.4. Removal of the Core from GA Crosslinked PVA Fibers

To remove template fibers, either solvent extraction or thermal degradation can be employed, depending on the nature of the polymer. In general both ways are suitable for PVA fibers. However, in case of thermal degradation there should be a reasonable decompostion temperature difference between fiber core and shell material.

Thermogravimetric analysis (TGA) was used to determine the thermal degradation properties of neat PVA and GA crosslinked PVA. The thermogravimety (TG) and differential thermogravimetry (DTG) curves are presented in Figure 4.8 and Figure 4.9, respectively.

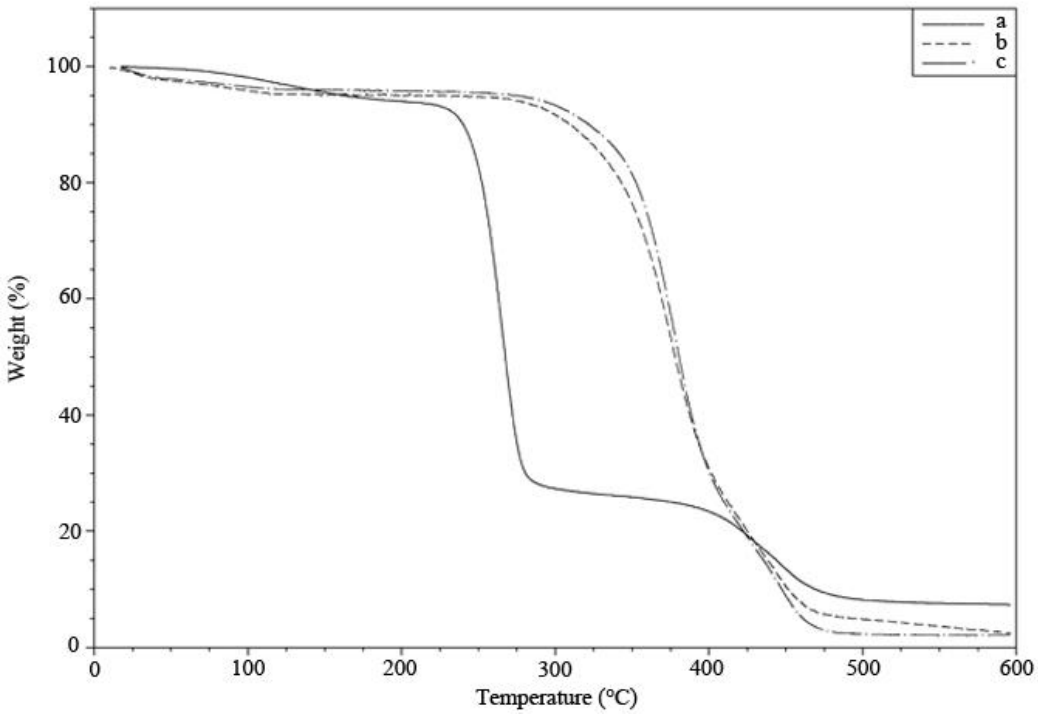


Figure 4.8. TG curves of neat PVA fibers (a), PVA fibers crosslinked in 0.02M GA (b), 0.2M GA (c) solutions.

According to TGA thermograms, it was observed that neat PVA has three main degradation steps. Around 100°C PVA looses about 5 per cent of its mass which is due to the

evaporation of absorbed moisture usually present in every hydrophilic material. The decomposition of PVA begins around 250°C and polymer lost 70 per cent of its mass at 280°C. The last step, around 430°C, corresponds to the breakage of the main chain and polymer lost 20 per cent of its mass and leaving merely 5 per cent char at 600°C [110].

It was observed that GA crosslinked PVA fibers also have three main degradation steps as shown in Figure 4.8 and Figure 4.9. In comparison to the neat PVA, it was seen that the first stage of weight loss was nearly similar showing 4 per cent of mass lost at 100°C. Furthermore, the degradation of crosslinked fibers was observed at a little higher temperatures, 340 and 440°C, which is due to the increased thermal stability as a result of crosslinking of PVA by GA (Figure 4.8b and Figure 4.9b). The increase in the GA concentration did not change the TG profile (Figure 4.8c and Figure 4.9c). The weight loss was continuous and there was no significant difference in the degradation stages. Clearly the decomposition temperatures of the core and the shell are quite close to each other. Therefore, it was imposible to remove unreacted PVA core templates by thermal degradation without any damage on GA crosslinked shells.

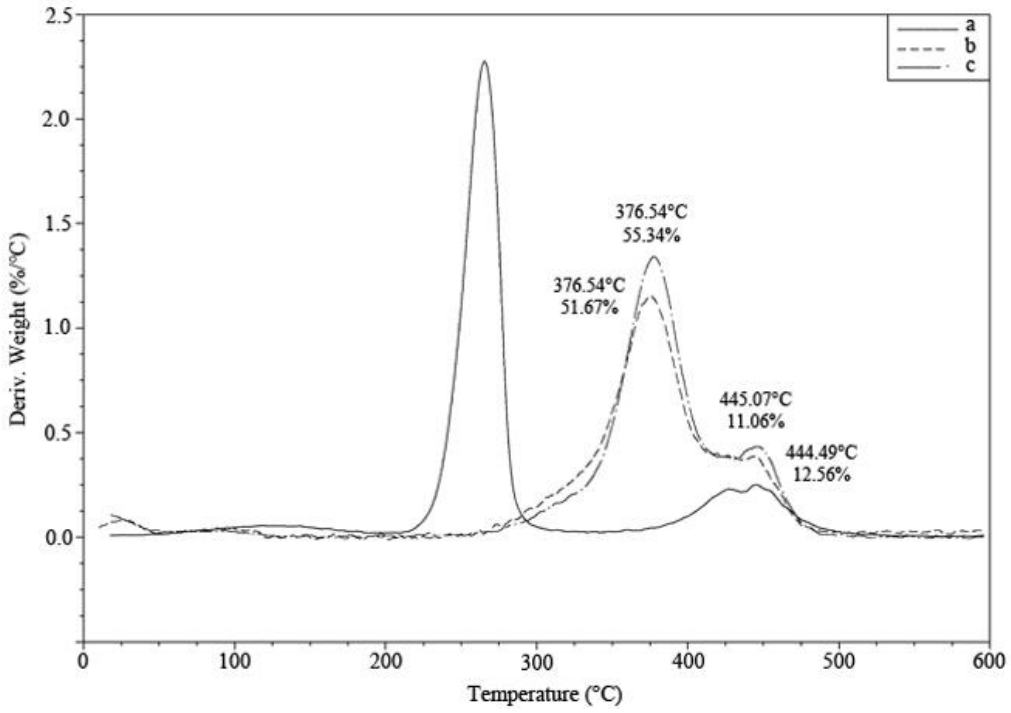


Figure 4.9. DTG curves of neat PVA fibers (a), PVA fibers crosslinked in 0.02M GA (b), 0.2M GA (c) solutions.

In case of solvent extraction, dimethyl sulfoxide, dimethyl formamide, water and several combinations of these solvents were tried. Water was found to be the best solvent since it dissolves PVA fibers completely without dissolving crosslinked shells. GA crosslinked PVA fibers were immersed in water at 70°C for different time periods. The dissolution of unreacted PVA core templates from GA crosslinked PVA fibers was monitored by scanning electron microscopy.

In case of neat PVA, the fibers gradually swell in water and become thinner and start to rupture until they dissolve completely. However, the shape of crosslinked fibers became irregular at the first stage and started to swell as inner PVA core swells and slowly dissolved from the open ends as shown in Figure 4.10. The dissolution front was seen to move inside the length of crosslinked fibers, as water started to penetrate from open ends.

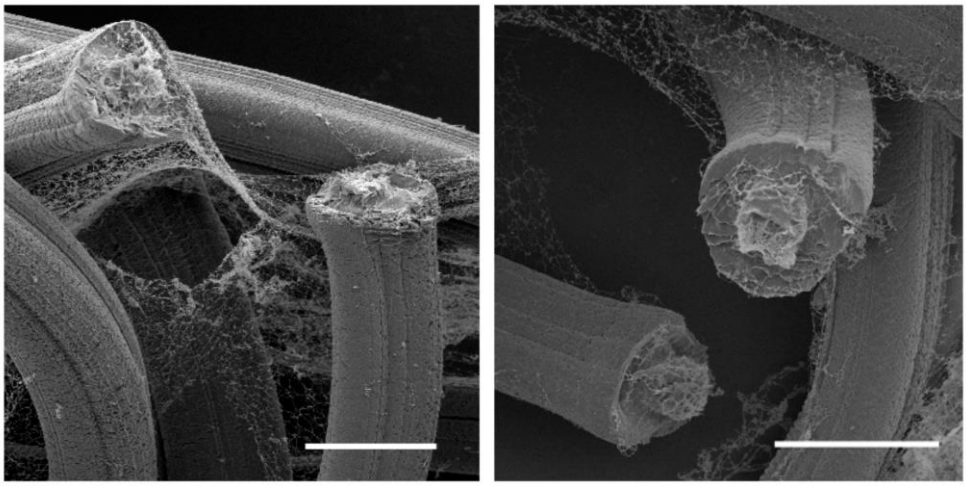


Figure 4.10. GA crosslinked PVA fibers after 1 min dissolution in water at 70^{o}C (Scale: 100 μm, PVA fiber used was crosslinked by 0.2M GA solution).

During dissolution of unreacted PVA core templates, sometimes precipitation of PVA was observed inside and outside of the microtubes. PVA was removed from the shells of crosslinked microtubes by dialysis against water at room temperature. The microtubes appear to contain some residues of PVA before dialysis (Figure 4.11a), whereas after dialysis the shape of the tubes indicate that they do not contain any solid PVA residues, as shown in Figure 4.11b.

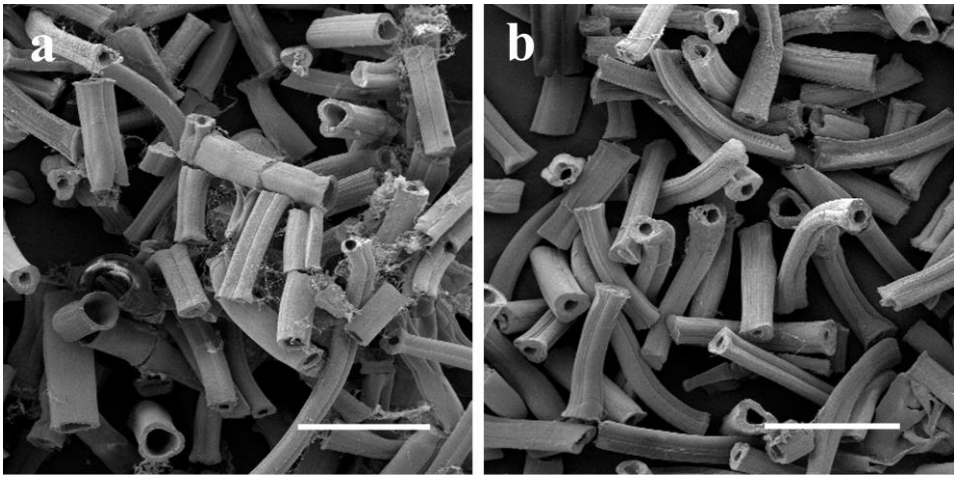


Figure 4.11. GA crosslinked PVA tubes before (a) and after dialysis (b) (Scale: 500µm).

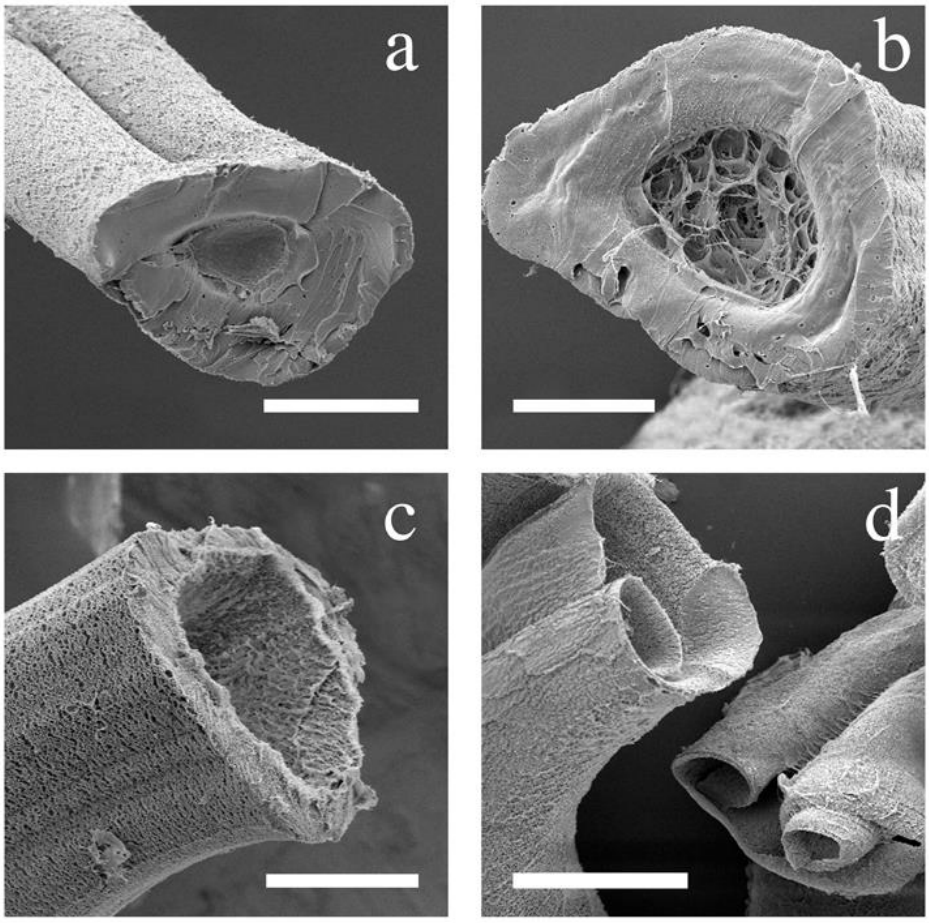


Figure 4.12. GA crosslinked PVA tubular structures after 2 min (a), 5 min (b), 10 min (c), 30 min (d) dissolution in water at 70°C (Scale bar: a, b and c=50µm, d=100µm).

Unreacted PVA fibers dissolved completely in water at 70^{o}C in 2 minutes; under the same conditions the core of crosslinked PVA fibers dissolved more slowly. The dissolution behaviour of PVA core was investigated by recording SEM images during dissolution. Figure 4.12 shows the SEM images of the crosslinked fibers after 2 min, 5 min, 10 min, and 30 min dissolution in water at 70^{o}C. The images clearly show that the shell gets thinner and the inner diameter increases as time goes on.

The dissolution time of the core from crosslinked fibers mainly depends on two factors. One is the length of the fiber and the other one is the thickness of the shell.

4.2.4.1. The effect of PVA fiber length. Length of the crosslinked fibers affects the dissolution of the inner core. Two kinds of samples were prepared to investigate the effect of fiber length on dissolution of the inner core. One is uncut (long) sample used immediately after crosslinking reaction. Such fibers probably do not contain open ends. The other is GA crosslinked PVA fibers that are cut to approximately 5mm length so that there are two open ends for each piece.

Figure 4.13a shows the uncut samples which were dissolved in water at 70°C for 10 minutes. Long crosslinked fibers did not form succesful tubular structures and the shells of these structures were ruptured during dissolution of the inner core.

In uncut samples water entered into the fibers by means of permeation through crosslinked shells. During penetration of water inside the core, unreacted PVA core swells with the crosslinked shell and the dissolution starts uniformly along the whole length of the crosslinked PVA fibers. The only possibility for the dissolved PVA to come out is to permeate out through crosslinked shell if there are no cracks on the shell. When there is no open ends and cracks that PVA could go out of, a pressure is created inside the core and the crosslinked shell is ruptured due to this high osmotic pressure during dissolution. Uncut fibers could not be made into tubes without shell rupture.

Figure 4.13b shows the cut samples which were dissolved in water at 70°C for 10 minutes. Cut and short crosslinked fibers did form succesful tubular structures having shells with uniform diameter. It was observed that PVA removal from the cut crosslinked samples

was easier than that of the uncut sample. The faster removal of PVA in the cut sample occured thanks to the presence of open ends. In addition to the permeation through the crosslinked shell water could now quickly enter into the tubes through the open ends. The dissolved PVA could also leave the tubes through the open ends. The significant effect of the presence of the open ends on the removal rate of PVA indicates that in general there are no holes or cracks on the crosslinked shells showing continuous crosslinking on the fiber surface.

According to these data maximum length of fibers that results in the formation of tubes was found to be as 5mm. Fibers longer than this length behaved inconsistently and would not form succesful tubular structures.

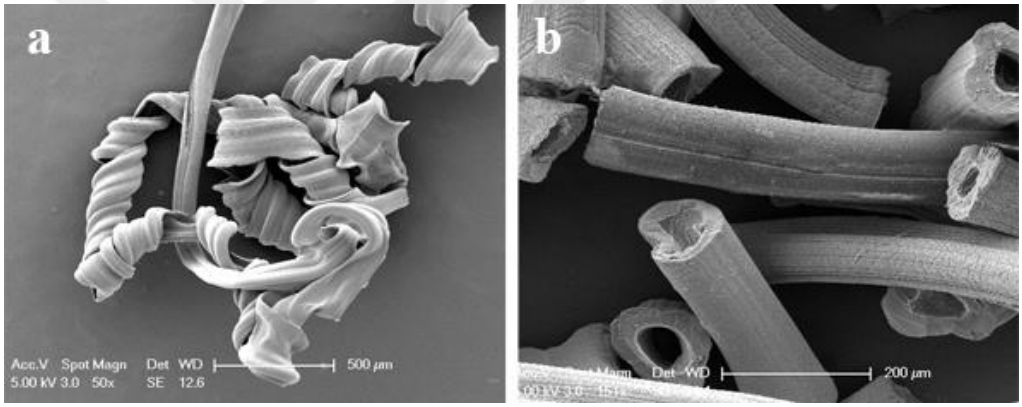


Figure 4.13. SEM images of the uncut (a) and cut GA crosslinked fibers (b) after dissolution.

4.2.4.2. The effect of crosslinked wall thickness. The dissolution time should be adjusted according to the thickness of the crosslinked shells. Since crosslinked shells swell in hot water, with longer dissolution time the shells with low thicknesses tend to be ruptured more easily. They would not stand the preasure created by dissolved PVA inside the core. The time needed for complete dissolution of PVA from GA crosslinked PVA fibers having 10-20 µm shell thicknesses was found to be approximately between 5 and 10 minutes (Figure 4.14a). Above 10 minutes the tubes were ruptured, rolled around themselves and became longitudinally curled as shown in Figure 4.14b.

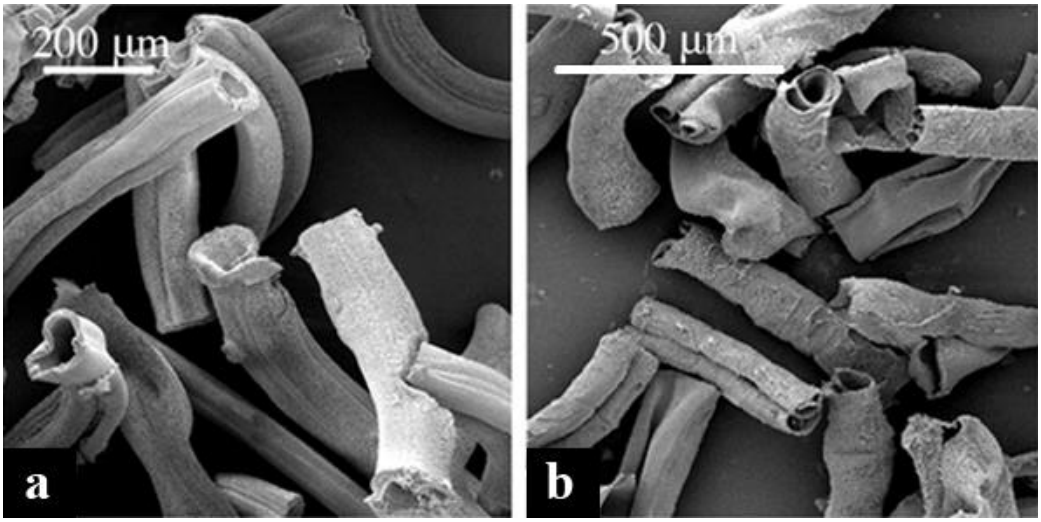


Figure 4.14. GA crosslinked PVA tubes (a) and rolled tubular polymeric films (b) after too much dissolution in water at 70°C.

4.2.5. Parameters That Affect Tube Wall Thickness of GA Crosslinked PVA Tubes

The effect of variables such as GA concentration, diffusion time of crosslinker solutions, reaction temperature and time on the thickness of the shell was investigated. It was found that the success of the surface reaction and the shell thickness depends on all of these parameters.

Diffusion time is the time that fibers were kept in crosslinker solutions. As diffusion time increases, the penetration probability of the crosslinker solution inside the core of the fibers becomes very high and therefore bulk crosslinking takes place and a water insoluble network is obtained. This is not suitable for our aim. However, by controlling the diffusion time of the crosslinker solution it is possible to control the shell thickness. The shell thickness increases with increasing diffusion time. However, beyond a certain time the fibers become bulk crosslinked and completely insoluble.

Reaction time is the time that the fibers were allowed to react with absorbed amount of GA. If reaction time increases the crosslinkers find time to penetrate further inside the core and fibers become bulk crosslinked. Reaction temperature is also an important parameter that has an effect on surface reaction. The extent of crosslinking reaction increases

as the temperature increases which reduces the possibility of surface reaction. However, increasing reaction temperature and decreasing reaction time may result in surface reaction. A large number of experiments were done to optimize these conditions. The crosslinking conditions that resulted in succesful tubular structures are summarized in Experimental section, Table 3.1.

In order to observe whether the reaction is limited to the surface or not fibers were swollen in water at 70°C. Figure 4.15 shows the cross sections of lightly crosslinked (a) and highly crosslinked (b) PVA fibers during dissolution of the inner core. Lightly crosslinked fibers start to dissolve however there is no change in the inner core of highly crosslinked ones showing their bulk crosslinked nature.

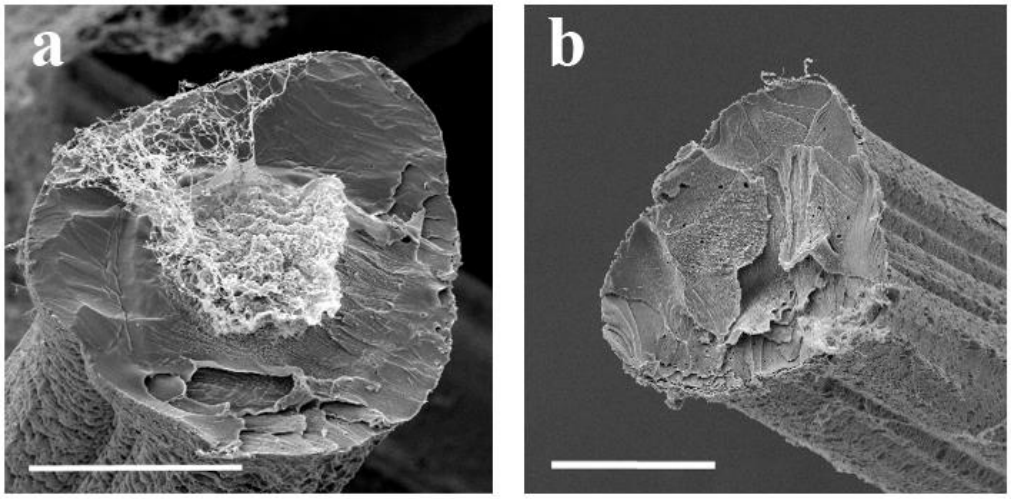


Figure 4.15. Cross sections of lightly crosslinked (a) and highly crosslinked PVA fibers (b) (Scale: 50μm).

In order to control the thickness of the shells it was found that changing the concentration of the crosslinker solutions gave better results then changing diffusion time, reaction time or temperature. The crosslinking reaction was done at six different concentrations of GA. The other parameters were kept constant as the concentration of GA solutions was changed. However, depending on the crosslinking density and the depth of the reaction only some of the fibers were succesfully converted to tubular structures.

After complete dissolution of the inner core GA crosslinked PVA tubular structures are formed (Figure 4.16). All are homogenous in thickness. Figure 4.16a and 4.16b show PVA tubes crosslinked with 0.02M GA, Figure 4.16c and 4.16d show PVA tubes crosslinked with 0.2M GA solution. Clearly, as the concentration increases the shell thickness of the tubes is increased.

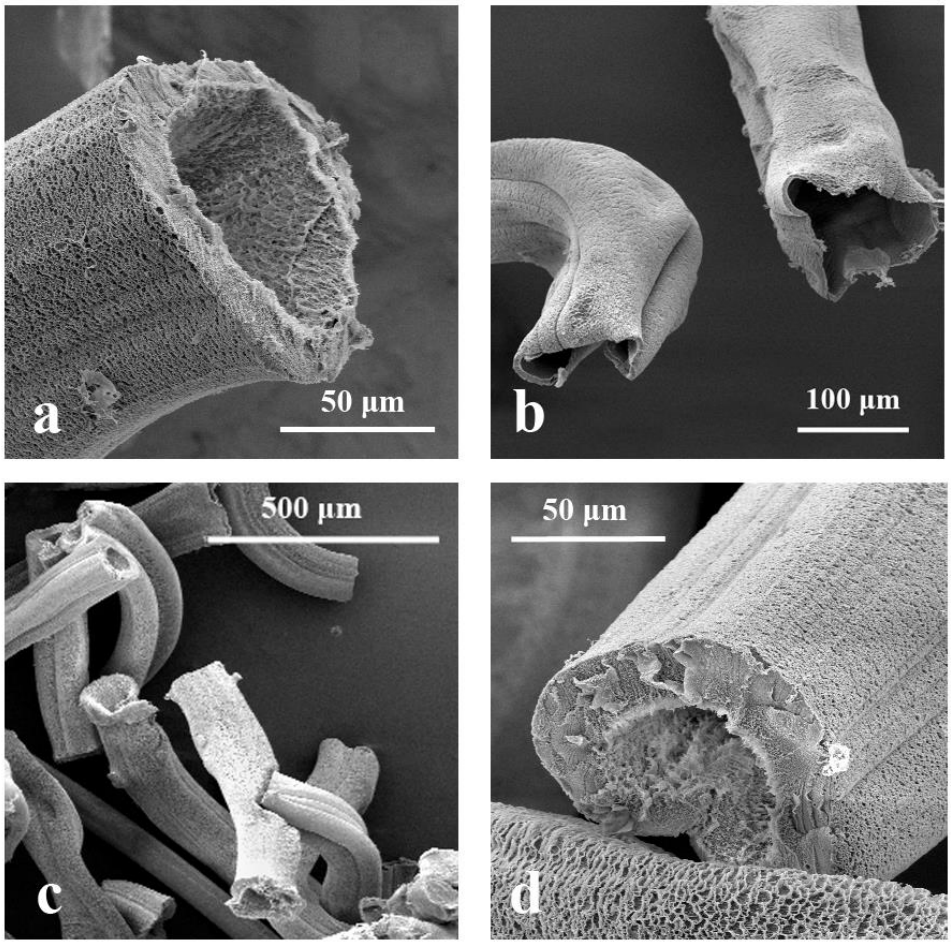


Figure 4.16. SEM images of crosslinked PVA polymeric tubes prepared in 0.02 M (a and b) and 0.2 M (c and d) glutaraldehyde solutions.

Crosslinked tubes couldn't be prepared by fibers reacted at lower GA concentrations than 0.02M. Their low crosslinked nature was confirmed by FTIR and water uptake results. During dissolution the lightly crosslinked shells could not stand the pressure created inside

by dissolved PVA and they ruptured easily. Crosslinking in concentrations above 0.2M, on the other hand, resulted in bulk crosslinking.

4.2.6. Dye Loading Properties of GA Crosslinked PVA Tubes

The shells of the GA crosslinked PVA tubes prepared in 0.02M and 0.2M GA solutions have uniform porous structure that look exactly like hydrogels, as shown in Figure 4.17. These tubes are glassy in dehydrated state but upon water penetration they swell and behave like an elastic gel. Such materials are known to be suitable for entrapment and controlled slow release of drugs or biological molecules. To simulate drugs Fluorescein dye was used as this molecule is readily observable in Fluorescence Microscopy.

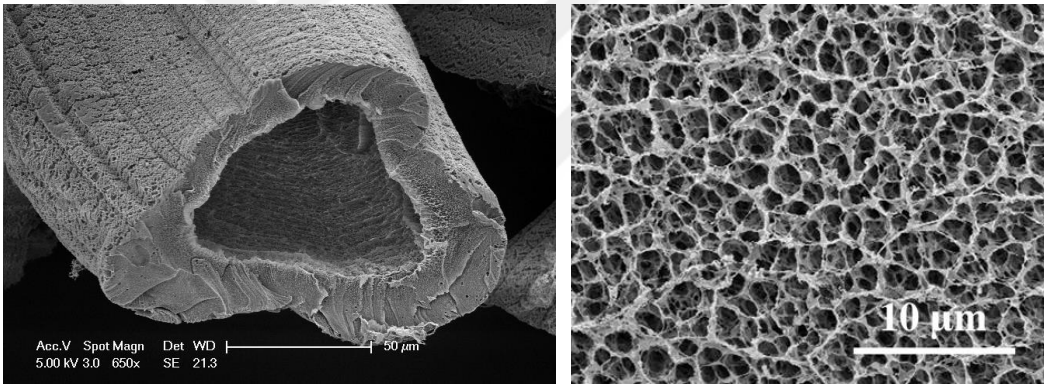


Figure 4.17. SEM images of the surface of PVA polymeric tubes crosslinked in 0.2M glutaraldehyde solutions.

Fluorescein dye was used for a load/release study in order to follow this process with optical microscopy. When these tubular hydrogels are placed into an aqueous medium containing dye molecules, some of the dye molecules pass through the core and fiber wall and may be entrapped inside the core or the molecules remain entrapped in the shell. If entrapped in the core the dye molecules will be released immediately after placing the crosslinked tubes into an aqueous environment. As this type of hydrogel is quite a hydrophilic system, it releases dye with a relatively high rate. This is not desirable to prolong dye release from such a system, the dye molecules must be entrapped in the shell. Optical microscopy images of tubes showed clearly that dye molecules were succesfully entraped into the shells and did not remain in the fiber cavities, as shown in Figure 4.18.

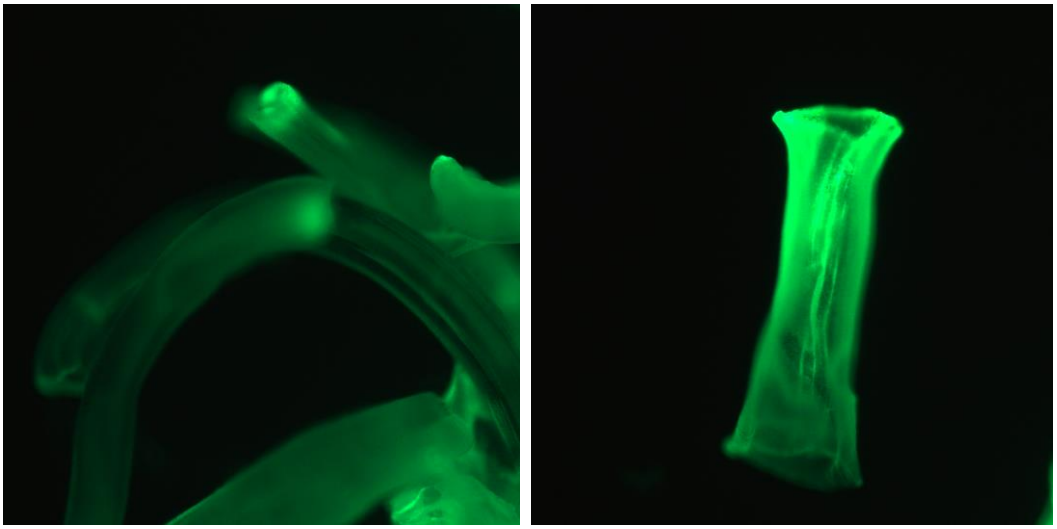


Figure 4.18. Optical microscopy images of fluorescein loaded PVA polymeric tubes crosslinked in 0.02M and 0.2M glutaraldehyde solutions.

The effect of several parameters such as initial dye concentration, crosslinking density or the thickness of the shells on the loading amount of dye molecules in the tubular hydrogels is summarized in Table 4.3.

Table 4.3. Loading amount of PVA polymeric tubes crosslinked in 0.02M and 0.2M glutaraldehyde solutions.

GA conc. (M)	**Thickness (µm)**	**Dye (w/v%) in the medium**	**Dye Loading (%)**
0.02	11	0.0200	5.88
0.02	11	0.0110	5.59
0.02	11	0.0048	5.21
0.2	20	0.0200	8.28
0.2	20	0.0110	8.03
0.2	20	0.0048	7.49

As Table 4.3 shows increasing the GA concentration from 0.02M to 0.2M increases the shell thickness also increases dye loading efficiency significantly. It seems that increasing shell thickness and crosslinking density has caused a better accomodation of the

dye solution in the tubular hydrogels. Similar properties were reported in the literature for GA crosslinked PVA films [59].

The amount of dye or drug molecules which can be loaded into a polymeric material, depends on three parameters, the dye/drug solubility in the initial solution, the solvent volume fraction of the crosslinked hydrogel, and the dye/drug partition coefficient between the polymer and the solution. If the crosslinking density is relatively high such that the network cannot accommodate the entire volume of the liquid, the solvent expels from the gel by contraction and this is known as syneresis [111]. The results show no decrease in loading efficiency by increasing crosslinking density or the thickness of the shells. It seems that increasing this parameter causes a better accommodation of dye and no syneresis has taken place in the concentrations used in this work. Changing the dye concentration from 0.02 to 0.0048 per cent (w/v) in the loading medium of the tubes also increases the loading efficiency significantly, as shown in Figure 4.19.

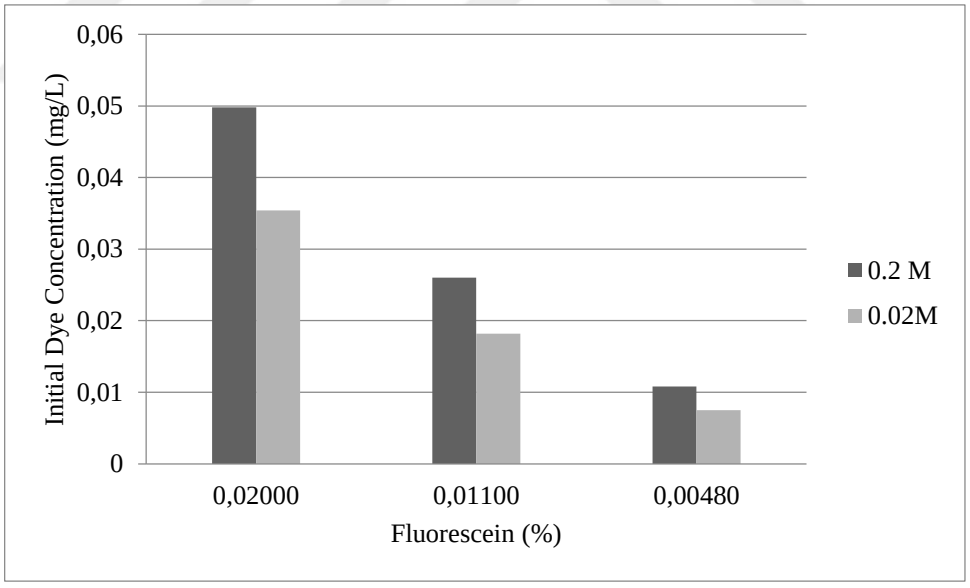


Figure 4.19. Initial dye concentrations of PVA polymeric tubes crosslinked in 0.02M and 0.2M glutaraldehyde solutions.

4.2.7. Dye Diffusion and Release Properties of the GA Crosslinked PVA Tubes

Rate of diffusion of dye molecules out of the crosslinked shells was monitored by measuring the difference between the concentration of the loaded tubes (C_0) and the concentration of water medim where dye released (C_t) in different time intervals. The concentration change (C_0-C_t) is inversely propotional to the rate of diffusion. The effect of pH on the rate of diffusion of dye molecules through GA crosslinked PVA tubular hydrogels is shown in Table 4.4. It seems that there is no significant difference between the diffusion of flourescein dye molecules at different pH values. This result is consistent with swelling data shown in Table 4.2 and it confirms that GA crosslinked PVA tubular hydrogels are not pH-sensitive.

Table 4.4. Effect of pH on release properties.

	Release (%) in 1h for 0.02M	**Release (%) in 1h for 0.2M**
pH 5	52.95±0.76	41.68±0.12
water	53.65±0.23	41.25±0.20
pH 9	57.12±0.51	43.42±0.23

Figure 4.20 indicates that increasing the crosslinking density decreases the diffusion of dye through PVA tubes significantly. This is probably due to the reduced free space available for solute transport, which essentially depends on the network structure. A similar behaviour for crosslinked PVA beads was also reported in the literature [112]. Decreasing GA concentration which corresponds to the decrease in shell thickness and crosslinking density, increases the diffusion of dye molecules. Higher swelling of tubular hydrogels produced by low GA concentration can explain the increase in diffusion by the free volume theory [113]. This theory was suggested for solute permeation in hydrogel films. It assumes that; solute diffuses only through aqueous regions, the solute diffuses through “fluctuating pores” by successive jumps, and the effective free volume available for transport is essentially the free volume of water in the hydrogel system.

Dye release studies show that as crosslinking density and thickness of the shells increases, the release rate of fluorescein dye from crosslinked shells decreases as shown in

Figure 4.20. Similarly, half life ($t_{1/2}$) of the dye release also increases with crosslinking and thickness. In one study the release of Santosol oil through PVA microcapsules showed the same pattern of release in the presence of different crosslinking agents [114].

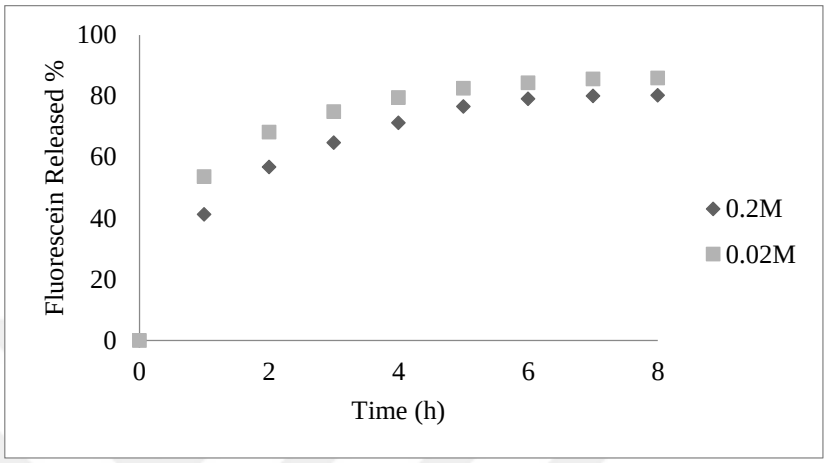


Figure 4.20. Plot of the released amount of fluorescein dye versus time for PVA polymeric tubes crosslinked in 0.02M and 0.2M glutaraldehyde solutions.

Figure 4.21 shows the effect of changes in fluorescein concentration on the release of dye molecules through PVA hydrogels crosslinked in 0.2M GA solution. The results show that increasing the dye content causes an increase in the rate of dye release as expected [115-116].

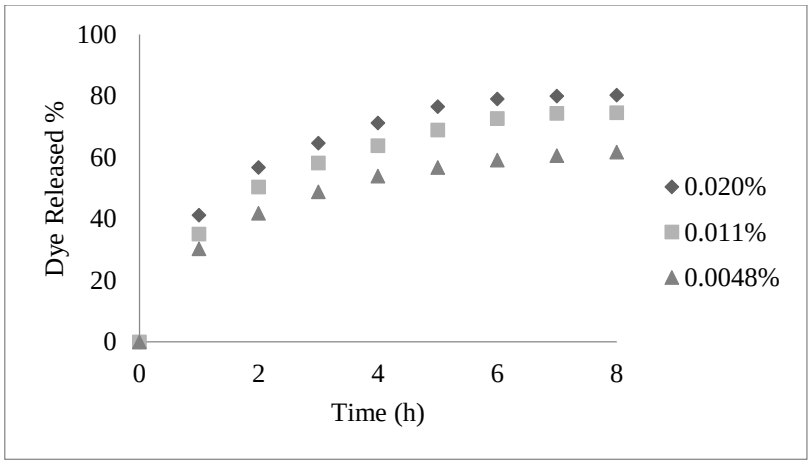


Figure 4.21. Effect of dye loading on the release from PVA tubular hydrogels crosslinked with 0.2M GA concentration.

The design of a prolonged drug delivey system is a serious business as lives may depend on the performance of the system. It would be presumtious to claim that a working controlled prolonged drug delivery system has been invented in this work. While all the necessary requirements have been met, much more work is needed. As Figure 4.19 shows increasing dye concentration in the soaking medium results in higher loading of dye in the crosslinked tubular hydrogels, increasing release per cent and therefore the diffusion (Figure 4.21). In general increasing the dye content acts as a driving force for water uptake which increases both release per cent. Decreasing the crosslinking density also increases the diffusion rate.

4.2.8. Contact Angle Measurements of GA Crosslinked PVA Films

PVA films were previously crosslinked with succinic anhydride and isocyanate functionalized soybean oil triglycerides in our group [117]. The crosslinking reaction was carried out with PVA films attached on glass slides so that only one side of the films was accessible for crosslinking. The two sides of such films had hydrophilicity differences. Triglyceride crosslinked side was hydrophobic wheras the other side was hydrophilic due to unreacted PVA. Such films with different surface properties may have potential applications as membranes with one-way permeability, in wound dressings and in biomedical applications such as enzyme purification.

The tubes obtained by this method should have similar properties. The crosslinked outer shell is expected to have a relatively hydrophobic property while the inner core should be more hydrophilic due to higher concentration of unreacted hydroxyl groups on the inside wall of the shells.

Hydrophilicity or wettability of crosslinked fibers can not be determined by contact angle (θ) measurements since they have no flat surfaces. In order to do contact angle measurements crosslinked films were prepared on microscope slides by using the same GA concentrations and same reaction conditions as fibers. When surface is more hydrophilic it can be easily wetted by water leading to smaller contact angles. Table 4.5 summarizes the results of contact angle measurements. It is concluded that, as GA content in the crosslinked films increases, the contact angle and hydrophobicity increase. The increase of overall

hydrophobicity of the outer surface with enhanced grafting of GA is due to the hydrophobic alkyl chains which are introduced onto PVA films by crosslinking.

Table 4.5. Contact angles (θ) of PVA and GA crosslinked PVA films.

GA concentration (M)	**Contact Angle (θ, degree)**
0	45
0.002	54
0.01	57
0.02	61
0.2	68
0.5	73
1	75

According to these results the outer shells of PVA polymeric tubes crosslinked in 0.02 M and 0.2M glutaraldehyde solutions were expected to have contact angles around 61 and 68°, respectively. This hydrophobicity difference may help to decrease the release rate of dye or drug molecules into an aquous medium and this is very important in prolonging the release.

4.2.9. Crosslinking of PVA Nanofibers with Glutaraldehyde

Compared to PVA micron size fibers, nanofiber mats need less diffusion time compared to micron size fibers due to their high specific surface area. It is expected that if the diffusion time of crosslinker solution increases, nanofiber mats become bulk crosslinked and will be completely insoluble in water. According to our previous experience from microfibers the crosslinker concentrations applied were 0.02M and 0.2M. Nanofibers were kept in these solutions only for 10 seconds, washed immediately with ethanol and crosslinked at 50^{o}C for 2.5 h. SEM images of crosslinked fibers before dissolution (a and b) and after dissolution (c and d) are shown in Figure 4.22. It was observed that in a low concentration the surface crosslinking of the nanofibers was achieved, while with a high concentration bulk crosslinking took place. In both cases no tubular formation was achieved. During dissolution as inner PVA core swells, very thin shells do not withstand the osmotic

stress created inside the core since there are no open ends and therefore the shells tend to be ruptured very fast.

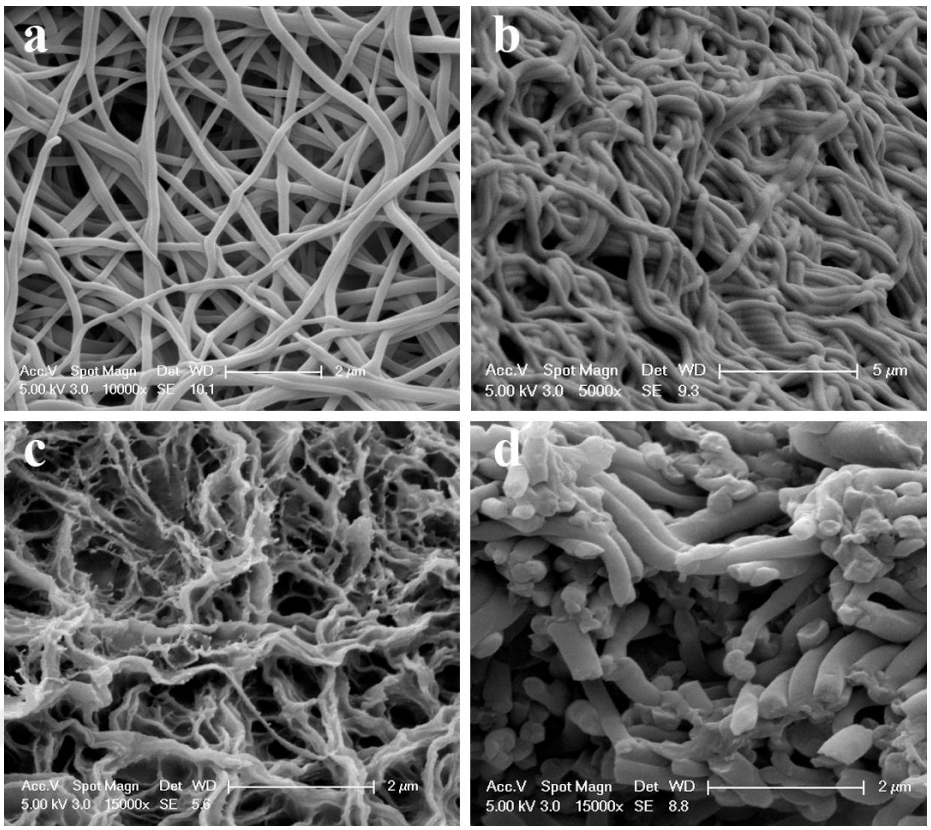


Figure 4.22. SEM images of crosslinked PVA nanofibers in 0.02M (a) and 0.2M (b) glutaraldehyde solutions and their dissolved products, respectively (c and d).

4.2.10. Crosslinking of PVA with Glyoxal

Glyoxal (GLY) is a difunctional aldehyde just like GA and it has been used as a crosslinker for PVA [118]. Like GA crosslinking reaction of PVA with GLY can be conducted under mild conditions which means PVA fiber templates may remain intact during the reaction. Therefore, GLY may be a good candidate to fabricate crosslinked tubular structures from PVA fibers.

The same procedure used for glutaraldehyde crosslinking was applied in the surface reaction of PVA with GLY. In this case ethanol which is a non-solvent for PVA was used as a reaction medium. PVA fibers were expected not to swell in ethanol although GLY used

contains 40 per cent of water and hence crosslinking agent could not penetrate inside the fiber matrix.

4.2.11. FTIR Characterization of GLY Crosslinked PVA Fibers

The crosslinking reaction is shown in Figure 1.15. The FTIR spectra of PVA fibers which were crosslinked with two different concentrations of GLY are shown in Figure 4.23. The reaction of PVA with GLY results in a reduction of the intensity of -OH stretching vibration peak (υ= 3310-3350 cm^{-1}) which is due to the consumption of hydroxyl groups upon reaction with GLY. The bands at 2941 and 2911 cm^{-1}corresponds to C-H stretching vibrations related to aldehydes, a duplet absorption with peaks attributed to the alkyl chain. The two peaks at 1431 and 1374 are from secondary –OH in plane bending and C-H wagging vibrations. There is an increase in the absorbance of the peak at 1374 cm^{-1} indicating the formation of an acetal ring as a result of the crosslinking reaction between hydroxyl groups of PVA and aldehyde groups of GLY. The bands at 1141 and 1091 cm^{-1} correspond to C-C stretching and C-O stretching vibrations of PVA where an intermolecular hydrogen bond is formed between two neigbouring –OH groups that are on the same side of the plane of the carbon chain which is related to crystallinity. The crystalline portion and the peak intensity of 1141 cm^{-1} is dependent on the number of neigbouring –OH groups of PVA. Increasing the density of GLY solution results in a decrease in the intensity of the peak at 1141 cm^{-1} and decrease in crystallinity.

Strong band from carbonyl group was also verified (C=O at υ= 1738-1713 cm^{-1}) and an increase in the intesity of this peak with GLY concentration was observed which is an unexpected situation. According to the spectra the presence of aldehyde peaks can be an evidence for unreacted pendant aldehyde groups on PVA chains created by monofunctional reaction of GLY.

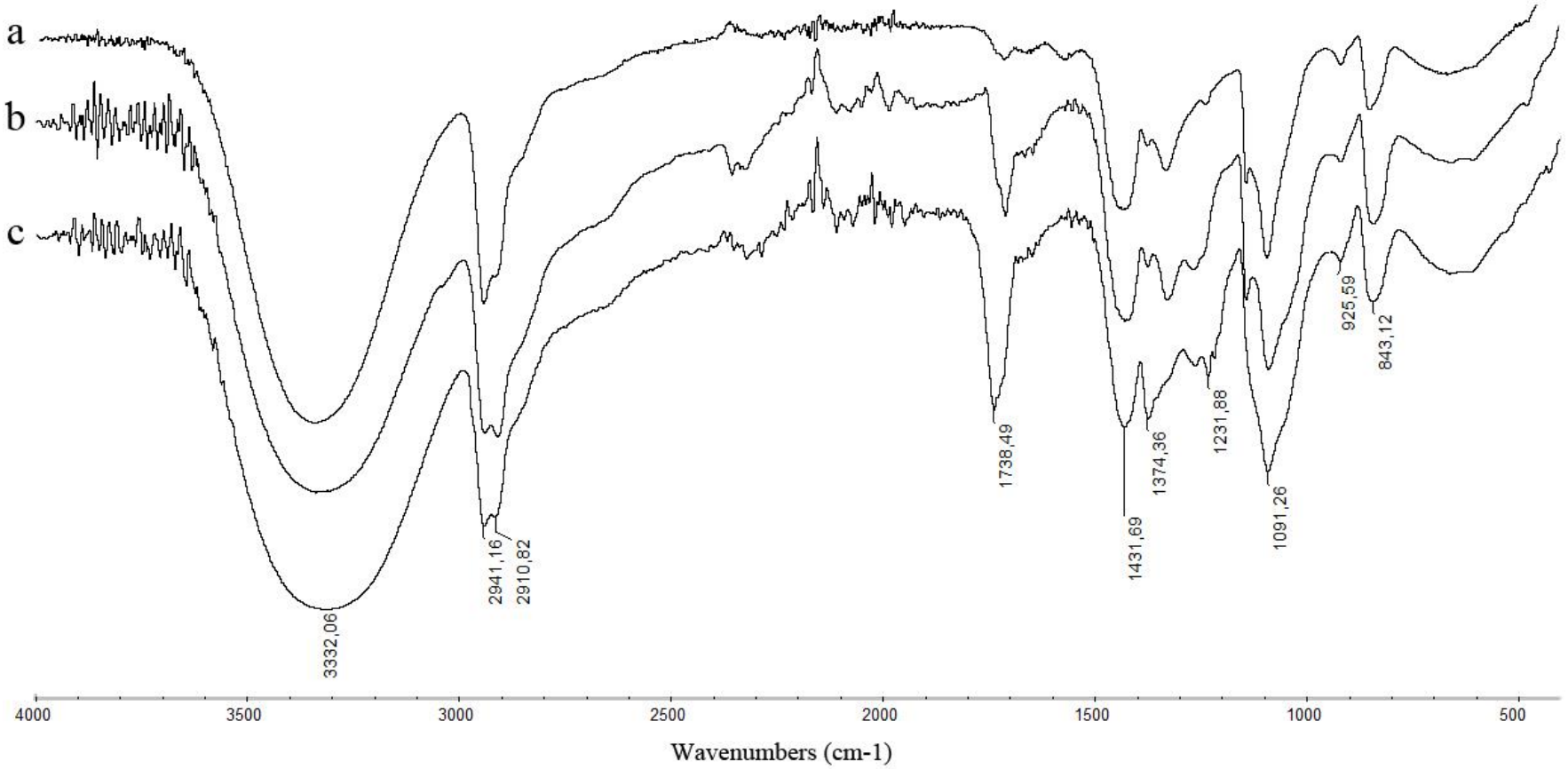
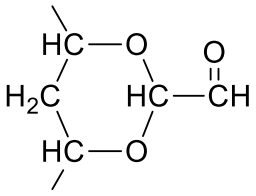


Figure 4.23. FTIR spectra of neat PVA (a) and PVA crosslinked in 0.002M (b) and 0.01M (c) glyoxal solutions.

From well known reaction mechanisms in the literature and FTIR spectra analysis, typical products of the reaction between PVA and GLY are shown in Figure 4.24. Four hydroxyl groups of PVA could react with one equivalent of GLY if both aldehyde groups of GLY monomer had reacted. The reactions between GLY and PVA can be intramolecular and/or intermolecular crosslinks, either make PVA insoluble, Figure 1.15 shows the expected chemical crosslinking reaction between PVA chains and GLY catalyzed by hydrochloric acid and the formation of structure a (Figure 4.24) was well documented [118]. 6 and 7 membered cyclic acetals are possible. According to the FTIR spectra mostly structure b (Figure 4.24) is formed by one-sided reaction of GLY and unreacted aldehyde pendant groups may remain on PVA chains. This possibility also renders the fibers insoluble in water which shows their crosslinked nature.



a. Cyclic Acetal Formation



b. Aldehyde Formation by One-sided Reaction

Figure 4.24. Expected crosslinked products by the reaction between PVA and GLY.

In order to quantitatively analyze FTIR spectral changes, the absorbance ratios of several functional groups to several reference peaks were determined which are shown in Table 4.6.

The ratio of the peak at 3300 cm^{-1} corresponding to hydroxyl groups to methylene stretching band around 2900 cm^{-1} was calculated in order to follow the change in the number of hydroxyl groups with increasing GLY concentration. It can be clearly observed that an

increase in GLY content resulted in the reduction of available hydroxyl groups and consequently higher degree of crosslinking.

Table 4.6. Absorbance ratios of several FTIR bands belong to PVA, crosslinked PVA in 0.002 and 1M GLY solutions.

	PVA	**GLY(0.002M) PVA**	**GLY(0.1M) PVA**
$\mathbf{A_{3300}/A_{2900}}$	6.97	4.17	3.31
$\mathbf{A_{1750}/A_{2900}}$	0.038	0.106	0.586
$\mathbf{A_{1141}/A_{1096}}$	0.057	0.045	0.032

The presence of monofunctional reaction was shown by the ratio of the peak at 1750 cm^{-1} corresponding to aldehyde group to the band at 2900 cm^{-1}. The absorbance ratio of the aldehyde group showed a huge increase with increasing GLY concentration of reaction solutions.

The relationship between crosslinking and crystallinity was established by using the ratio between 1141 and 1096 cm^{-1} peaks. The crystallinity depends on the number of –OH groups which are able to form hydrogen bonds. As GLY content increases the number of available –OH groups decreases which reduces crystallinity.

4.2.12. Determination of Crosslinking Density for GLY Crosslinked PVA Fibers by Swelling

The degree of swelling is dependent upon the crosslink density of polymer networks. Two different GLY concentrations lead to significant difference in water uptake properties of crosslinked PVA networks. By increasing the concentration of crosslinking agent chain entanglement occurs which would result in highly crosslinked rigid structure and a decreased network expansion and this in turn reduces the swelling or water uptake of the gels significantly.

Water uptake is around 20 and 15 per cent for crosslinked fibers in 0.002M and 0.1M GLY reaction solutions. This shows that in these low and high monomer concentrations the

reaction may not be limited to the surface since all monomers penetrate inside the fiber matrix to cause bulk crosslinking which will be investigated in the following template removal section.

4.2.13. Removal of the Core from GLY Crosslinked PVA Fibers

The chemical properties of GLY crosslinked PVA is very similar to GA crosslinked PVA and so both of them were expected to have similar thermal properties. Since there is no significant difference in degradation stages of PVA and aldehyde crosslinked PVA fibers solvent extraction method was used to remove unreacted PVA core templates. GLY crosslinked PVA fibers were immersed in water at 70°C for different time periods. After dissolution crosslinked fibers were monitored by scanning electron microscopy.

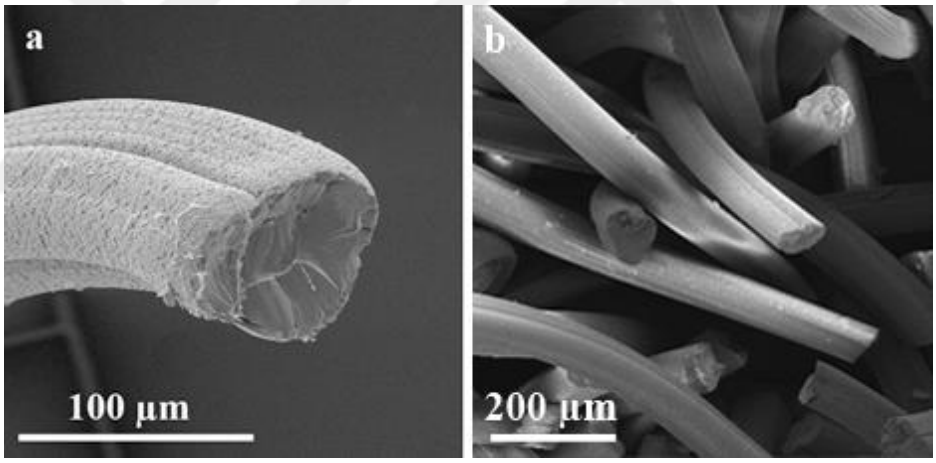


Figure 4.25. SEM images of crosslinked PVA fibers in 0.002M (a) and 0.1M (b) GLY solutions.

According to SEM images shown in Figure 4.25, unfortunately, it was observed that no tubular structures were formed. As shown in the GA case it is predicted that the crosslinking reaction in ethanol is a surface reaction. However, in this case this prediction was not confirmed by SEM images. It seems that both low and relatively high concentrations of GLY solutions cause bulk crosslinking. GLY molecules are smaller then GA and compared to GA the diffusion of GLY into the polymer matrix is expected to be very high which increases the possibility of bulk reaction. This situation was also confirmed by FTIR

spectroscopy. According to FTIR spectra the stretching vibration of aldehyde peaks is very intense (Figure 4.23b and Figure 4.23c) which also proves the bulk reaction. Therefore, these results showed that GLY monomer is not suitable for fabrication of crosslinked tubular structures since it results in bulk crosslinking. No differentiation was possible between the core and the shell. The same crosslinking reaction was not repeated with nanofibers due to the bulk crosslinking possibility.

4.3. Fabrication and Characterization of Diisocyanate Crosslinked PVA Tubular Structures

Reaction of PVA with diisocyanates is one of the techniques used in the literature especially for crosslinking of PVA. In general crosslinking reactions of PVA with diisocyanates can be conducted with or without using catalysts and this reaction results in the formation of urethane or urethane-urea bridges. Most of the literature examples were applied in bulk, there are only a few examples showing the surface crosslinking of PVA with diisocyanates [82, 119]. PVA fibers and films were reacted with hexamethylene diisocyanate to introduce isocyanate groups on the surface of PVA. Residual isocyanate groups were hydrolyzed to primary amine functionalities in order to get biocompatible materials since amine groups on PVA are used to bind biomolecules such as heparin (anticoagulant) or fibrinolytic enzymes. PVA was also crosslinked by using triisocyanates in the presence of enzyme to prepare membranes [120].

General crosslinking reaction mechanism is shown in Figure 1.18. The crosslinking comes from the reaction of both isocyanate ends of the crosslinker with surface –OH groups of PVA. Unlike dialdehyde monomers, if only one end of isocyanates react with PVA, there will be no crosslinking reaction and only the monomers graft onto the polymer chain which results in both –NCO or $–NH_2$ functionalities on the surface. In this study careful adjustment of monomer concentration was made so that while keeping control of crosslinker diffusion to a thin outer shell, the reaction of both isocyanate ends was triggered.

4.3.1. Crosslinking Reaction of Poly(vinyl alcohol) with Hexamethylene Diisocyanate

In a general procedure hexamethylene diisocyanate (HMDI) was absorbed onto PVA fibers from different concentrations of crosslinker solutions at room temperature. Excess HMDI which does not penetrate inside the fiber matrix in a given time duration was washed off from the surface of the fibers. The reaction occurs without using any catalyst. After complete crosslinking reaction, the unreacted core was removed. The selection of solvent, concentration of HMDI monomer solutions and diffusion time of these monomer solutions inside PVA fiber matrix have a significant effect to confine the reaction on the surface.

Non-solvents for PVA which are miscible with HMDI were tried as a reaction medium. In the literature it was reported that since this is a heterogenous reaction, it is difficult to get reproducable data on the extent of reaction [82]. Surface crosslinking with HMDI was carried out in dimethyl formamide (DMF), acetone, and toluene at the same temperature and the same HMDI concentrations under nitrogen atmosphere to investigate the effect of solvent on the extent of crosslinking. Using different solvents will bring different swelling environments which may change the extent of surface reaction.

4.3.2. FTIR Characterization of PVA Fibers Reacted with HMDI in Different Solvents

FTIR spectra of PVA fibers reacted with HMDI in different solvents like DMF, acetone and toluene are shown in Figure4.26a, Figure4.26b and Figure4.26c, respectively. The spectrum of PVA fibers crosslinked with 0.1M HMDI solution in DMF (Figure 4.26a) shows a distinct new band at 1693 cm^{-1} which is attributed to C=O stretching of the urethane groups formed. The –NH stretching vibrations of the urethane group cannot be distinguished since they overlap with unreacted –OH stretching vibrations of PVA at 3319 cm^{-1}. However, –NH bending can be seen at 1556 cm^{-1}. The backbone aliphatic C–H stretching vibrations give sharp bands at 2940 and 2914 cm^{-1}. The stretching vibrations of methylene groups in HMDI may overlap with these bands. However, it is obvious that the band at 2860 cm^{-1} corresponds to C–H stretching vibrations of HMDI. Ether linkage (C–O–C) which is found in PVA and HMDI crosslinked PVA is assigned at 1090 cm^{-1}. The characteristic bands for the –NCO groups are usually observed in the range of 2260 cm^{-1}. The disappearance of this

stretching vibration band suggests that there is no unreacted isocyanate groups left in the reaction which occurs in DMF.

The spectra of PVA fibers reacted with HMDI in acetone and toluene (Figure 4.26b and Figure 4.26c, respectively) show similar bands. The broad band at 3324 cm^{-1} related to both –NH stretchings of amide and –OH groups of unreacted PVA. The peaks at 2932 cm^{-1} and 2856 cm^{-1} correspond to C–H stretchings of alkyl groups. A small shoulder around 1682 cm^{-1} can be attributed to C=O stretchings of the urethane groups formed, as shown as Figure 4.27 (structure **a** or **b**). The band at 1617 cm^{-1} is related to C=O of the urea group ,the band at 1571 cm^{-1} corresponds to amide group shown in Figure 4.27 structure **e** and **f**. The band at 1252 cm^{-1} corresponds to another type of amide shown in structure **d** in Figure 4.27 [121]. All of these assignments suggest the formation of urethane-urea linkages between PVA and HMDI [122]. Ether linkage (C–O–C) is assigned at 1090 cm^{-1}. The characteristic bands for the –NCO groups is observed in the range of 2270 cm^{-1}, showing that some unreacted –NCO groups exist after the reaction which may be an evidence for functionalization of PVA with HMDI shown in structure **b** and **e** in Figure 4.27. If acetone or toluene is used as a reaction medium, apparently the extent of crosslinking is low. The isocyanate mostly reacts with one end only and very little crosslinking is observed. Therefore, surface crosslinking reaction was decided to be conducted in DMF.

From well known reaction mechanisms in the literature typical products of the reaction between PVA and HMDI are shown in Figure 4.27. Two hydroxyl groups of PVA undergo reaction with one mole of HMDI if both isocyanate ends of HMDI monomer are reacted. The reactions between HMDI and PVA can be intermolecular (a) and/or intramolecular (b), either make PVA insoluble, as shown in Figure 1.18. According to surface reactions reported in the literature [82, 120] structure **b** (Figure 4.27) may be formed by monofunctional reaction of HMDI and unreacted isocyanate pendant groups may remain on PVA chains. However, this is not desirable since this possibility will not render the fibers insoluble in water. Therefore, the selection of solvent is very important.

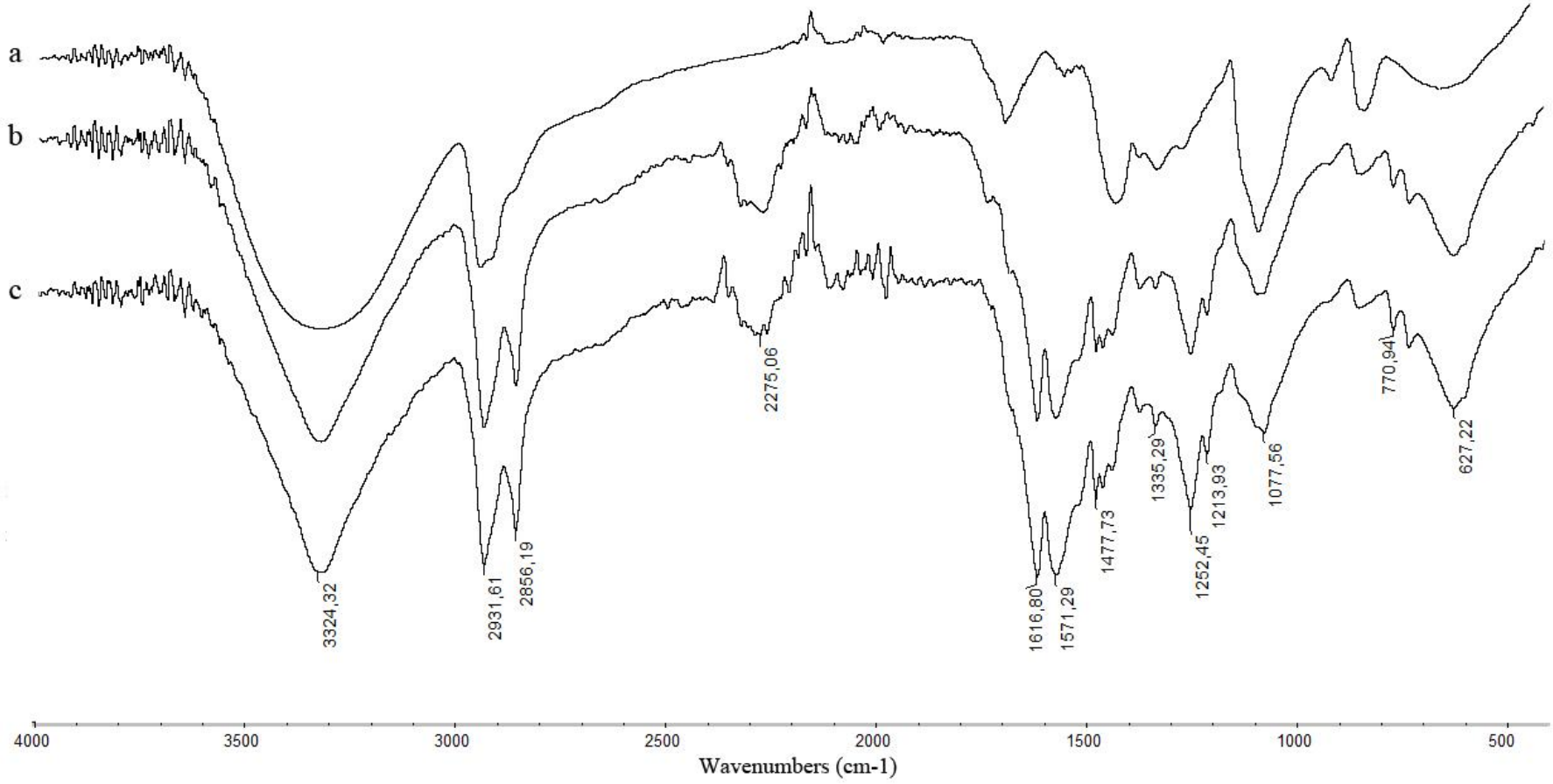


Figure 4.26. FTIR spectra of PVA crosslinked with 0.1M HMDI solutions prepared in DMF (a), acetone (b), and toluene (c).

HMDI is a flexible, linear, and symmetrical molecule with two primary aliphatic isocyanate groups which are expected to have equal reactivities. However, as a general rule, each isocyanate groups of a diisocyanate has different reactivities, in spite of the perfect symmetry of the molecule. During the reaction a diisocyanate is first converted into urethane isocyanate. The second isocyanate group has a much lower reactivity than the first one, because the urethane group, due to its electron releasing effect, decreases the reactivity. The reactivity ratios of isocyanate groups in HMDI against hydroxyl groups was reported as $K_1/K_2=2$ [123]. Therefore, the hydroxyl groups of PVA on the surface should be easily accesible for the second isocyanate group of the monomer to increase the possibility of the crosslinking reaction. PVA does not swell in acetone or toluene since they are not very good solvents for PVA. One end of the isocyanate can react with surface hydroxyls, however, the other end which will have lower reactivity may not penetrate inside the matrix and due to the distance between these two functional groups, crosslinking reaction may not take place even though the reaction is conducted in these solvents at long reaction times. If DMF is used as solvent, PVA will swell adequately and HMDI penetrates inside the fiber matrix and the crosslinking reaction is expected to be uniformly distributed throughout the matrix. In order to keep the reaction only on the surface, PVA fibers were kept in monomer solutions prepared in DMF at a limited time to cause an appreciable swelling and penetration of crosslinking agent in the surface PVA chains. However, increasing the concentration of HMDI monomer solutions and the diffusion time of these monomer solutions into the fiber matrix may increase the probability of bulk reaction. Numerous concentrations and swelling times were tried. The reaction conditions are summarized in Table 3.3. Star (*) labelled conditions resulted in the formation of tubular structures.

In some cases due to moisture and water inside the reaction medium, isocyanate ends may be transformed into amine groups, as shown in Figure 4.27 c. The reaction between isocyanates and water leads to the production of gaseous carbon dioxide and an amino group which can react with a free isocyanate group to form urea linkages (Figure 4.28). The crosslinked and functionalized PVA products are depicted in Figure 4.27 d, e, and f. Reactivity of primary amine groups with isocyanates is much faster than with primary alcohols or water. The reaction of primary hydroxyl groups or water with isocyanate groups is around three times faster than secondary hydroxyl groups of PVA [124]. Therefore, in the presence of even a little amount of moisture many isocyanates may be converted into amines

and/or some of the isocyanate functional fibers (structure e, Figure 4.27) may become amine functionalized (structure f, Figure 4.27) and these amines may react with other isocyanate groups of HMDI or the other isocyanate functionalized PVA fibers, which may result in a crosslinked network (structure d, Figure 4.27) through urethane-urea bridges. According to FTIR spectra both of these structures appear to be formed in the presence of acetone or toluene which may be due to several reasons. Unlike DMF, the crosslinking reaction of PVA with HMDI in these solvents is very slow and this reaction results mostly in monofunctionalization.

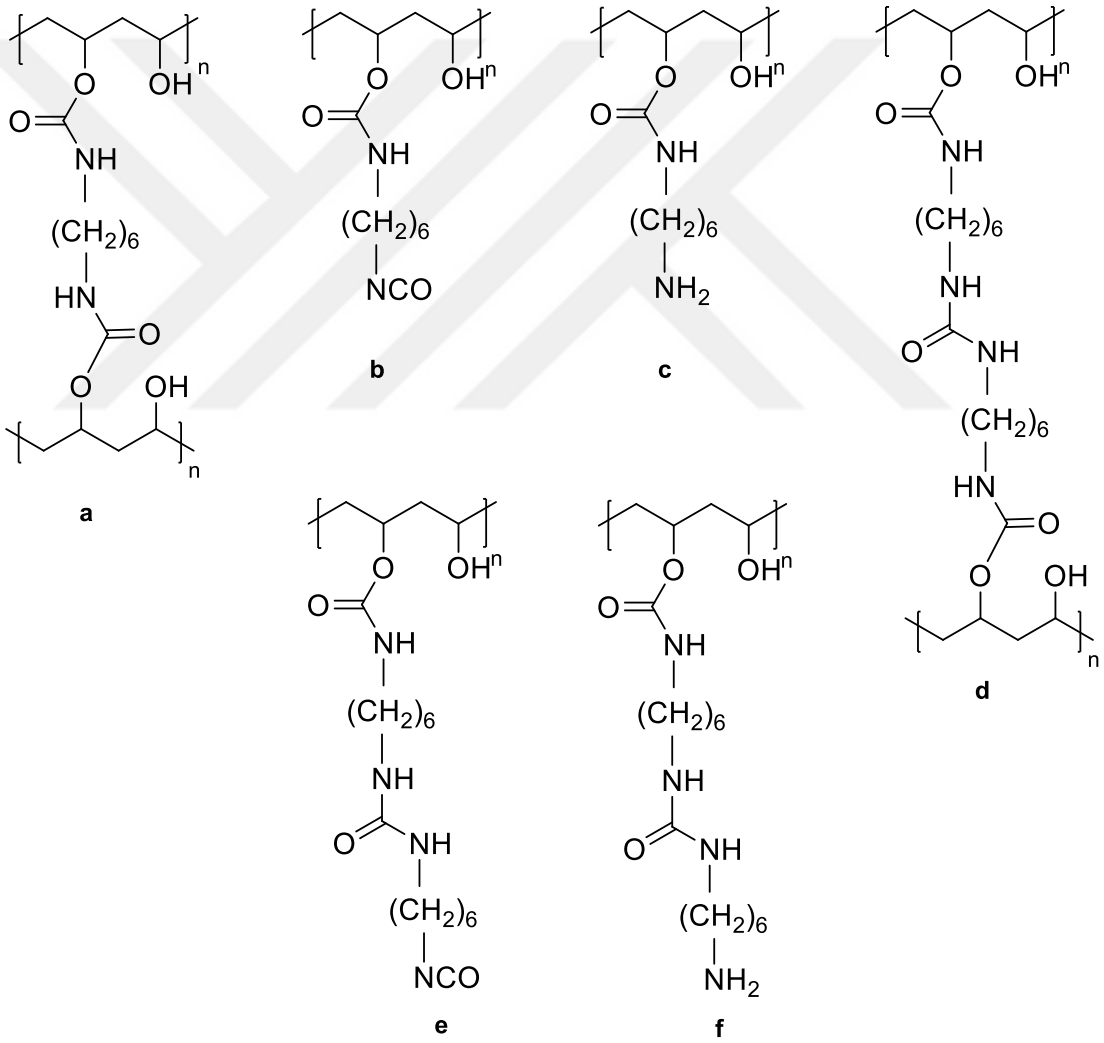


Figure 4.27. Expected products by the reaction between PVA and HMDI.

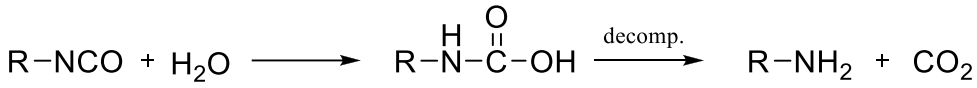


Figure 4.28. The reaction of isocyanates with moisture (water) and monomers with amine functionalities.

Five different concentrations of HMDI reaction solutions were used for FTIR and crosslinking density characterization by swelling. The diffusion time of monomers, reaction temperature and duration were kept constant as the concentration of HMDI solutions was changed. All samples were used after dissolution of unreacted PVA. However, depending on the crosslinking density only some of the fibers were succesfully resulted in tubular structures. Similar to the GA case, crosslinked tubes could only be prepared from fibers that had just the right crosslinking ratio.

The FTIR spectra of HMDI crosslinked PVA fibers are shown in Figure 4.29(b-f) and vibration band frequencies are summarized in Table 4.7.

There are several changes observed with increasing HMDI solution concentration, as shown in Figure 4.29. The reaction of PVA with HMDI results in a reduction of the intensity of –OH stretching vibration peak (υ= 3310-3350 cm^{-1}). This spectral change is due to the consumption of hydroxyl groups upon reaction with isocyanates. When the concentration of HMDI increases, the peak around 3320 cm^{-1} becomes more likely corresponding to the total amount of stretching vibrations of –OH groups and –NH groups of polyurethane formed after the reaction. FTIR spectra of HMDI crosslinked PVA samples show an increase in the intesity of the band at 2863 cm^{-1} which may be related to C-H stretchings of HMDI. Furthermore, there is an increase in the absorbance of the peak at 1693 cm^{-1} indicating C=O of the urethane group formed. For high concentrations above 0.1M of HMDI the peaks around 1627 and 1556 cm^{-1} corresponding to C=O and N-H stretchings of urea groups become visible showing the presence of reaction between HMDI molecules with themselves. Increasing the concentration, excess HMDI molecules which could not react with PVA surface hydroxyls prefer to react with each other resulting urea and isocyanate formation. The intensity of the peak at 1144 cm^{-1} which is related to the C-C symmetric stretchings decreases with crosslinking of PVA with HMDI. As expected, the crystalline portion

depends on the number of -OH groups on PVA chain which are able to form hydrogen bonds. As HMDI content increases crosslinking density, the number of available –OH groups decreases which reduces crystallinity. Furthermore, the absence of –NCO bands at 2260 cm^{-1} shows there is no pendant –NCO groups remaining on the surface.

Table 4.7. Vibration band frequencies of PVA and HMDI crosslinked PVA.

	Chemical Groups	**Wavenumber (cm^{-1})**
PVA **PVA-HMDI**	O-H from intermolecular and intramolecular hydrogen bonds Overlapped O-H stretchings and N-H stretchings	υ 3550-3200 (broad)
PVA **PVA-HMDI**	C-H from alkyl groups C-H from alkyl groups	υ 2940-2914 υ 2914-2863
PVA **PVA-HMDI**	C=O of acetate C=O of urethane and urea	υ 1714-1666 υ 1693 and 1627
PVA-HMDI	N-H bending	υ 1556
PVA **PVA-HMDI**	Secondary –OH in plane bend. C-H wagging of CH_2	υ 1430-1332
PVA **PVA-HMDI**	Ester C=O Amide N-H υ C=N	υ 1263
PVA	C-C-C symmetrical stretching (sensitive to crystallinity)	υ 1144
PVA **PVA-HMDI**	C-O-C	υ 1090

In order to quantitatively analyze FTIR spectral changes, the absorbance ratios of several functional groups to several reference peaks were determined and plotted. The methylene stretching band at 2900 cm^{-1} was taken as a reference peak. The ratio of the peak at 3320 cm^{-1} corresponding to hydroxyl groups to this reference peak was plotted against HMDI content in the reaction solution. The graph is shown in Figure 4.30. It can be clearly observed that an increase in HMDI content results in higher degree of crosslinking and consequently the reduction of available hydroxyl groups.

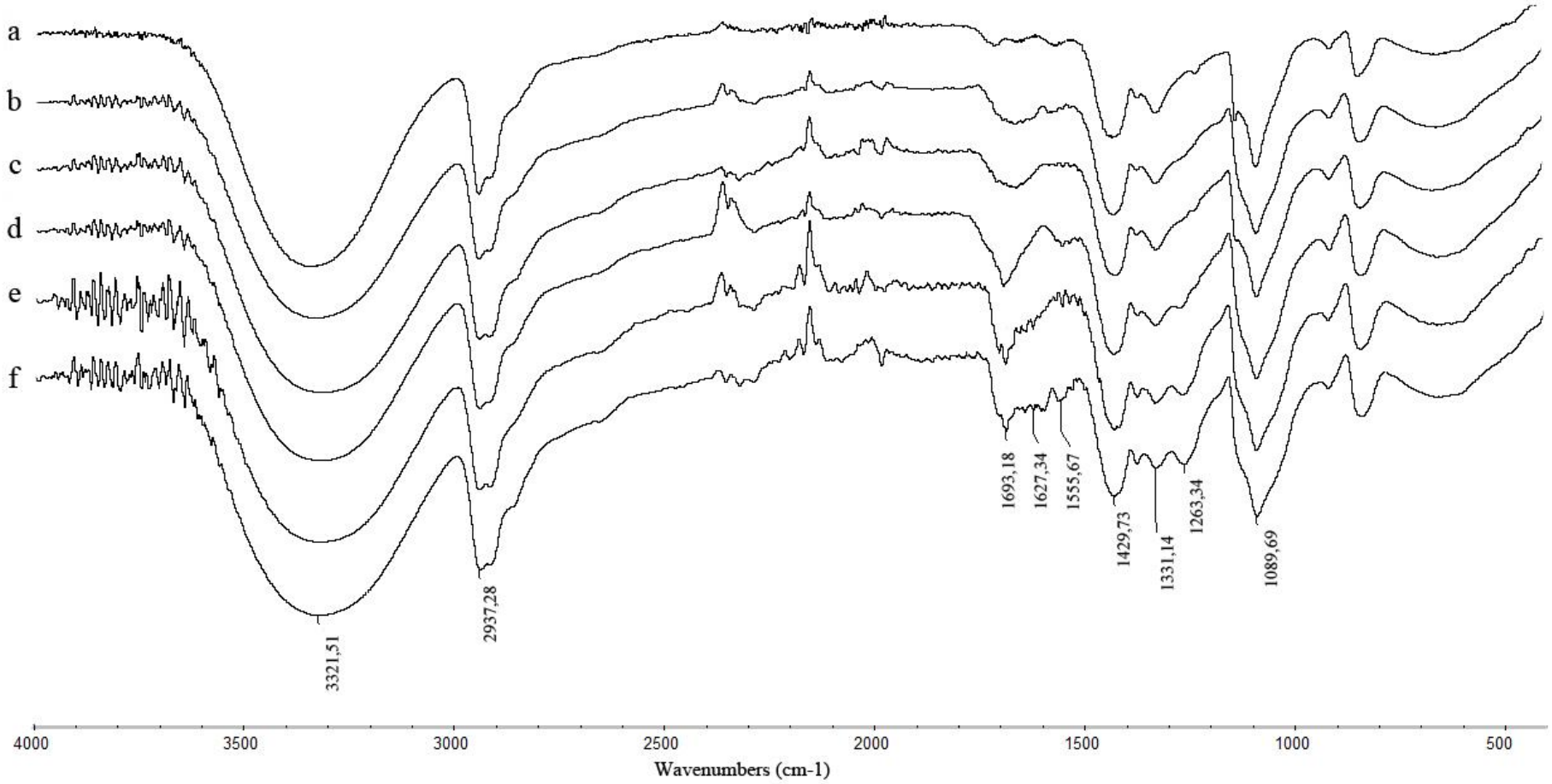


Figure 4.29. FTIR spectra of neat PVA (a) and PVA crosslinked in 0.01M (b), 0.04M (c), 0.1M (d), 0.2M (e), and 0.3M (f) HMDI solutions in dimethyl formamide.

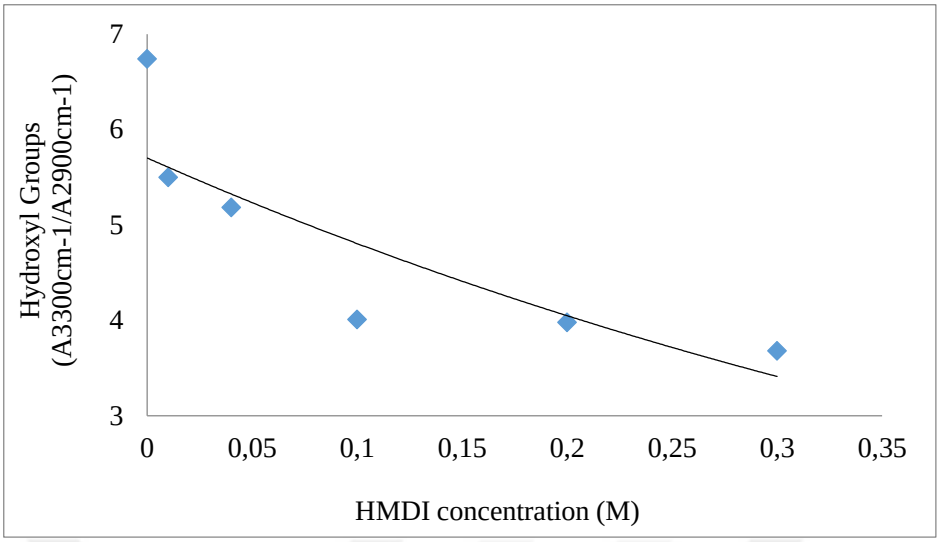


Figure 4.30. Absorbance ratio of the peak at 3300 cm^{-1} to a reference peak (2900 cm^{-1}) on crosslinked PVA with different HMDI content in reaction solution.

The ratio of the peak around 1693 cm^{-1} corresponding to both urea and urethane groups to 2900 cm^{-1} was plotted against HMDI content in the reaction solution to show the extend of crosslinking reaction. The graph is shown in Figure 4.31. The absorbance ratio of the urethane carbonyl group showed a constant increase with HMDI concentration in reaction solution while that of hydroxyl groups decreased.

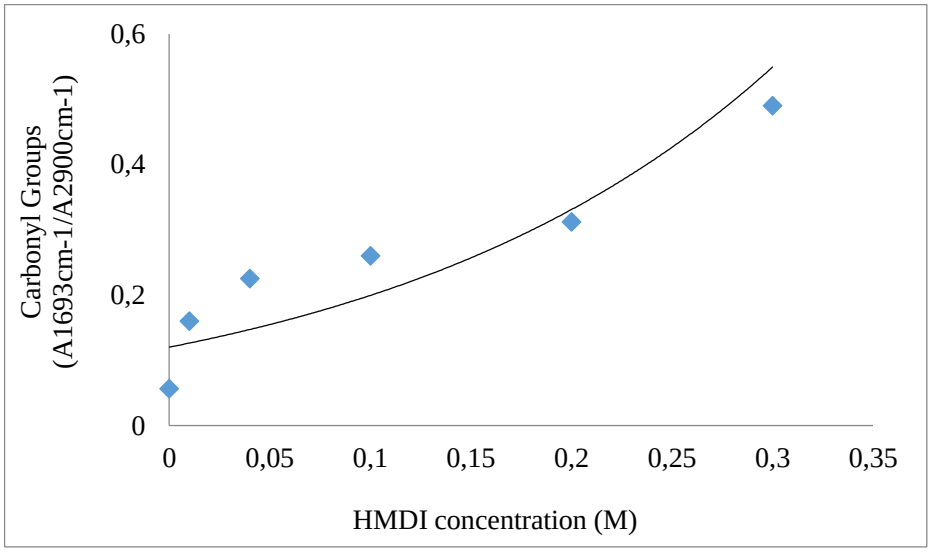


Figure 4.31. Absorbance ratio of the peak at 1693 cm^{-1} to a reference peak (2900 cm^{-1}) on crosslinked PVA with different HMDI content in reaction solution.

From absorption ratio of hydroxyl and urethane/urea carbonyl groups to methylene stretchings obtained from FTIR spectra, it can be said that the decrease in hydroxyl groups is attributed to the urethane or/and urea formation, therefore, the increase in the absorbtion value of carbonyl group is attributed to crosslinking reaction.

The degree of crystallinity was also obtained from FTIR spectroscopy through the peak at 1141 cm^{-1} which is related to the C-C symmetric stretchings and 1090 cm^{-1} which corresponds to C-O stretchings of PVA chain where an intramolecular hydrogen bond is formed between two neighbouring –OH groups. The ratio of absorbances of the 1141 cm^{-1} and 1096 cm^{-1} band was calculated for each sample obtained by reaction solutions having different HMDI concentrations. The correlation between crosslinking and crystallinity was established in Figure 4.32. As HMDI content increases, crosslinking density and the number of available –OH groups decreases which reduces crystallinity.

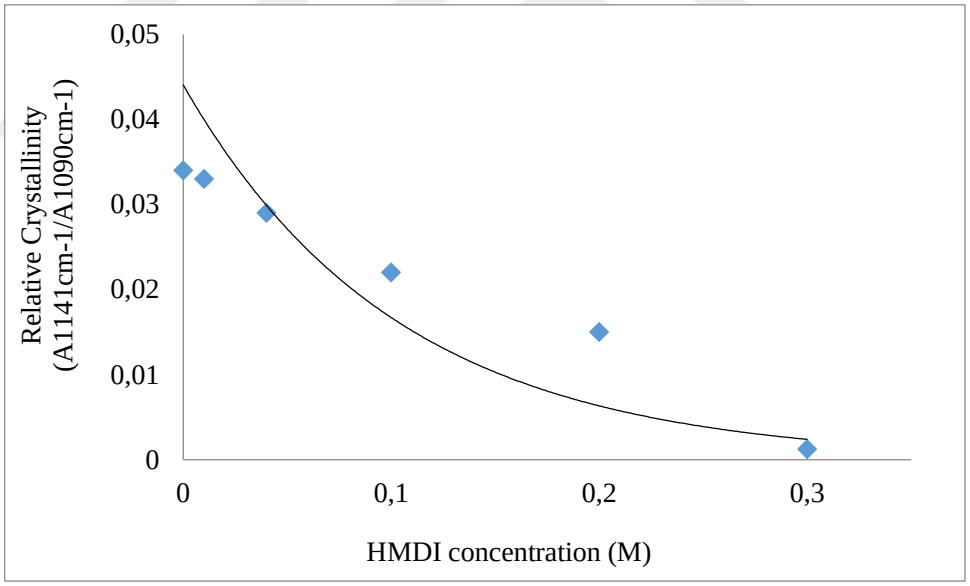


Figure 4.32. Absorbance ratio of the peak at 1141 cm^{-1} to a reference peak (1090 cm^{-1}) on crosslinked PVA with different HMDI content in reaction solution.

4.3.3. Determination of Crosslinking Density for HMDI Crosslinked PVA Fibers by Swelling

In order to investigate pH dependence of the crosslinked fibers used, degree of swelling was obtained for PVA fibers crosslinked with 0.2M HMDI solution at 12 h time intervals at different pH values and mean value was recorded. Table 4.8 shows the variation of equilibrium swelling of HMDI crosslinked PVA fibers in pH 5, pH 9 and water. As this table shows there is almost no difference between swelling ratio of PVA at different pH values. In other words PVA used in this study is almost neutral regarding to pH stimuli. Furthermore, it shows completed crosslinking which means there is no pendant $–NH_2$ and/or –NCO groups remaining on the fibers which may increase the degree of swelling in pH 5 since amine groups can be protonated by addition of $[H^+]$ ions by decreasing pH. The chains may then become highly ionic and these charges repel each other, increasing the swelling ratio. Therefore, in general all swelling measurements were done in water.

Table 4.8. Effect of pH on swelling of PVA fibers crosslinked in 0.2M HMDI solution.

	Swelling (%) **Mean value ± SD (n=3)**
pH 5	235.62±0.6
water	232.18±0.9
pH 9	228.17±0.4

The effect of different HMDI content in reaction solutions on the crosslinking density of PVA was studied by using swelling characteristics of the crosslinked PVA fibers. The effect of HMDI concentration on the swelling properties of PVA is shown in Figure 4.33. It was observed that crosslinking of PVA with HMDI results in a decrease in the number of hydroxyl groups of PVA and an increase in the amount of alkyl chains which reduces the affinity of the polymer for water leading to a reduction in the swelling ratio. Different HMDI concentrations lead to differences in water uptake properties of crosslinked PVA networks. By increasing the concentration of crosslinking agent chain entanglement occurs which would result in highly crosslinked structure and a decreased network expansion is predicted. However, the lenght of the crosslinker is relatively high compared to GA which may not result in a strictly crosslinked network. With low HMDI concentrations both the extent of

crosslinking and thickness of the crosslinked surface was relatively low and tubular structures could not be formed since very thin crosslinked shells could not not stand the pressure created inside the core and ruptured during dissolution process. Therefore, instead of tubular structures, very thin and very soft polymeric films were formed. In general it may be concluded that by increasing HMDI concentration, the crosslinking density increases and this in turn reduces the swelling or water uptake of the gels significantly.

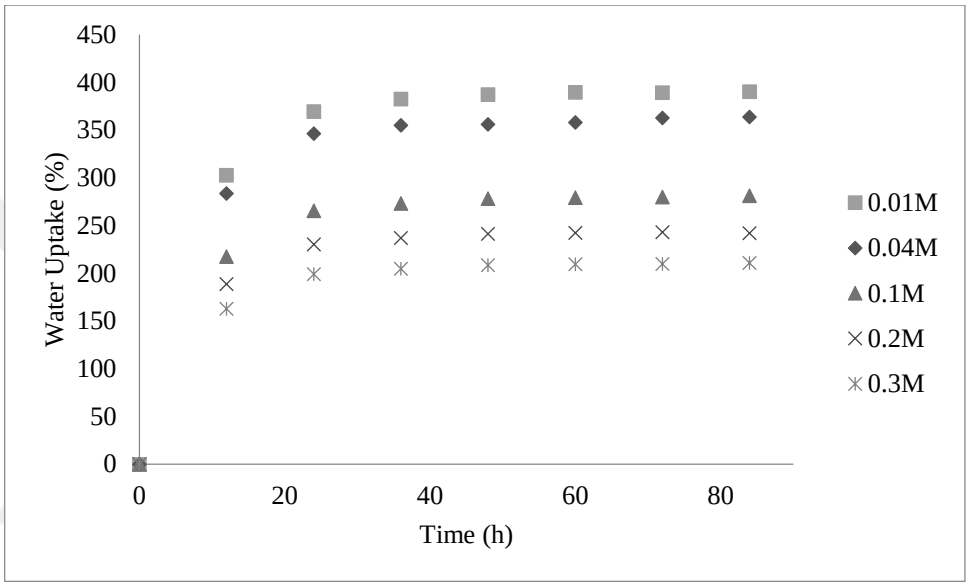


Figure 4.33. Effect of different HMDI content in reaction solutions on the swelling of crosslinked PVA in water.

Water uptake per cent is very high for crosslinked fibers at 0.01M and 0.04M HMDI reaction solutions, respectively compared to the fibers crosslinked in 0.1 0.2, and 0.3M HMDI reaction solutions. This shows that in low crosslinker concentrations the extent of the reaction is very low which may cause a very lightly crosslinked shell which will be investigated in template removal section.

4.3.4. Removal of the Core from HMDI Crosslinked PVA Fibers

To remove template fibers, either thermal degradation or solvent extraction were discussed. In the previous case there was no reasonable decomposition temperature difference between PVA core and GA crosslinked shells. Thermal properties of HMDI

crosslinked PVA shells were also investigated in order to decide whether the core can be removed by thermal degradation or not.

TG and DTG curves of PVA and crosslinked PVA samples are presented in Figure 4.34 and Figure 4.35, respectively.

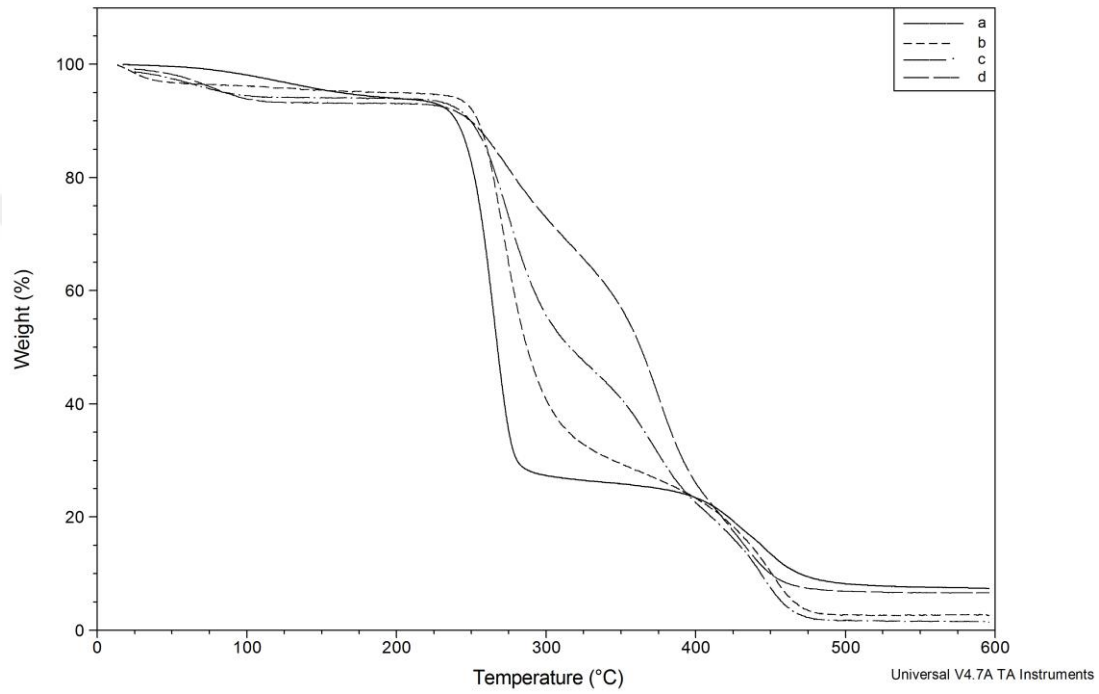


Figure 4.34. TG curves of neat PVA fibers (a), PVA fibers crosslinked in 0.1M (b), 0.2M (c), and 0.3M (d) HMDI solutions.

According to TGA thermograms, it was observed that HMDI crosslinked PVA has three main degradation steps similar to PVA. In comparison to the neat PVA, it was seen that the first stage of weight loss was nearly similar, however, the degradation of HMDI crosslinked fibers occured at a little higher temperature than PVA but at a lower temperature than GA crosslinked shells. The temperatures in these degradation stages and the weight loss per cent are summarized in Table 4.9. Clearly, the decomposition temperature difference between core and shells is not enough to remove core fibers via thermal degradation.

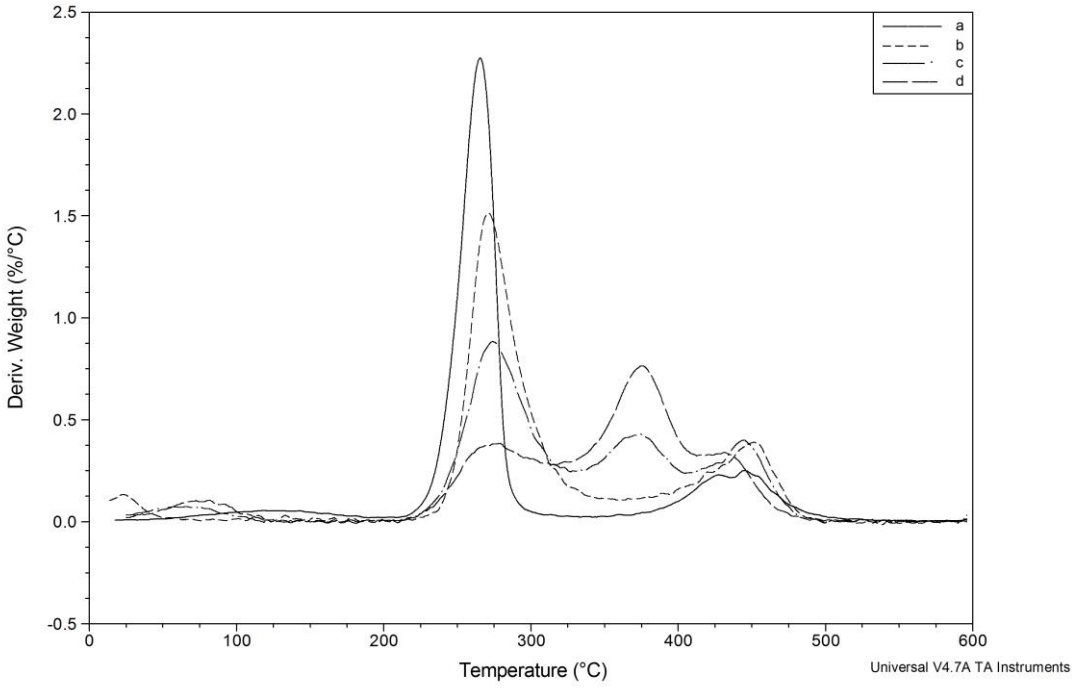


Figure 4.35. DTG curvesof neat PVA fibers (a), PVA fibers crosslinked in 0.1M HMDI (b), 0.2M HMDI (c), and 0.3M (d) solutions.

Table 4.9. The degradation temperatures and loss percentages of neat PVA fiber (a), PVA fibers crosslinked in 0.02M GA (b), 0.2M GA (c), 0.1M HMDI (d), 0.2M HMDI (e), and 0.3M HDI solutions.

	1.Deg. Step		**2.Deg. Step**		**3.Deg. Step**	
	Temp (°C)	**Loss (%)**	**Temp (°C)**	**Loss (%)**	**Temp (°C)**	**Loss (%)**
PVA	115	5.5	263	68.3	439	18.8
0.02M GA	71	4.8	362	69.7	454	20.0
0.2M GA	69	3.9	366	69.9	462	24.5
0.1M HMDI	67	4.7	275	67.4	446	24.9
0.2M HMDI	71	4.6	319	72.2	447	20.9
0.3M HMDI	77	6.0	316	67.2	440	14.0

In case of solvent extraction, water was found to be the best solvent since it dissolves PVA fibers completely without dissolving any crosslinked shells, as discussed in the previous

section. The dissolution of unreacted PVA core templates from HMDI crosslinked PVA fibers was monitored by scanning electron microscopy.

4.3.4.1. The effect of fiber lenght and wall thickness on the removal of the PVA core from HMDI Crosslinked PVA Fibers. The dissolution behaviour of PVA core was very similar to that of the GA crosslinked tubes. Crosslinked fibers started to dissolve after being cut so that water can enter into the fibers from two open ends and by means of permeation through crosslinked shells as well. Like GA crosslinked fibers the shape of HMDI crosslinked fibers start to swell as inner PVA core swells and the dissolution front was seen to move inside the length of crosslinked fibers. Figure 4.36a and Figure 4.36b shows HMDI crosslinked fibers after 1 minute and 5 minutes dissolution.

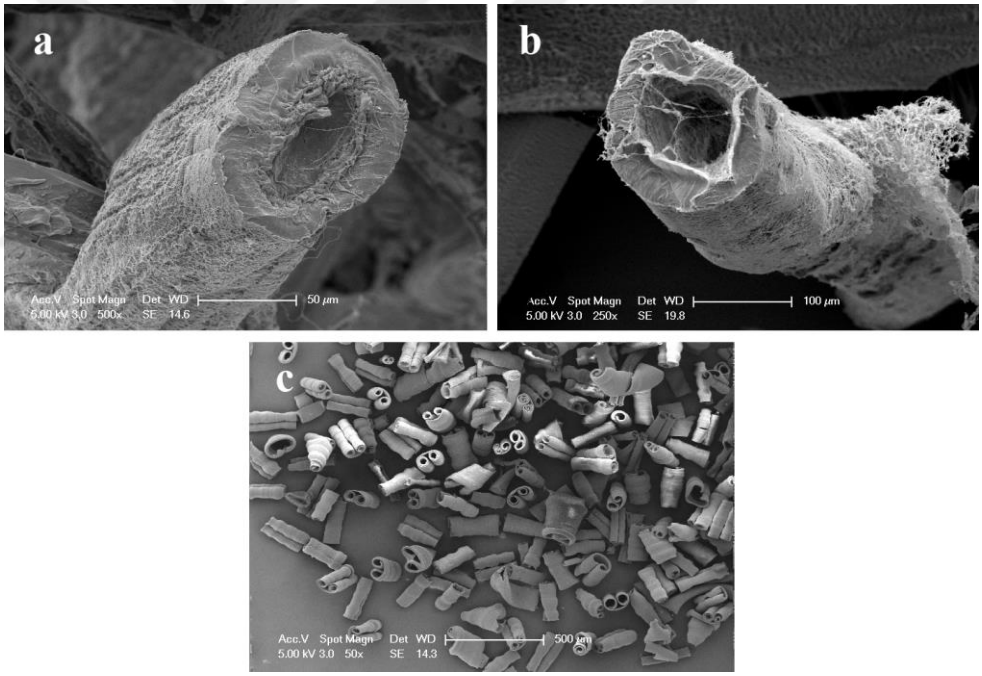


Figure 4.36. HMDI crosslinked PVA fibers after 1 min (a) and 5 min (b) 30 min (c) dissolution in water at 70°C (PVA fiber used was crosslinked by 0.2M HMDI concentration).

As discussed in the previous section the dissolution time of the core from crosslinked fibers mainly depends on two factors. One is the length of the fiber and the other one is the thickness of the shell. The length of the crosslinked fibers was kept constant around 5 mm to be successfully dissolved from open ends without leaving any residual PVA inside and

the dissolution time was adjusted according to the thickness of the shells. The time needed for complete dissolution of PVA from HMDI crosslinked fibers having 10-30 μm shell thicknesses was found to be between 5-10 minutes. Above this duration the tubes were ruptured and became longitudinally curled as shown in 4.36c. The curling direction was not random. The tubes always curled in such a way as to leave the more highly crosslinked region on the outside of the curled structure.

4.3.5. Parameters That Affect Tube Thickness in HMDI Crosslinked Fibers

The success of surface reaction as well as shell thickness depends on several parameters like HMDI concentration, diffusion time of the crosslinker, reaction temperature and time.

As diffusion time increases the penetration of the crosslinker solution inside the core becomes very high and therefore bulk crosslinking takes place which is not suitable for our aim. The solvent for this reaction is DMF in which PVA is slightly soluble in. However, by controlling the diffusion time it is possible to restrict the reaction only on the surface as well as controlling the thickness of the shells. As expected, the shell thickness increases with increasing the diffusion time.

In order to control the thickness of the shells concentration of the monomer solutions was changed instead of diffusion time, reaction time and temperature. The crosslinking reaction was conducted in five different concentrations of HMDI. The other parameters were kept constant as the concentration of HMDI solutions was changed. However, depending on the crosslinking density and the depth of the reaction only some of the fibers were succesfully yielded tubular structures.

After complete dissolution of the core SEM images of HMDI crosslinked PVA microfibers are shown in Figure 4.37.

Figure 4.37a and Figure 4.37b show lightly crosslinked fibers after dissolution. No tubular formation was observed. Figure 4.37c, Figure 4.37d, and Figure 4.37e show PVA

tubes crosslinked with 0.1M, 0.2M, and 0.3M HMDI solutions. As the concentration was increased, the thickness of the tubes was increased from 14.7 to 30 μm.

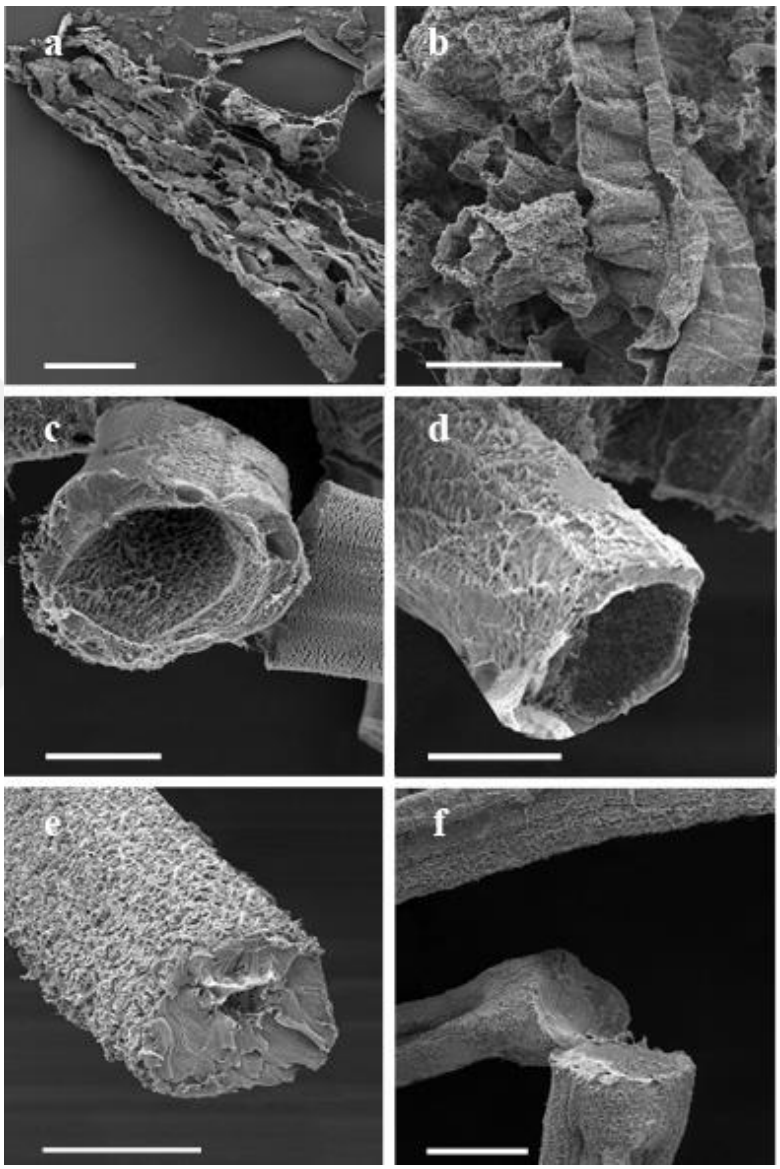


Figure 4.37. SEM images of crosslinked PVA polymeric tubes in 0.01M (a), 0.04M (b), 0.1M (d), 0.2M (e), 0.3M HMDI solutions and bulk crosslinked fibers in 1M HMDI solution (Scale=100 μm).

Crosslinked tubes couldn't be prepared by fibers reacted at lower HMDI concentrations than 0.1M. Their low crosslinked nature was also confirmed by FTIR and water uptake results. During dissolution the lightly crosslinked shells could not stand the osmotic pressure created inside the core by dissolved PVA and they ruptured easily.

Crosslinking in concentrations above 0.3M, on the other hand, resulted in bulk crosslinked fibers.

4.3.6. Dye Loading Properties of HMDI Crosslinked PVA Tubes

Figure 4.38a shows the surface of PVA tubular structure crosslinked in 0.2M HMDI solution. The shells of the HMDI crosslinked PVA tubes have uniform porous structure in general which is expected to be glassy in dehydrated state and upon water penetration swell and behave like an elastic gel.

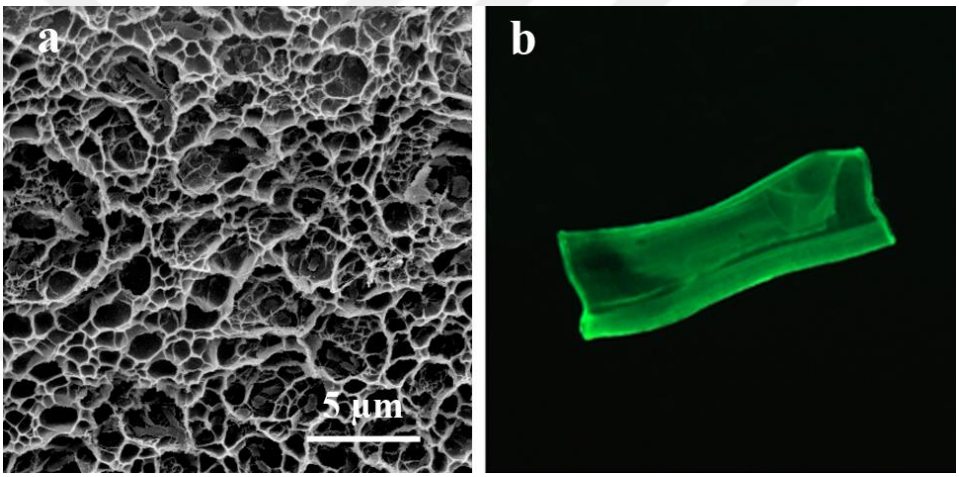


Figure 4.38. SEM imageof the surface of PVA polymeric tubes crosslinked in 0.2MHMDI solutions (a) and optical microscopy image (b) of these tubes after loaded with fluorescein dye.

Similar to GA crosslinked tubes fluorescein dye was used for a load/release study in order to follow this process with optical microscopy. As expected dye molecules were succesfully entrapped into the shells and did not remain in the fiber cavities, depicted in Figure 4.38b.This case is favorable, since if dye molecules are entrapped inside the core cavities, they will be released immediately after placing the crosslinked tubes into an aquous environment. However, by entapping dye molecules inside the shells, a system which may have a potential to be used as a drug delivery purpose can be created.

The effect of several parameters such as initial dye concentration, crosslinking density or the thickness of the shells on the loading amount of dye molecules in the tubular hydrogels

are summarized in Table 4.10. In general changing the dye concentration from 0.02 to 0.0048 per cent (w/v) in the loading medium of the crosslinked tubes increases the loading efficiency significantly, shown in Figure 4.39.

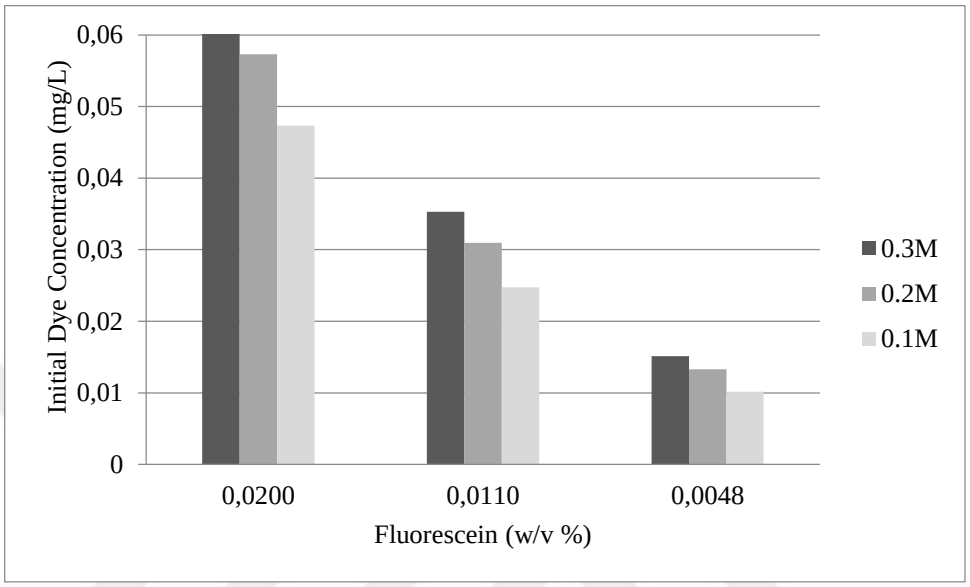


Figure 4.39. Initial dye concentrations of PVA polymeric tubes crosslinked in 0.1M, 0.2M and 0.3M HMDI solutions.

As Table 4.10 shows increasing the HMDI reaction concentration from 0.1M to 0.3M increases the shell thickness and dye loading efficiency significantly. It seems that increasing the shell thickness and crosslinking density has caused a better accomodation of the dye solution in the tubular hydrogels and no syneresis was observed. Similar properties were reported for GA crosslinked tubular hydrogels as well. Compared to GA crosslinked shells the dye loading efficiency is a little higher for HMDI crosslinked shells which may be due to their enhanced swelling properties, reported in Figure 4.33.

Table 4.10. Loading amount of PVA polymeric tubes crosslinked in 0.1M, 0.2M and 0.3M HMDI solutions.

HMDI conc. (M)	Thickness (μm)	Dye (w/v%) in the medium	Dye Loading (%)
0.1	14.7	0.0200	7.86
0.1	14.7	0.0110	7.47
0.1	14.7	0.0048	7.06
0.2	20	0.0200	9.52
0.2	20	0.0110	9.35
0.2	20	0.0048	9.22
0.3	30	0.0200	11.48
0.3	30	0.0110	10.67
0.3	30	0.0048	10.51

4.3.7. Dye Diffusion and Release Properties of the HMDI Crosslinked PVA Tubes

Diffusion rate of dye molecules from the crosslinked shells was monitored by measuring the concentration difference between loaded tubes (C_0) and the concentration of water medium where the dye was released (C_t) at different time intervals. The concentration change (C_0-Ct) is inversely propotional to the rate of diffusion. The effect of pH on the rate of diffusion of dye molecules through HMDI crosslinked PVA tubular hydrogels is shown in Table 4.11. It seems that there is no significant difference between the diffusion of flourescein dye molecules at different pH values. This result is in coincidence with swelling data shown in Table 4.8 and it confirms that HMDI crosslinked PVA tubular hydrogels are not pH-sensitive.

Dye release studies show that as crosslinking density and thickness of the shells increases, the release rate of fluorescein dye from crosslinked shells decreases while half life ($t_{1/2}$) of the dye released increases, as shown in Figure 4.40. This is related probably to increased chain entanglement or hinderence due to the degree of crosslinking. Therefore, a crosslinked network structure may reduce available free space for solute transport. On the other hand, decreasing HMDI concentration which corresponds to the decrease in shell thickness and crosslinking density increases the diffusion rate of dye molecules.

Table 4.11. Effect of pH on release percentage of dye from HMDI crosslinked PVA tubes.

	Release (%) in 1h for 0.1M	**Release (%) in 1h for 0.2M**	**Release (%) in 1h for 0.3M**
pH 5	53.00±0.9	52.68±0.7	48.51±0.7
water	53.79±0.7	53.26±0.1	46.49±0.5
pH 9	55.81±0.4	54.61±0.3	49.88±0.5

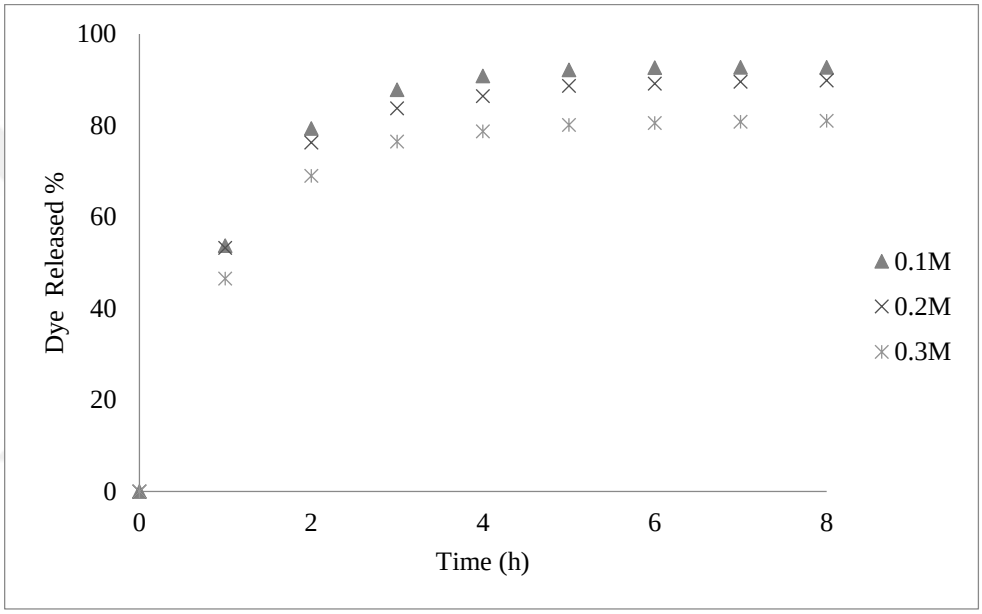


Figure 4.40. Plot of per cent release of fluorescein dye versus time for PVA polymeric tubes crosslinked in 0.1M, 0.2M and 0.3M HMDI solutions.

Figure 4.41 shows the effect of changes in fluorescein concentration on the release of dye molecules through PVA hydrogels crosslinked in 0.2M HMDI solution. The results show that increasing the dye content causes an increase in the rate of dye release.

As Figure 4.39 shows increasing dye concentration in the soaking medium results in higher loading of the dye in the crosslinked tubular hydrogels, increasing release per cent and therefore the diffusion as shown in Figure 4.41. In general increasing the dye content acts as a driving force for water uptake which increases release rate. Decreasing the crosslinking density also increases the diffusion rate.

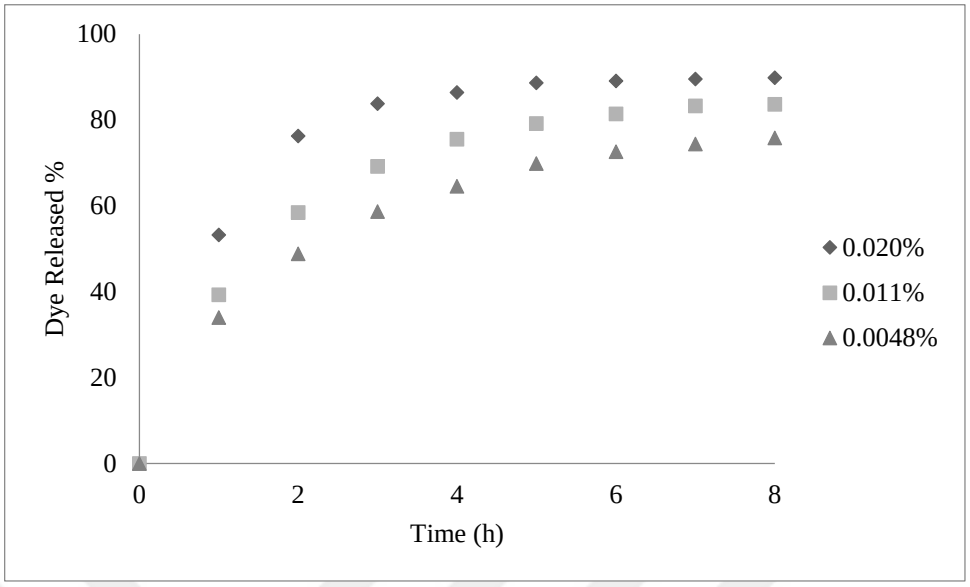


Figure 4.41. Effect of dye loading on the fluorescein released from PVA tubular hydrogels crosslinked in 0.2M HMDI concentration.

4.3.8. Contact Angle Measurements of HMDI Crosslinked Films

The crosslinked outer shell is expected to have a relatively hydrophobic property while the inner core should be more hydrophilic due to higher concentration of unreacted hydroxyl groups on the inside wall of the shells. In order to do contact angle measurements crosslinked films were prepared on microscope slides by using the same HMDI concentrations and the same reaction conditions as fibers. Table 4.12 summarizes the results of contact angle measurements. It is concluded that, as HMDI content in crosslinked films increases, the contact angle and hydrophobicity increases. The increase of overall hydrophobicity of the outer surface with enhanced grafting of HMDI is due to the long hydrophobic alkyl chains (6 C in lenght) which were introduced onto PVA films by crosslinking.

According to these results the outer shells of PVA polymeric tubes crosslinked in 0.1M, 0.2M and 0.3M HMDI solutions are expected to have contact angles around 65 and 75°, respectively. This hydrophobicity difference may help to decrease the release rate of dye or drug molecules into an aquous medium which is very important in prolonging the release.

Table 4.12. Contact angle (θ)values of PVA and HMDI crosslinked PVA films.

HMDI concentration (M)	**Contact Angle (θ, degree)**
0	45
0.01	57
0.04	58
0.1	65
0.2	71
0.3	75

4.3.9. Crosslinking of Poly(vinyl alcohol) Nanofibers with HMDI

Due to their high specific surface area of nanofibers diffusion time of crosslinker solution applied was only 2 seconds. According to our previous experience from microfibers the crosslinker concentration applied was 0.1M. It is expected that if the diffusion time and concentration of crosslinker solution increases, nanofiber mats become bulk crosslinked and will be completely insoluble in water. SEM images of crosslinked fibers before dissolution (a) and after dissolution (b) are shown in Figure 4.42. Despite such a low concentration and diffusion time of crosslinker solution, the surface crosslinking of the nanofibers was achieved. However, after dissolution process no tubular formation was observed which is a sign of bulk crosslinking. Therefore, it is concluded that this method is not suitable for the fabrication of nanotubes.

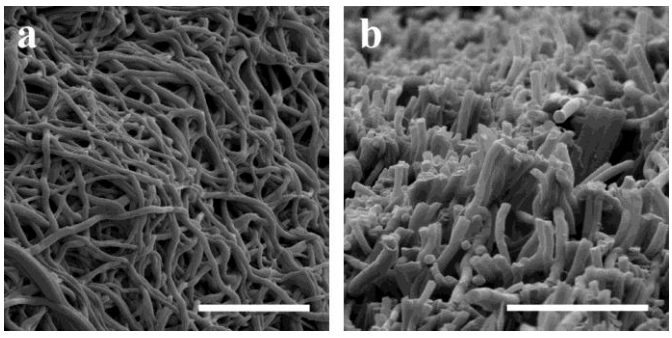


Figure 4.42. SEM images of crosslinked PVA nanofibers in 0.1M HMDI solution (a) and its product after water dissolution (b).

4.3.10. Crosslinking of PVA with Other Diisocyanates

Isophorone diisocyanate (IPDI) and 2,4-toluene diisocyanate (2,4-TDI) are difunctional compounds which can be used as crosslinkers for PVA. It is known that the isocyanate group of 2,4-TDI in the *para* position is approximately four times higher than the reactivity of the isocyanate groups in the *ortho* position and at least two times higher than the isocyanate group in HMDI [125]. In general the isocyanate groups of a diisocyanate have different reactivities. The different reactivity of isocyanate groups in 2,4-TDI against hydroxyl groups is $K_1/K_2=12$. The *ortho* isocyanate of 2,4-TDI may not react until the concentration of the *para* isocyanate has been sufficiently depleted. However, both ortho and para isocyanate groups could react almost simultaneously at a very high temperature (T≈125°C) [123].

IPDI, on the other hand, has both primary and secondary isocyanate ends having definetely different reactivities. According to the literature relative reactivities of the primary and secondary isocyanate groups in urethane formation depend on the catalyst, the reaction temperature and the reactivity of alcohol [126, 127]. IPDI reacts mainly with the secondary isocyanate group without catalyst addition. At high temperatures, the difference in reactivity between the secondary and primary isocyanate groups is reduced. On the other hand, with increasing steric hindrance of the alcohol, the urethane formation reaction proceeds more selectively towards to formation of primary than secondary urethanes. It is supposed that the reaction will proceed mainly between the hydroxyl group of PVA and the secondary isocyanate group of IPDI.

The crosslinking reaction with IPDI has been proven by FTIR spectrum, shown in Figure 4.43b. This FTIR spectrum belongs to PVA microfiber crosslinked in 0.2M IPDI solution in DMF. The broad band at 3330 cm^{-1} related to both –NH stretchings of amide and –OH group stretchings of unreacted hydroxyl groups of PVA. The peaks at 2944 cm^{-1} and 2913 cm^{-1} correspond to C-H stretchings of alkyl groups. The broad peak around 1738 cm^{-1} can be attributed to C=O stretchings of the urethane groups formed after the reaction of PVA with IPDI and free urea carbonyl absorption band [128] formed after the reaction between IPDI molecules. The band at 1633 cm^{-1} is related to C=O of the urea group , the band at 1556 cm^{-1} corresponds to amide group shown in Figure 4.44 structures a and c. The band at 1235

cm^{-1} also corresponds to an amide structure. All of these assignments suggest the formation of urethane-urea linkages between PVA and IPDI. Ether linkage (C-O-C) is assigned at 1092 cm^{-1}. The characteristic bands for the -NCO groups is observed in the range of 2270 cm^{-1} which does not exist in the spectrum showing that there is no unreacted –NCO groups left after the reaction. This may be an evidence for crosslinking or amine functionalization of PVA with IPDI.

After the reaction three types of constitutional units are predicted. A unit with two urethane groups after the crosslinking reaction of two isocyanate groups and two hydroxyl groups of PVA (Figure 4.44, unit **a**), an unreacted hydroxyethylene unit of PVA (Figure 4.44, unit **b**) and a unit with one urethane group which was formed by the reaction between the hydroxyl group of hydroxy ethylene monomeric unit on PVA and one isocyanate group of IPDI and a free isocyanate group at the end of branch, from which the amino group could be formed by the reaction with humidity (Figure 4.44, unit **c**). Urea segments could be present in the units of **a** and **c**.

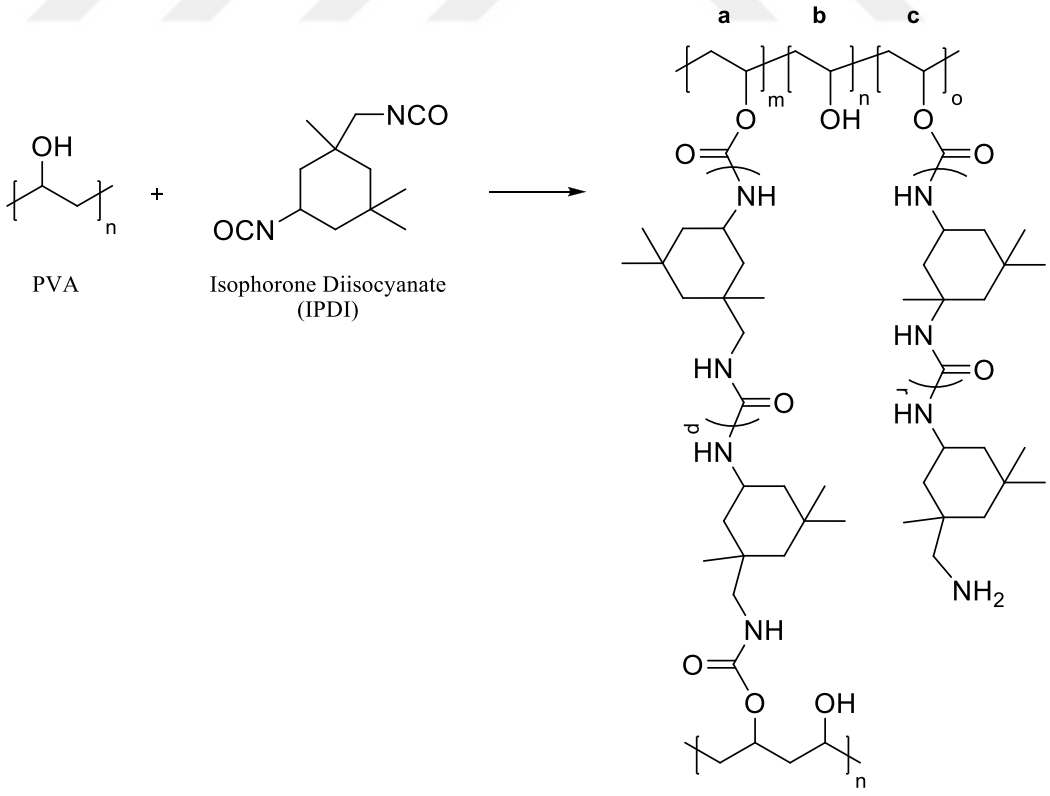


Figure 4.43. Expected products by the reaction between PVA and IPDI.

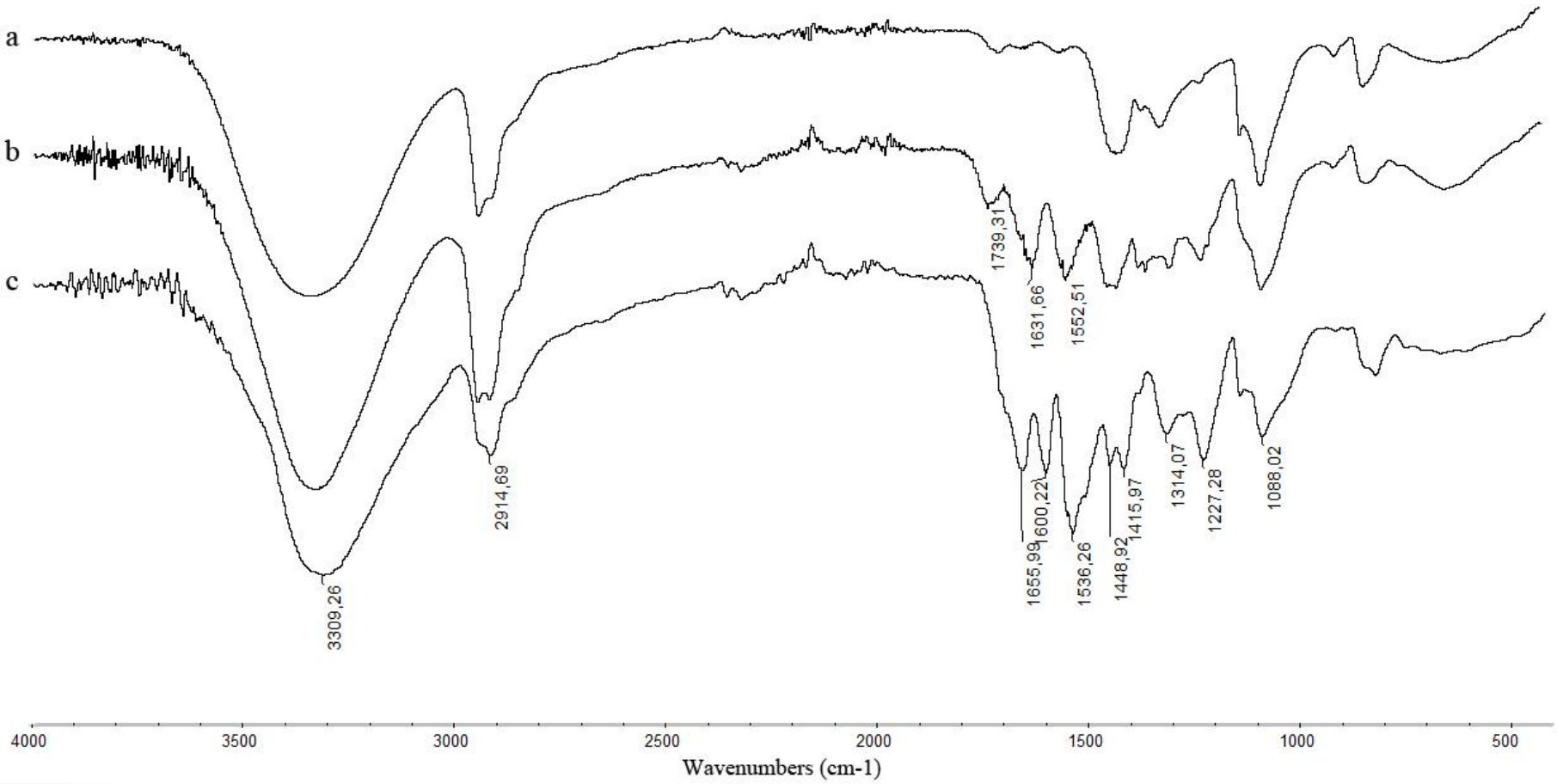


Figure 4.44. FTIR spectra of PVA (a) and PVA crosslinked in 0.2M IPDI (b) and 0.2M 2,4-TDI solutions in DMF.

The crosslinking reaction with 2,4-TDI has also been proven by FTIR, shown in Figure 4.43c. The FTIR spectrum of PVA fiber crosslinked in 0.2M 2,4-TDI solution in DMF show similar bands as IPDI with some slight changes in their position. A broad band at 3309 cm^{-1} related to both –NH stretchings of amide and –OH group stretchings of unreacted PVA. The peaks at 2930 cm^{-1} and 2915 cm^{-1} correspond to C-H stretchings of alkyl groups. A small shoulder around 1705 cm^{-1} can be attributed to C=O stretchings of the urethane groups formed. The band at 1655 cm^{-1} is related to C=O of the urea group , the band at 1600 cm^{-1} corresponds to amide group shown in Figure 4.45 structures a and c. The band at 1227 cm^{-1} also corresponds to an amide structure. All of these assignments suggest the formation of urethane-urea linkages between PVA and 2,4-TDI. Ether linkage (C-O-C) is assigned at 1088 cm^{-1}. There is no band observed asround 2270 cm^{-1} showing that there is no unreacted –NCO groups left after the reaction which may be an evidence for crosslinking or amine functionalization of PVA with 2,4-TDI.

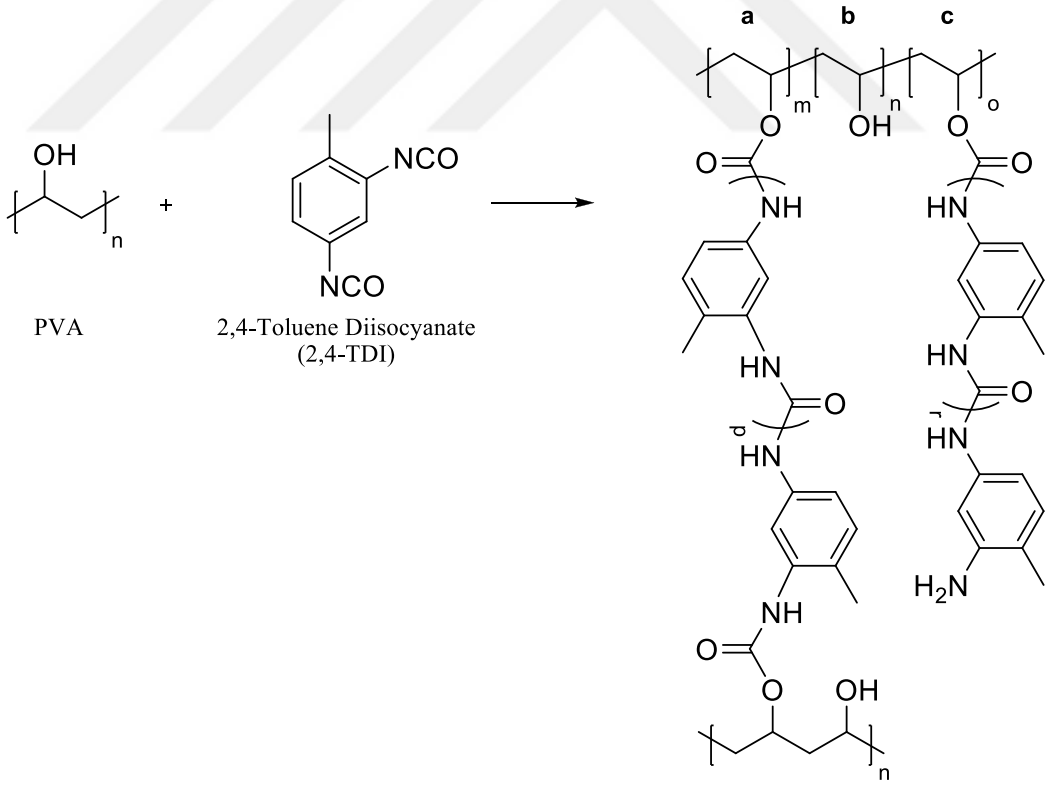


Figure 4.45. Expected products by the reaction between PVA and 2,4-TDI.

4.3.11. Removal of the Core from IPDI and 2,4-TDI Crosslinked PVA Fibers

Solvent extraction method was used to remove unreacted PVA core templates. Both IPDI and 2,4-TDI crosslinked fibers were immersed in water at 70°C for different time periods. After dissolution process crosslinked fibers were monitored by scanning electron microscopy.

According to SEM images shown in Figure 4.46 it was observed that the crosslinking reaction with IPDI and 2,4-TDI in DMF is definetely a surface reaction. However, microparticles of 5-35 μm diameter and some surface porosity on the PVA fibers is observed during IPDI crosslinking. This may be due to the moisture remaining in the fibers. Very little amount of moisture is enough to start this reaction. Porous poly(urethane urea) microparticles in the size of 2-10 μm from PVA and IPDI in DMSO/water was reported in the literature [129]. After dissolution of the inner core tube formation was observed. The shells seem continuously crosslinked with IPDI; however, some cracks are observed on the shells which may be due to inhomogenous crosslinking (Figure 4.46c and Figure 4.46d).

Figure 4.46e shows 2,4-TDI crosslinked PVA fibers before dissolution. No continuous crosslinking was observed on the surface since there are many cracks on the shells. This layer with many cracks may be a result of the reaction between crosslinkers instead of PVA. Similar surface reaction with similar reaction conditions was repeated with PVA films. This also resulted in the formation of a thin shell with many cracks on it, Figure 4.46f. Therefore, it is concluded that 2,4-TDI is not a good crosslinker to be used in fabrication of tubular structures from PVA fiber templates. However, IPDI has a potential if right crosslinking conditions are found.

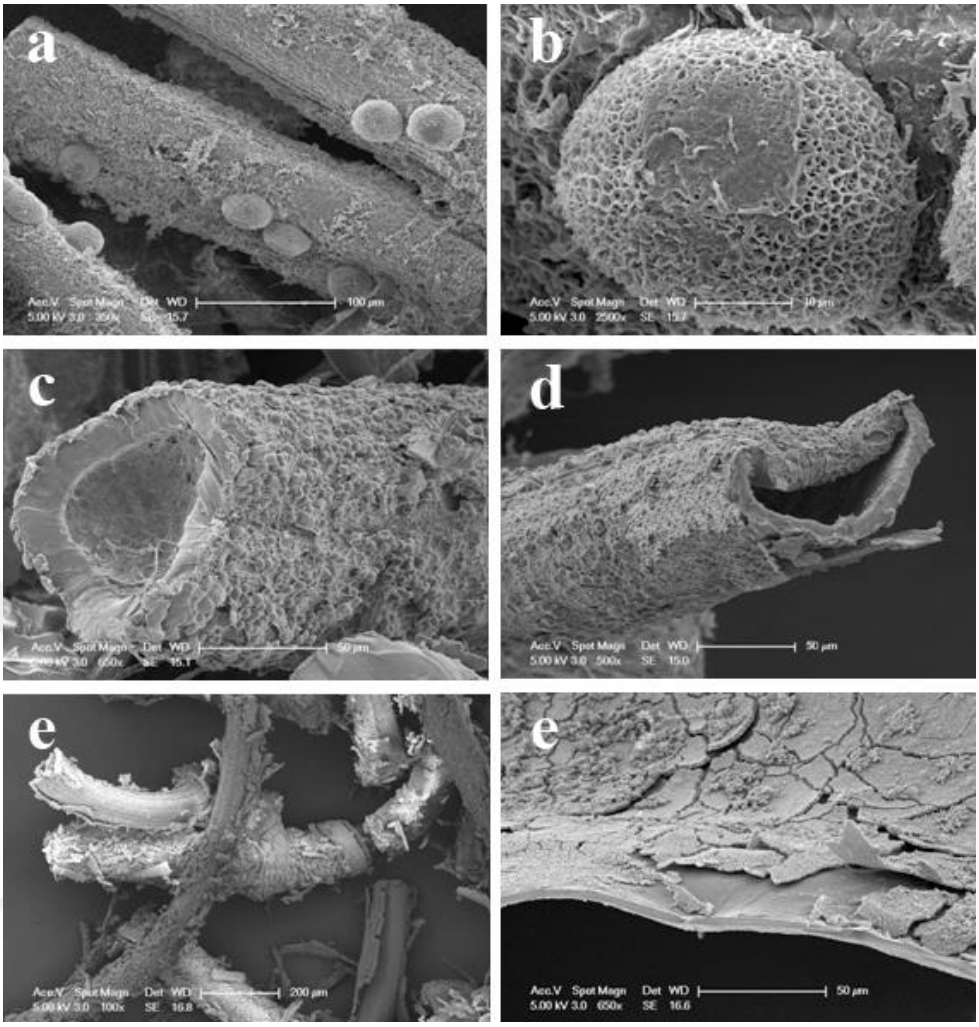


Figure 4.46. SEM images showing the surface of crosslinked PVA fibers in 0.2M IPDI solution before dissolution (a and b), after 2 min dissolution (c), after complete dissolution (d), and the surface of crosslinked PVA fibers (e) and film (f) in 0.2M 2,4-TDI solution before dissolution.

4.4. Modification of Poly(vinyl alcohol) with Acryloyl Chloride or Alkoxysilane and Crosslinking of Modified Fibers with Mono- or Difunctional Hardeners

One of the most common ways to prepare photoreactive PVA is to introduce double bond functionalities on polymer chain. Then, photo-crosslinkable monomers can react with these double bonds to prepare hydrogel like materials.

4.4.1. Grafting of Acryloyl Chloride on PVA Fibers and FTIR Characterization of the Product

Acryloyl chloride (AC) is a suitable monomer for grafting onto PVA. It will react with PVA to give ester linkages. The esterification by Schotten-Baumann reaction enables degrees of modification to be reached which depend on the chemical reactivity of the pendant unit introduced. High degrees of modification can be only obtained with water-stable acid chlorides. The most common way to esterify polymers containing hydroxylic groups with acid chlorides uses a homogenous medium by solution in an appropriate solvent. In case of PVA these solvents must be very polar such as dimethyl sulfoxide (DMSO). However, since only surface functionalization is required in this study, toluene which is a non-solvent for PVA was used as a reaction medium. The reaction was carried out with slight excess of AC. The use of toluene led to long reaction times such as 48 h. In general the reactions with acid chlorides in polar solvents for longer reaction times do not increase the degree of substitution due to hydrolysis of acid chloride. However, since toluene was used as a reaction medium, the reaction time was extended. Despite long reaction times steric crowding leads to low degree of esterification as seen by considerable number of hydroxyl groups which remained in the product as shown by FTIR characterization in Figure 4.47b.

The FTIR spectrum of PVA fibers modified with AC is nearly similar with the FTIR spectrum of neat PVA except the carbonyl band at 1730 cm^{-1} corresponding to ester carbonyl of the acrylate. A quantitative analysis on FTIR spectral changes can be also made according to the absorbance ratios of several functional groups to a reference peak. The results are summarized in Table 4.13.

Table 4.13. Absorbance ratios of several FTIR bands belong to PVA and PVA-*g*-AC.

	PVA	**PVA-*g*-AC**
$\mathbf{A_{3330}/A_{2900}}$	5.99	5.04
$\mathbf{A_{1730}/A_{2900}}$	0.0736	0.379

Methylene stretching band around 2900 cm^{-1} was taken as a reference peak. It was observed that the ratio of the peak at 3330 cm^{-1} corresponding to –OH stretchings and the ratio of the peak at 1730 cm^{-1} belongs to carbonyl stretchings to this reference peak decreases

and increases, respectively. This shows the decrease in the number of –OH groups and an increase in the number of ester carbonyl groups through the modification of PVA with AC.

4.4.2. Grafting of 3-trimethoxysilyl propylmethacrylateon PVA Fibers and FTIR and SEM Characterization of the Product

Another way used to introduce photoreactive double bond functionalities on PVA polymer surface was to react PVA fibers with 3-trimethoxysilyl propylmethacrylate (MPS). One end of MPS contains organofunctional group which is methacrylate and the other end contains trimethoxy silyl groups (-Si-$(OCH_3)_3$) which will be hydrolyzed to silanol (-Si-$(OH)_3$ groups, as shown 1.26. Silanol ends of hydrolyzed MPS will condense with PVA hydroxyl groups or with themselves to form hybrid organic-inorganic surface having methacrylate functionalities. Expected reaction is shown in Figure 4.48.

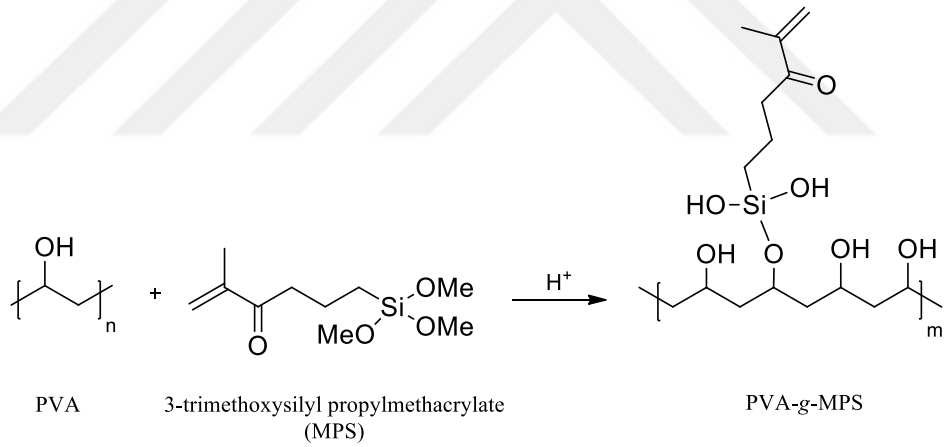


Figure 4.47. Expected product after the grafting of 3-trimethoxysilyl propylmethacrylate on PVA.

The extent of functionalization or crosslinking reaction on the surface of PVA is too small to be quantitatively determined with FTIR spectroscopy; however, it can be said that at least one hydroxyl group of silanol may condense with PVA chains. In the literature hybrid materials were synthesized by reacting PVA with three different alkoxysilanes: tetraethoxysilane (TEOS), 3 mercaptopropyltrimethoxysilane (MPTMS) and 3-glycidoxypropyltrimethoxysilane (GPTMS) in solution [97].

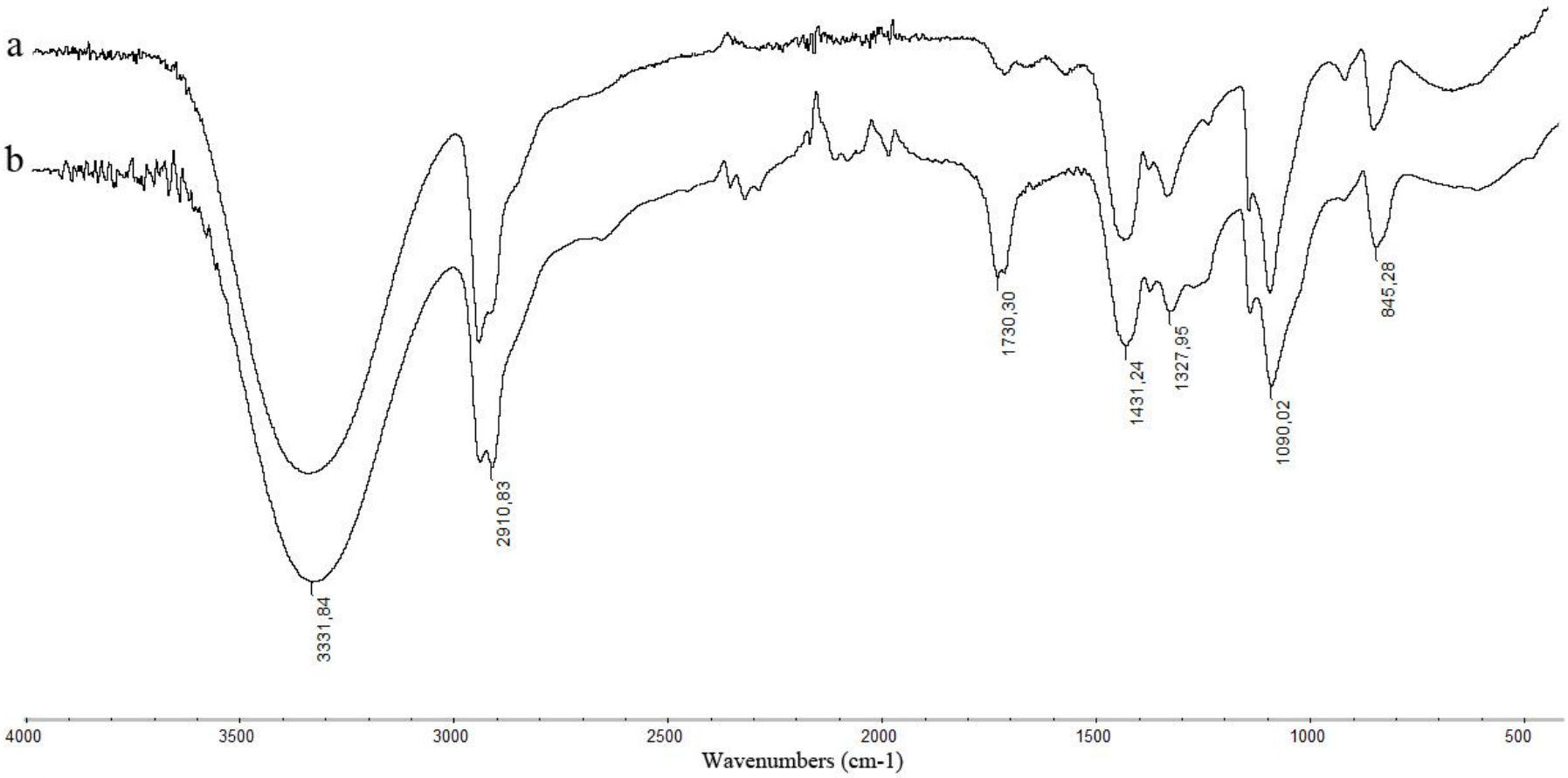


Figure 4.48. FTIR spectra of PVA (a) and acryloyl chloride grafted PVA (PVA-g-AC) (b).

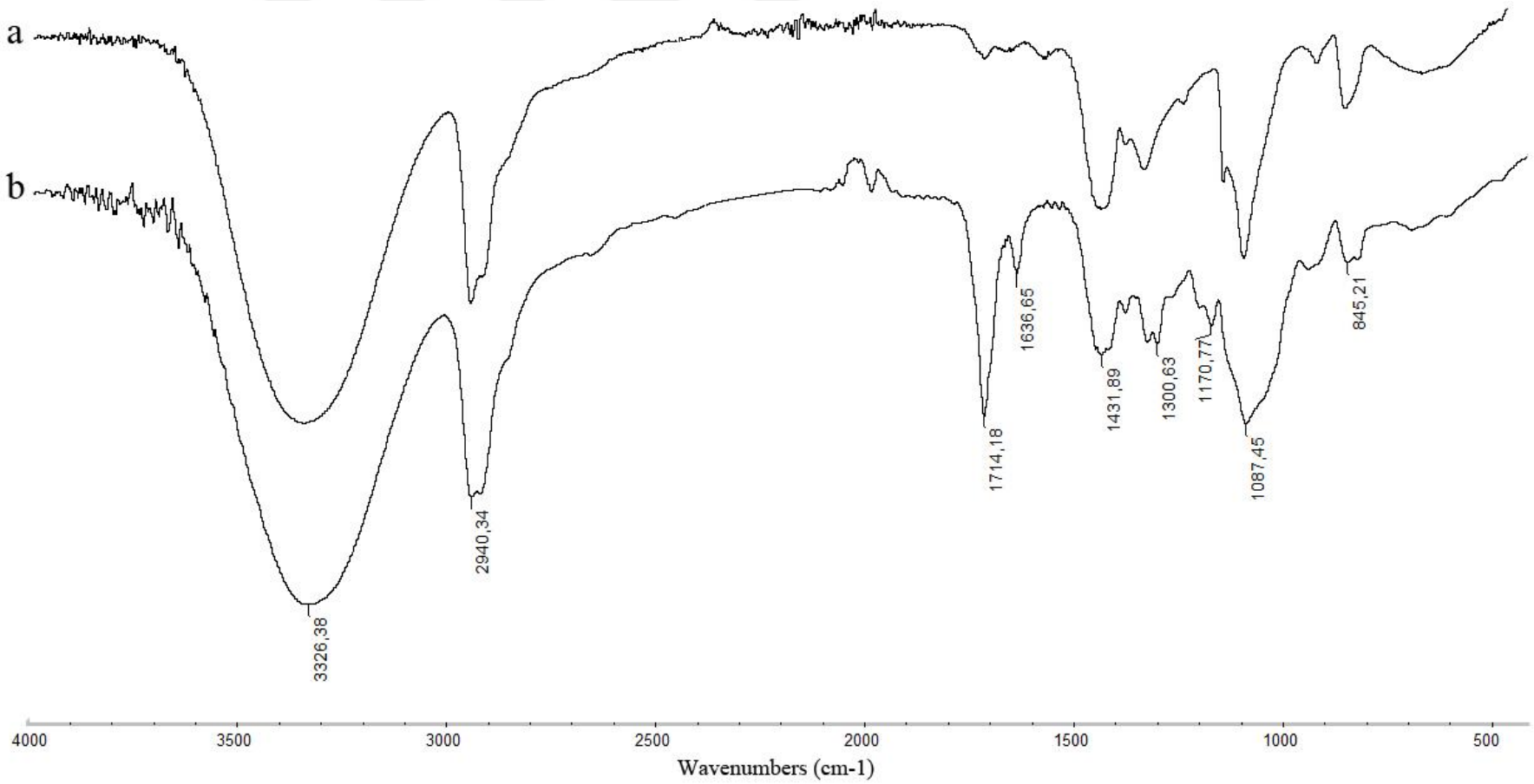


Figure 4.49. FTIR spectra of PVA (a) and 3-trimethoxysilyl propylmethacrylate modified PVA (PVA-g-MPS) (b).

FTIR spectrum shown in Figure 4.49b confirms the presence of methacrylate groups. Among several peaks (Si-O-, -CH_2), this spectrum shows an important peak at 1715 cm^{-1} that is characteristic of the 3-trimethoxysilyl propylmethacrylate (MPS), associated with the methacrylate carbonyl (C=O) vibration band. The peak at 1634 cm^{-1} corresponds to the methacrylate double bond stretchings. It can be observed that major vibration bands (Si-O-Si, υ=1087 cm^{-1}; Si-OH, υ=845 cm^{-1}) associated with polysiloxane (R-Si-O-) reactions of hydrolysis and condensation added to PVA. Furthermore, the absorption peaks in the region from υ=1200 to 1171 cm^{-1} can be attributed to Si-alkyl bonds, indicating some hybrid organic-inorganic structure formation [130]. In the frequency range from 3500 to 3100 cm^{-1} which is the same as the FTIR spectrum of the neat PVA mainly related to hydroxyl groups

The surface morphology and thickness of the fibers were monitored by scanning electron microscopy. SEM images shown in Figure 4.50 also confirm the surface modification, while the thickness of the fibers did not change much.

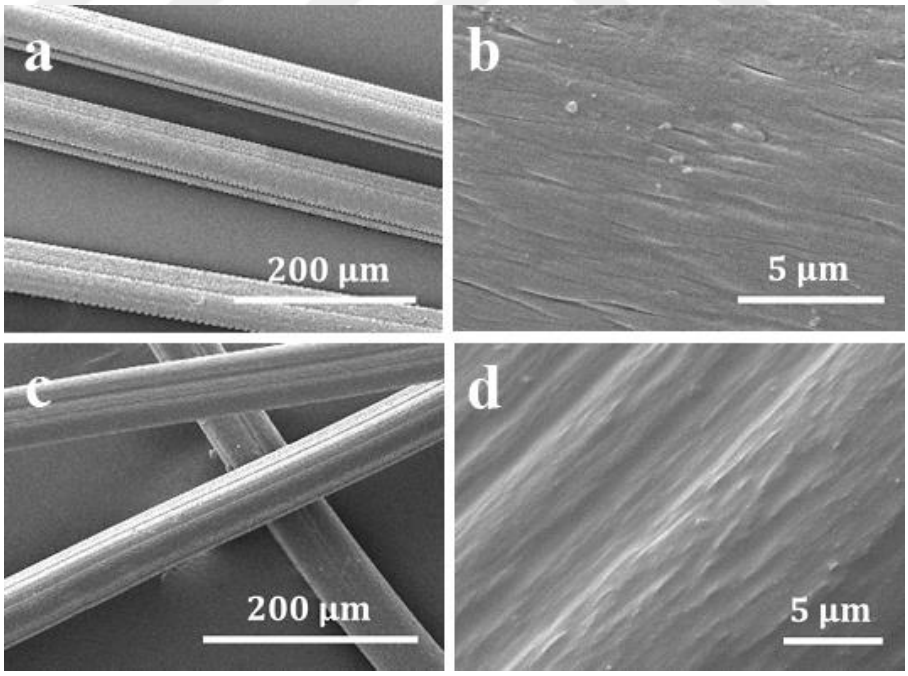


Figure 4.50. SEM images showing PVA fibers and their surface morphologies before (a and b) and after (c and d) 3-trimethoxysilyl propylmethacrylate modification.

4.4.3. Surface Photopolymerization of Modified PVA Fibers and Characterization of Fibers after Complete Dissolution of Templates

To produce a water insoluble network on these functionalized PVA fibers dip-coating method was used. In this process double bond functionalized fibers which were cast on glass slides were dipped in a container having a solution of mono- and/or diacrylate monomers. The fibers were then exposed to UV light with appropriate conditions (exposure time, and light intensity). The monomer solutions and conditions tried are summarized in Experimental Section Table 3.4.

Three important parameters are involved in this process: the tube thickness, the concentration and the surface tension. These parameters are very important to fabricate shells having uniform thicknessess. The modified PVA fibers should be completely wetted in equal thickness by crosslinker solution. The other parameter is the crosslinking density, which depends on the crosslinker solutions used. The increase in the crosslinking density results in more rigid shells while with less crosslink density relatively flexible shells can be fabricated. To produce a shell which can swell and be flexible enough to allow water penetration inside and egres of the dissolved core outside without damaging itself is a challenging process.

SEM images shown in Figure 4.51a, Figure 4.51b and Figure 4.51c belong to dissolved fibers of MPS modified PVA after dip coating with poly(ethyleneglycol) diacrylate (PEGDA), 1,6-hexanedioldiacrylate (HDODA) and 2-hydroxyethylmethacrylate (HEMA) (100 wt% each in 0.5M solution). Both images show ruptured walls. This probably results from osmotic pressure created inside by dissolution of the core. The speed of template dissolution and permeability of the shells are affected by the extent of osmotic stress. The shells of these fibers are so thick and so extensively crosslinked that they cannot conform and expand with the swollen core. The osmotic pressure simply ruptures the rigid shells. Therefore, the shell material sould be designed as a flexible hydrogel that can swell in the presence of water and enable the dissolution of the PVA core without rupturing the shells.

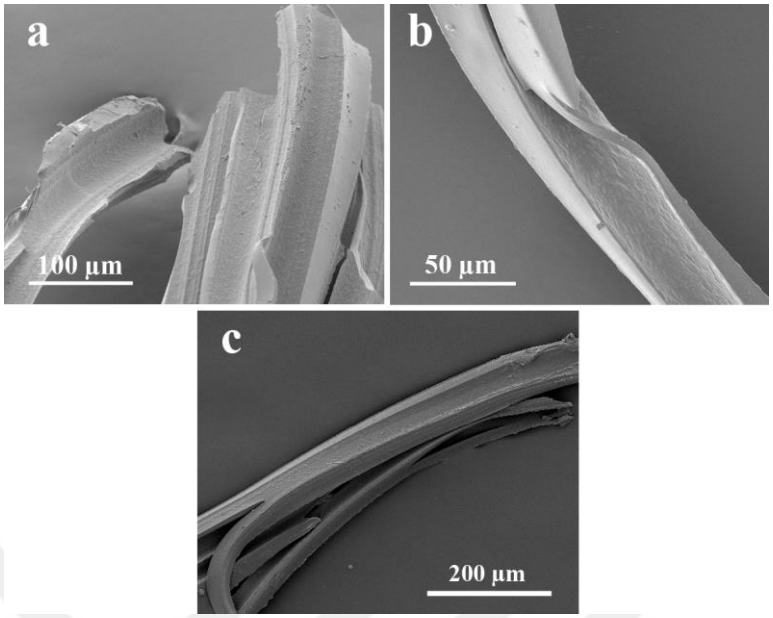


Figure 4.51. SEM images of dissolved PVA-*g*-MPS fibers after dip coating with PEGDA (a), HDODA (b) and HEMA (c) (100 wt% each in 0.5M solution).

Therefore, the combination of mono and long difunctional acrylates were used as the shell material. The monomer solution applied on MPS and AC grafted PVA fibers via UV-assisted dip coating was HEMA/PEGDA(80/20) prepared in 1M solution. To investigate the effect of silane network on the solubility of inner PVA core, dissolution behaviour of PVA-*g*-AC and PVA-*g*-MPS core fibers were compared. Figure 4.52 shows the SEM images of these fibers and their shell surfaces after dissolution.

The inner core of the PVA fibers grafted with AC has a porous surface which look very permeable (Figure 4.52a and Figure 4.52b). On the other hand, the inner core of MPS modified fibers has a non porous surface and some rupture perforations inside are visible (Figure 4.52c and Figure 4.52d). While silane network is forming a supporting layer inside the tubular structures, it may decrease water permeability of the shells.

Also, these images show that introducing PEGDA into the crosslinker mixture created a porous network. However, despite all the experiments done with acrylate monomers, no continuous tubular structures could be formed. Therefore, it is concluded that this method is not suitable for the fabrication of tubular structures from PVA fiber templates.

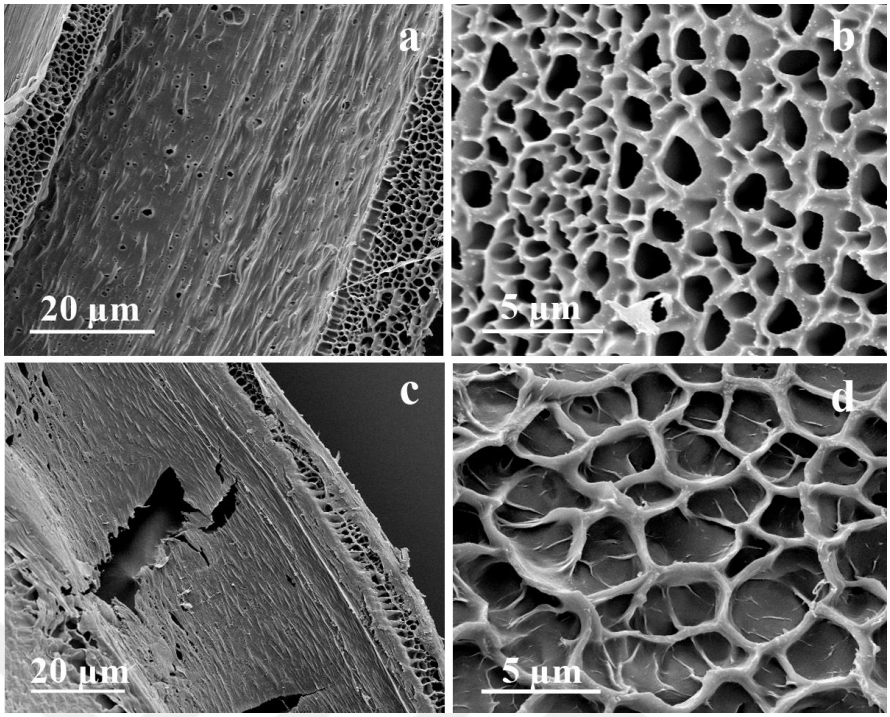


Figure 4.52. SEM images of dissolved PVA-*g*-AC (a and b) and PVA-*g*-MPS (c and d) fibers after dip coating with HEMA/PEGDA(80/20) prepared in 1M solution.

5. CONCLUSIONS

The fabrication of hollow polymeric structures by using poly(vinyl alcohol) fiber templates was demonstrated. The surface of PVA fibers were crosslinked and tube formation was observed after the selective removal of the unreacted PVA core. Two methods were applied to get crosslinked shells on PVA fibers. In the first method the surface of PVA was crosslinked directly with dialdehydes or diisocyanates. In the second method acrylate functionalities were introduced on PVA surface and these groups were further reacted with photopolymerizable monomers. After many experiments the former was found to be the most suitable method to prepare hollow polymeric structures. Depending on the reaction conditions tubes whose shells are adjusted in terms of crosslinking and thicknesses were prepared.The surface of the shells had uniform and porous structures. Such materials may be used in entrapment and release of drugs or biological molecules. The effect of tubular geometry, hydrophilicity difference between inner and outer shells, crosslinking density and thickness on load/relase properties were discussed.In spite of many promissing results, much more work is needed to design a prolonged delivery system.

In general microfibers were used in this study. The technique and crosslinking reactions which are applied on microfibers were investigated in order to check the applicability of this method on nanofibers. However, it was found that using the reactivity of PVA fibers to create crosslinked shells for the fabrication of hollow structures is not a suitable method for nanofiber templates. In some cases the crosslinking reaction occured selectively on the surface of PVA nanofibers; however, to remove inner unreacted core from very tiny fibers is still a great challenge.

REFERENCES

1. Fu, G. D., G. L. Li, K.G. Neoh, and E.T. Kang, "Hollow Polymeric Nanostructures-Synthesis, Morphology and Function", *Progress in Polymer Science*, Vol. 36, pp.127-167, 2011.

2. Bognitzki, M., W. Czado, T. Frese, A. Schaper, M. Hellwig, M. Steinhart, A. Greiner, and J. H. Wendorff, "Nanostructured Fibers via Electrospinning", *Advanced Materials*, Vol. 13, pp. 70-72, 2001.

3. Edelmann, F. T., "Fullerene Pipes, Tube-in-Tube Membranes, and Carbon-Nanotube Tips: Adding New Dimensions to Molecular Technology", *Angewandte Chemie-International Edition*, Vol. 38, pp. 1381-1387, 1999.

4. Ghadiri, M. R., J. R. Granja, and L. K. Buehler, "Artificial Transmembrane Ion Channels From Self-assembling Peptide Nanotubes", *Nature*, Vol. 369, pp. 301-304, 1994.

5. Dersch, R., T. Liu, A. K. Schaper, A. Greiner, and J. H. Wendorff, "Electrospun Nanofibers: Internal Structure and Intrinsic Orientation", *Journal of Polymer Science: Part A: Polymer Chemistry*, Vol. 41, pp. 545-553, 2003.

6. Iijima, S., "Helical Microtubules of Graphitic Carbon", *Nature*, Vol. 354, pp. 56-58, 1991.

7. Martin, C. R., "Template Synthesis of Electronically Conductive Polymer Nanostructures", *Accounts of Chemical Research*, Vol. 28, pp. 61-68, 1995.

8. Martin, C. R., "Nanomaterials: A Membrane-Based Synthetic Approach", Science, Vol. 266, pp. 1961-1966, 1994.

9. Schnur, J. M., "Lipid Tubules: A Paradigm for Molecularly Engineered Structures", *Science*, Vol. 262, pp. 1669-1676, 1993.

10. Whitesides, G. M., J. P. Mathias, and C. T. Seto, "Molecular Self-Assembly and Nanochemistry: A Chemical Strategy for the Synthesis of Nanostructures", *Science*, Vol. 254, pp. 1312-1319, 1991.

11. Ozin, G. A., "Nanochemistry: Synthesis in Diminishing Dimensions", *Advanced Materials*, Vol. 4, pp. 612-649, 1992.

12. Evans, E., H. Bowman, A. Leung, D. Needham, and D. Tirrell, "Biomembrane Templates for Nanoscale Conduits and Networks", *Science*, Vol. 273, pp. 933-935, 1996.

13. Anilkumar, P., and M. Jayakannan, "Single-Molecular-System-Based Selective Micellar Templates for Polyaniline Nanomaterials: Control of Shape, Size, Solid State Ordering, and Expanded Chain to Coillike Conformation", *Macromolecules*, Vol. 40, pp. 7311-7319, 2007.

14. Liu, J., and M. X. Wan, "Synthesis, Characterization and Electrical Properties of Microtubules of Polypyrrole Synthesized by a Template-Free Method", *Journal of Materials Chemistry*, Vol. 11, pp. 404-407, 2001.

15. Chern, C. S., "Emulsion Polymerization Mechanisms and Kinetics", *Progress in Polymer Science*, Vol. 31, pp. 443-486, 2006.

16. Wan, M., "A Template-Free Method Towards Conducting Polymer Nanostructures", *Advanced Materials*, Vol. 20, pp. 2926-2932, 2008.

17. Anilkumar, P. and M. Jayakannan, "Fluorescent Tagged Probing Agent and Structure-Directing Amphiphilic Molecular Design for Polyaniline Nanomaterials via Self-Assembly Process", *Journal of Physical Chemistry C*, Vol. 111, pp. 3591-3600, 2007.

18. Georgakilas, V., F. Pellarini, M. Prato, D. M. Guldi, M. Melle-Franco, and F. Zerbetto, "Supramolecular Self-Assembled Fullerene Nanostructures", *Proceedings of the National Academy of Sciences of the United States of America*, Vol. 99, pp. 5075-5080, 2002.

19. Shimizu, T., *Self-Assembled Nanomaterials II*, Springer,Berlin Heidelberg, 2008.

20. Hamley, I. W., *Block Copolymers in Solution: Fundamentals and Applications*, John Wiley & Sons Ltd., Chichester, 2012.

21. Yu, Y., and A. Eisenberg, "Control Of Morphology through Polymer-Solvent Interactions in Crew-Cut Aggregates of Amphiphilic Block Copolymers", *Journal of the American Chemical Society*, Vol. 119, pp. 8383-8384, 1997.

22. Rank, A., S. Hauschild, S. Förster, and R. Schubert, "Preparation Of Monodisperse Block Copolymer Vesicles via a Thermotropic Cylinder-Vesicle Transition", *Langmuir*, Vol. 25, pp. 1337-1344, 2009.

23. Olsen, B. D. and R. A. Segalman "Self-assembly of Rod-Coil Block Copolymers", *Materials Science and Engineering R*, Vol. 62, pp. 37-66, 2008.

24. Martin, C. R., "Membrane-Based Synthesis of Nanomaterials", *Chemistry of Materials*, Vol. 8, pp. 1739-1746, 1996.

25. Brumlik, C. J., and C. R. Martin, "Template Synthesis of Metal Microtubules", *Journal of the American Chemical Society*, Vol. 113, pp. 3174-3175, 1991.

26. Martin, C. R., and R. V. Parthasarathy, "Polymeric Microcapsule Arrays", *Advanced Materials*, Vol. 7, pp. 487–488, 1995.

27. Parthasarathy, R. V.,and C. R. Martin, "Synthesis of Polymeric Microcapsule Arrays and Their Use for Enzyme Immobilization", *Nature*, Vol. 369, pp. 298-301, 1994.

28. Steinhart, M., J. H. Wendorff, A. Greiner, R. B. Wehrspohn, K. Nielsch, J. Schilling, J. Choi, and U. Gösele, "Polymer Nanotubes by Wetting of Ordered Porous Templates", *Science*, Vol. 296, p. 1997, 2002.

29. Martin, C. R., "Template Synthesis of Electronically Conductive Polymer Nanostructures", *Accounts of Chemical Research*, Vol. 28, pp. 61-68, 1995.

30. Fan, R., Y. Wu, D. Li, M. Yue, A. Majumdar, and P. Yang, "Fabrication of Silica Nanotube Arrays from Vertical Silicon Nanowire Templates", *Journal of the American Chemical Society*, Vol. 125, pp. 5254-5255, 2003.

31. Wu, C. G., and T. Bein, "Conducting Carbon Wires in Ordered, Nanometer-Sized Channels", *Science*, Vol. 266, pp. 1013–1015, 1994.

32. Beck, J. S., J. C. Vartuli, W. J. Roth, M. E. Leonowicz, C. T. Kresge, K. D. Schmitt, C. T-W. Chu, D. H. Olson, E. W. Sheppard, S. B. McCullen, J. B. Higgins, and J. L. Schlenker, "A New Family of Mesoporous Molecular Sieves Prepared with Liquid Crystal Templates", *Journal of American Chemical Society*, Vol.114, pp. 10834-10843, 1992.

33. Cepak, V. M., and C. R. Martin, "Preparation of Polymeric Micro- and Nanostructures Using a Template-Based Deposition Method", *Chemistry of Materials*, Vol. 11, pp. 1363-1367, 1999.

34. Kriha, O., P. Göring, M. Milbradt, S. Agarwal, M. Steinhart, R. Wehrspohn, J. H. Wendorff, and A. Greiner, "Polymer Tubes with Longitudinal Composition Gradient by Face-to-Face Wetting", *Chemistry of Materials*, Vol. 20, pp. 1076-1081, 2008.

35. Tan, J., X. L. She, F. Yuan, S. Yang, and D. Zhou, "Preparation of Acrylonitrile-Butadiene-Styrene Terpolymer Nanotubes with Array Structure in Anodic Aluminium Oxide Membrane Using Wetting Techniques", *Journal of Porous Materials*, Vol. 15, pp. 619-623, 2008.

36. McCann, J. T., D. Li, and Y. Xia, "Electrospinning of Nanofibers with Core-Sheath, Hollow, or Porous Structures", *Journal of Materials Chemistry*, Vol. 15, pp. 735-738, 2005.

37. Greiner, A., and J. H. Wendorff, "Electrospinning: A Fascinating Method for the Preparation of Ultrathin Fibers", *Angewandte Chemie-International Edition*, Vol. 46, pp. 5670-5703, 2007.

38. Liu, T., "Preparation of a Novel Micro/nano Tubes via Electrospun Fiber as a Template", *Journal of Materials Science&Technology*, Vol. 20, pp. 613-616, 2004.

39. Deitzel, J. M., J. Kleinmeyer, D. Harris, and N. C. Beck Tan, "The Effect of Processing Variables on the Morphology of Electrospun Nanofibers and Textiles", *Polymer*, Vol. 42, pp. 261-272, 2001.

40. Fong, H., I. Chun, and D. H. Reneker, "Beaded Nanofibers Formed during Electrospinning", *Polymer*, Vol. 40, pp. 4585-4592, 1999.

41. Kumar, A., *Nanofibers*, InTech, Croatia, 2010.

42. Zhang, L., and Y-L. Hsieh, "Carbon Nanofibers with Nanoporosity and Hollow Channels from Binary Polyacrylonitrile Systems", *European Polymer Journal*, Vol. 45, pp. 47-56, 2009.

43. Dror, Y., W. Salalha, R. Avrahami, E. Zussman, A. L. Yarin, R. Dersch, A. Greiner, and J. H. Wendorff, "One-step Production of Polymeric Microtubes by Co-electrospinning", *Small*, Vol. 3, pp. 1064-1073, 2007.

44. Hou, H., Z. Jun, A. Reuning, A. Schaper, J. H. Wendorff, and A. Greiner, "Poly(p-xylylene) Nanotubes by Coating and Removal of Ultrathin Polymer Template Fibers", *Macromolecules*, Vol. 35, pp. 2429-2431, 2002.

45. Bognitzki, M., H. Hou, M. Ishaque, T. Frese, M. Hellwig, C. Schwarte, A. Schaper, J. H. Wendorff, and A. Greiner, "Polymer, Metal, and Hybrid Nano- and Mesotubes by Coating Degradable Polymer Template Fibers (TUFT Process)", *Advanced Materials*, Vol. 12, pp. 637-640, 2000.

46. Mark, J. E., *Polymer Data Handbook*, Oxford University Press, New York, 1999.

47. Huang, Z-M., Y-Z. Zhang, M. Kotaki, and S. Ramakrishna, "A Review on Polymer Nanofibers by Electrospinning and Their Applications in Nanocomposites", *Composites Science and Technology*, Vol. 63, pp. 2223-2253, 2003.

48. R. A. Caruso, J. H. Schattka, and A. Greiner., "Titanium Dioxide Tubes from Sol-Gel Coating of Electrospun Polymer Fibers", *Advanced Materials*, Vol. 13, pp.1577-1579, 2001.

49. Finch, C. A. *Poly(vinyl alcohol) Development*, John Wiley & Sons Ltd, Chichester, 1992.

50. Chiellini, E., A. Corti, S. D'Antone, and R. Solaro, "Biodegradation of Poly(vinyl alcohol) Based Materials", *Progress in Polymer Science*, Vol. 28, pp. 963-1014, 2003.

51. DeMerlis, C. C. and D. R. Schoneker, "Review of the Oral Toxicity of Polyvinyl Alcohol (PVA)", *Food and Chemical Toxicology*, 41, 319-326, 2003.

52. Hassan C. M. and N. A. Peppas, "Structure and Applications of Poly(vinyl alcohol) Hydrogels Produced by Conventional Crosslinking or by Freezing/Thawing Methods", *Advances in Polymer Science*, Vol. 153, pp. 37-65, 2000.

53. Wang, T., M. Turhan, and S. Gunasekaran, "Selected Properties of pH-sensitive, Biodegradable Chitosan–Poly(vinyl alcohol) Hydrogel",*Polymer International*, Vol. 53, pp. 911-918, 2004.

54. Peppas, N. A., *Hydrogels in Medicine and Pharmacy 2*, CRC Press, Florida, 1986.

55. Tang, X. and S. Alavi, "Recent Advances in Starch, Polyvinyl Alcohol Based Polymer Blends, Nanocomposites and Their Biodegradability", *Carbohydrate Polymers*, Vol. 85, pp. 7-16, 2011.

56. Bonakdar, S.; S. H. Emami, M. A. Shokrgozar, A. Farhadi; S. A. H. Ahmadi; and A. Amanzadeh, "Preparation and Characterization of Polyvinyl Alcohol Hydrogels Crosslinked by Biodegradable Polyurethane for Tissue Engineering of Cartilage", *Materials Science and Engineering C*, Vol. 30, pp. 636-643, 2000.

57. Xu, B., H. A. Toutanji, J. Gilbert, "Impact Resistance of Poly(vinyl alcohol) Fiber Reinforced High-Performance Organic Aggregate Cementitious Material", *Cement and Concrete Research*, Vol. 40, pp. 347-351, 2010.

58. Nuttelman, C. R.; S. M. Henry, and K. S. Anseth, "Synthesis and Characterization of Photocrosslinkable, Degradable Poly(vinyl alcohol)-based Tissue Engineering Scaffolds", *Biomaterials*, Vol. 23, pp. 3617-3626, 2002.

59. Basak, P., B. Adhikari, and A. K. Sen, "Surface Cross-Linked Poly(Vinyl Alcohol) Hydrogel for Colon Targeted Drug Release", *Polymer-Plastics Technology and Engineering*, Vol. 50, pp. 1357-1361, 2011.

60. Orienti, I., R. Trere, and V. Zecchi, "Hydrogels Formed by Cross-Linked Polyvinylalcohol as Colon-Spesific Drug Delivery Systems", *Drug Development and Industrial Pharmacy*, Vol. 27, pp. 877-884, 2001.

61. Brazel, C. S. and N. A. Peppas, "Mechanisms of Solute and Drug Transport in Relaxing, Swellable, Hydrophilic Glassy Polymers", *Polymer*, Vol. 40, pp. 3383-3398, 1999.

62. Morita, R., R. Honda, and Y. Takahashi, "Development of Oral Controlled Release Preparations, a PVA Swelling Controlled Release System (SCRS): I. Design of SCRS and its Release Controlling Factor", *Journal of Controlled Release*, Vol. 63, pp. 297-304, 2000.

63. Huang, X., and C. S. Brazel, "Analysis of Burst Release of Proxyphylline from Poly(vinyl alcohol) Hydrogels", *Chemical Engineering Communications*, Vol. 190, pp. 519-532, 2003.

64. Gholap, S. G., J. P. Jog, and M. V. Badiger, "Synthesis and Characterization of Hydrophobically Modified Poly(vinyl Alcohol) Hydrogel Membrane", *Polymer*, Vol. 45, pp. 5863-5873, 2004.

65. Ruiz, J., A. Mantecon, and V. Cadiz, "Synthesis and Properties of Hydrogels from Poly (vinyl alcohol) and Ethylenediaminetetraacetic Dianhydride", *Polymer*, Vol. 42, pp. 6347-6354, 2001.

66. Trieu, S. and S. Qutubuddin, "Poly(vinyl alcohol) Hydrogels: 2. Effects of Processing Parameters on Structure and Properties", *Polymer*, Vol. 36, pp. 2531-2539, 1995.

67. Liou, F. J. and Y. J. Wang, "Preparation and Characterization of Crosslinked and Heat-treated PVA-MA Films", *Journal of Applied Polymer Science*, Vol. 59, pp. 1395-1403, 1996.

68. Mallapragada, S. K. and N. A. Peppas, "Dissolution Mechanism of Semicrystalline Poly(vinyl alcohol) in water", *Journal of Polymer Science: Part B: Polymer Physics*, Vol. 34, pp. 1339-1346, 1996.

69. Gohil, J. M., A. Bhattacharya, and P. Ray, "Studies on the Crosslinking of Poly(vinyl alcohol), *Journal of Polymer Research*, Vol. 13, pp. 161-169, 2006.

70. Kenawy, E-R., M. H. El-Newehy, and S. S. Al-Deyab, "Controlled Release of Atenolol from Freeze/Thawed Poly(vinyl Alcohol) Hydrogel", *Journal of Saudi Chemical Society*, Vol. 14, pp. 237-240, 2010.

71. He, G., H. Zheng, and F. Xiong, "Preparation and Swelling Behavior of Physically Crosslinked Hydrogels Composed of Poly(vinyl Alcohol) and Chitosan", *Journal of*

Wuhan University of Technology, Materials Science Edition, Vol. 23, pp. 816-820, 2008.

72. Bolto, B., T. Tran, M. Hoang, and Z. Xie, "Crosslinked Poly(vinyl Alcohol) Membranes", *Progress in Polymer Science*, Vol. 34, pp. 969-981, 2009.

73. Hickey, A. S. and N. A. Peppas, "Mesh Size and Diffusive Characteristics of Semicrystalline Poly(vinyl Alcohol) Membranes Prepared by Freezing/Thawing Techniques", *Journal of Membrane Science*, Vol. 107, pp. 229-237, 1995.

74. Chapiro, A., *Radiation Chemistry of Polymeric Systems*, Interscience Publishers, New York, 1962.

75. Charlesby, A., *Atomic Radiation and Polymers*, Pergamon Press, Oxford, 1960.

76. Katz, M. G. and T. Wydeven, "Selective Permeability of PVA Membranes. I. Radiation-Crosslinked Membranes", *Journal of Applied Polymer Science*, Vol. 26, pp. 2935–2946, 1981.

77. Ikada, Y. and T. Mita, "Preparation of Hydrogels by Radiation Technique", *Radiation Physics and Chemistry*, Vol. 9, pp. 633-645, 1977.

78. Wang, B., M. Kodama, S. Mukataka, and E. Kokufuta, "On the Intermolecular Crosslinking of PVA Chains in an Aqueous Solution by γ-ray Irradiation", *Polymer Gels and Networks*, Vol. 6, pp. 71-81, 1998.

79. Chen, N., L. Li, and Q. Wang, "New Technology for Thermal Processing of Poly(vinyl alcohol)", *Plastics, Rubber and Composites*, Vol. 36, pp. 283-290, 2007.

80. Wang, Q., J. Gao, Y. Dan, and Z. Chen, "Preparation of Novel Polymer Materials through Intermolecular Complexation", *Materials Science and Engineering:C*, Vol. 10, pp. 135-140, 1999.

81. Gimenez, V., A. Mantecon, J. C. Ronda, and V. Cadiz, "Poly (vinyl Alcohol) Modified with Carboxylic Acid Anhydrides: Crosslinking through Carboxylic Groups", *Journal of Applied Polymer Science*, Vol. 65, pp. 1643-1651, 1997.

82. Caro, S. V., C. S. P. Sung, and E. W. Merrill, "Reaction of Hexamethylene Diisocyanate with Poly(Vinyl Alcohol) Films for Biomedical Applications", *Journal of Applied Polymer Science*, Vol. 20, pp. 3241-3246, 1976.

83. Lang, K., S. Sourirajan, T. Matsuura, and G. Chowdhury, "A Study on the Preparation of Polyvinyl Alcohol Thin-Film Composite Membranes and Reverse Osmosis Testing", *Desalination*, Vol. 104, pp. 185-196, 1996.

84. Smets, G. and B. Petit, "Kinetics of Acetalization of Polyvinyl Alcohol and of Hydrolysis of Acetalized Polyvinyl Alcohol", *Macromolecular Chemistry and Physics*, Vol. 33, pp. 41-54, 1959.

85. Kim K-J., S-B. Lee, and N. W. Han, "Effects of the Degree of Crosslinking on Properties of Poly(vinyl alcohol) Membranes", *Polymer Journal-Nature*, Vol. 25, pp. 1295-1302, 1993.

86. Hansen, E. W., K. H. Holm, D. M. Jahr, J. K. Olafsen, and A. Stori, "Reaction of Poly(vinyl alcohol) and Dialdehydes during Gel Formation Probed by ^{1}H n.m.r.- A Kinetic Study", *Polymer*, Vol. 38, pp. 4863-4871, 1997.

87. Zhang, H. Z., B. L. Liu, R. Luo, Y. Wu, and D. Lei, "The Negative Biodegradation of Poly(vinyl alcohol) Modified by Aldehydes", *Polymer Degradation and Stability*, Vol. 91, pp. 1740-1746, 2006.

88. Krumova, M., D. López, R. Benavente, C. Mijangos, and J.M. Pereña, "Effect of Crosslinking on the Mechanical and Thermal Properties of Poly(Vinyl Alcohol)", *Polymer*, Vol. 41, pp. 9265-9272, 2000.

89. Loughlin, R. G., M. M. Tunney, R. F. Donnelly, D. J. Murphy, M. Jenkins, and P. A. McCarron, "Modulation of Gel Formation and Drug-Release Characteristics of Lidocaine-Loaded Poly(Vinyl Alcohol)-Tetraborate Hydrogel Systems Using Scavenger Polyol Sugars", *European Journal of Pharmaceutics and Biopharmaceutics*, Vol. 69, pp. 1135-1146, 2008.

90. Bo, J., "Study on PVA Hydrogel Crosslinked by Epichlorohydrin", *Journal of Applied Polymer Science,* Vol. 46, pp. 783-786, 1992.

91. Huang, R. Y. M. and J. W. Rhim, "Modification of Poly (Vinyl Alcohol) Using Maleic Acid and Its Application to the Separation of Acetic Acid‐Water Mixtures by the Pervaporation Technique", *Polymer International*, Vol. 30, pp. 129-135, 1993.

92. Tsai, C-E., C-W. Lin, and B-J. Hwang, "A Novel Crosslinking Strategy for Preparing Poly(vinyl Alcohol)-Based Proton-Conducting Membranes with High Sulfonation", *Journal of Power Sources*, Vol. 195, pp. 2166-2173, 2010.

93. Mühlebach, A., B. Müller, C. Pharisa, M. Hofmann, B. Seiferling, and D. Guerry, "New Water-Soluble Photo Crosslinkable Polymers Based on Modified Poly(vinyl Alcohol)", *Journal of Polymer Science Part A: Polymer Chemistry*, Vol. 35, pp. 3603-3611, 1997.

94. Schmedlen, R. H., K. S. Masters, and J. L. West, "Photocrosslinkable Polyvinyl Alcohol Hydrogels that can be Modified with Cell Adhesion Peptides for Use in Tissue Engineering", *Biomaterials*, Vol. 23, pp. 4325-4332, 2002.

95. Kuo, S. M., S. J. Chang, and Y. Jiin, "Properties of PVA-AA Cross-linked HEMA-based Hydrogels", *Journal of Polymer Research*, Vol. 6, pp. 191-196, 1999.

96. Xue, J., T. Wang, J. Nie, and D. Yang, "Preparation and Characterization of a Bioadhesive with Poly (vinyl alcohol) Crosslinking Agent", *Journal of Applied Polymer Science*, Vol. 127, pp. 5051-5058, 2013.

97. Andrade, G., E. F. Barbosa-Stancioli, A. A. Piscitelli Mansur, W. L. Vasconcelos, and H. S. Mansur, "Design of Novel Hybrid Organic–Inorganic Nanostructured Biomaterials for Immunoassay Applications", *Biomedical Materials*, Vol. 1, pp. 221-234, 2006.

98. Sanchez, C., B. Lebeau, F. Ribot, and M. In, "Molecular Design of Sol–Gel Derived Hybrid Organic–Inorganic Nanocomposites", *Journal of Sol-Gel Science and Technology*, Vol. 19, pp. 31-38, 2000.

99. Mansur, H. S., R. L. Oréfice, A. A.P. Mansur, "Characterization of Poly(vinyl alcohol)/poly(ethylene glycol) Hydrogels and PVA-derived Hybrids by Small-angle X-ray Scattering and FTIR Spectroscopy", *Polymer*, Vol. 45, pp. 7193-7202, 2004.

100. Peppas, N. A., "Infrared Spectroscopy of .Semicrystalline Poly(vinyl alcohol) Networks", *Macromolecular Chemistry*, Vol. 178, pp. 595-601, 1977.

101. Isasi, J. R., L. C. Cesteros, and I. Katime, "Hydrogen Bonding and Sequence Distribution in Poly(vinyl acetate-co-vinyl alcohol) Copolymers", *Macromolecules*, Vol. 27, pp. 2200-2205, 1994.

102. Figueiredo, K. C. S., T. L. M. Alves, and C. P. Borges, "Poly(vinyl alcohol) Films Crosslinked by Glutaraldehyde Under Mild Conditions", *Journal of Applied Polymer Science*, Vol. 111, pp. 3074-3080, 2009.

103. Wang, Y. and Y. L. Hsieh, "Crosslinking of Polyvinyl Alcohol (PVA) Fibrous Membranes with Glutaraldehyde and PEG Diacylchloride", *Journal of Applied Polymer Science*, Vol. 116, pp. 3249-3255, 2010.

104. Immelman, E., R. D. Sanderson, E. P. Jacobs, and A. J. Van Reenen, "Poly (vinyl alcohol) Gel Sublayers for Reverse Osmosis Membranes. I. Insolubilization by Acid-Catalyzed Dehydration", *Journal of Applied Polymer Science*, Vol. 50, pp. 1013-1034, 1993.

105. Lindemann, M. K., *Encyclopedia of Polymer Science and Technology*, 1971.

106. Yeom, C.-K. and K.-H. Lee, "Pervaporation Separation of Water-Acetic Acid Mixtures through Poly(vinyl alcohol) Membranes Crosslinked with Glutaraldehyde", *Journal of Membrane Science*, Vol. 109, pp. 257-265, 1996.

107. Elliot, J. E., M. Macdonald, J. Nie, and C. N. Bowman, "Structure and Swelling of Poly(acrylic acid) Hydrogels: Effect of pH, Ionic Strenght and Diluton on the Crosslinked Polymer Structure", *Polymer*, Vol. 45, pp. 1503-1510, 2004.

108. Kim C. J. and P. I. Lee, "Composite Poly(vinyl alcohol) Beads for Controlled Drug Delivery", *Pharmaceutical Research*, Vol. 9, pp. 10-16, 1992.

109. Korsmeyer, R. W. and N. A. Peppas, "Effect of the Morphology of Hydrophilic Polymer Matrices on the Diffusion and Release of Water Soluble Drugs", *Journal of Membrane Science*, Vol. 9, pp. 211-227, 1981.

110. McNeill, I. C., "Thermal Degradation Mechanisms of Some Addition Polymers and Copolymers", *Journal of Analytical and Applied Pyrolysis*, Vol. 40, pp. 21-41, 1997.

111. Martin, A., J. Swarbrick, and A. Cammarata, *Physical Pharmacy: Physical Chemical Principles in Pharmaceutical Sciences*, Lee and Febiger, Philadelphia, 1993.

112. Kim, C. J. and P. I. Lee, "Effect of Loading on Swelling Controlled Drug Release from Hydrophobic Polyelectrolyte Gel Beads", *Pharmaceutical Research*, Vol. 9, pp.1268-1274, 1992.

113. Yasuda, H., A. Peterlin, C. K. Colton, K. A. Smith, and E. W. Merrill, "Permeability of Solutes through Hydrated Polymer Membranes. III. Theoretical Backgroud for the Selectivity of Dialysis Membranes", *Die Macromolecular Chemie*, Vol. 126, pp. 177-186, 1969.

114. Bachtsi, A. R., and C. Kiparissides, “Synthesis and Release Studies of Oil-containing Poly(vinyl alcohol) Microcapsules Prepared by Coacervation”, *Journal of Controlled Release*, Vol. 38, pp. 49-58, 1996.

115. Hopfenberg, H. B., A. Apicella, and D. E., Saleeby, “Factors Affecting Water Sorption in and Solute Release from Glassy Ethylene-vinyl alcohol Copolymers”, *Journal of Membrane Science*, Vol. 8, pp. 273-282, 1981.

116. Lee, P. I., “Dimensional Changes during Drug Release from a Glassy Hydrogel Matrix”, *Polymer Communications*, Vol. 24, pp. 45-47, 1983.

117. Cavusoglu, J. and S. H. Kusefoglu, “Oleophilic Modification of Poly(vinyl alcohol) films by functionalized soybean oil triglycerides”, *Journal of Applied Polymer Science*, Vol. 119, pp. 2431-2438, 2011.

118. Zhang, Y., P. C. Zhu, and D. Edgren, “Crosslinking Reaction of Poly(vinyl alcohol) with Glyoxal”, *Journal of Polymer Research*, Vol. 17, pp. 725-730, 2010.

119. Varma, D. S. and C. Nedungadi, “Modification of Poly(vinyl Alcohol) Fibers by Hexamethylene Diisocyanate”, *Journal of Applied Polymer Science*, Vol. 20, pp. 681-688, 1976.

120. Galiatsatos, C., K. Hajizadeh, J. E. Mark, and W. R. Heineman, “A New Method for Enzyme Membrane Preparation Based on Polyurethane Technology: Electrode Modification for Sensor Development”, *Biosensors*, Vol. 4, pp. 393-402, 1989.

121. Straksys, A., T. Kochane, and S. Budriene, “Synthesis and Characterization of Poly(urethane-urea) Microparticles from Poly(vinyl alcohol) and Binary Blends of Diisocyanates and their Application for Immobilization of Maltogenic α-amylase”, *Chemija*, Vol. 24, pp. 160-169, 2013.

122. Zhang, S., Z. Ren, S. He, and C. Zhu, "FTIR Spectroscopic Characterization of Polyurethane-urea Model Hard Segments (PUUMHS) based on Three Diamine Chain Extenders”,*Spectrochimica Acta Part A*, Vol. 66, pp.188-193, 2007.

123. Lonescu, M., *Chemistry and Technology of Polyols for Polyurethanes*, Rapra Technology, Shropshire, 2005.

124. Ajithkumar, S., S. S. Kansara, and N. K. Patel, "Kinetics of castor oil based polyol-toluene diisocyanate reactions", *European Polymer Journal*, Vol. 34, pp. 1273-1276, 1998.

125. Randall, D., *The Urethane Book*, Wiley, NewYork, 2002.

126. Götz, H., U. Beginn, C. F. Bartelink, H. J. M. Grünbauer, and M. Möller, "Preparation of Isophorone Diisocyanate Terminated Star Polyethers", *Macromolecular Materials and Engineering*, Vol. 287, pp. 223-230, 2002.

127. Lomölder, R., F. Plogmann, and P. Speier, "Selectivity of Isophorone Diisocyanate in the Urethane Reaction Influence of Temperature, Catalysis, and Reaction Partners", *Journal of Coatings Technology*, Vol. 69, pp. 51-57, 1997.

128. Hong, K. and S. Park, "Preparation of Polyurea Microcapsules with Different Composition Ratios: Structures and Thermal Properties", *Materials Science and Engineering*, Vol. 272, pp. 418-421, 1999.

129. Straksys, A., T. Kochane, and S. Budriene, "Preparation and Characterization of Porous Poly(urethane-urea) Microparticles from Poly(vinyl alcohol) and Isophorone Diisocyanate", *Chemija*, Vol. 26, pp. 132-140, 2015.

130. Mark, J. E., "Ceramic-Reinforced Polymers and Polymer-modified Ceramics", *Polymer Engineering & Science*, Vol. 36, pp. 2905-2920, 1996.